UNIVERSIDADE FEDERAL DA BAHIA
INSTITUTO DE GEOCIÊNCIAS
PROGRAMA DE PESQUISA E PÓS-GRADUAÇÃO EM GEOLOGIA
ÁREA DE CONCENTRAÇÃO:
PETROLOGIA, METALOGÊNESE E EXPLORAÇÃO MINERAL

DISSERTAÇÃO DE MESTRADO

OS RIFTES ESTATERIANO E TONIANO DO SETOR SUL DO AULACÓGENO DO PARAMIRIM, PALEOPLACA SÃO FRANCISCO-CONGO: NOVOS DADOS, CORRELAÇÕES REGIONAIS E INVERSÃO TECTÔNICA

CAROLINE NOVAIS BITENCOURT

SALVADOR-BA
2017

OS RIFTES ESTATERIANO E TONIANO DO SETOR SUL DO AULACÓGENO DO PARAMIRIM, PALEOPLACA SÃO FRANCISCO-CONGO: NOVOS DADOS, CORRELAÇÕES REGIONAIS E INVERSÃO TECTÔNICA

Caroline Novais Bitencourt

Orientadora: Profa. Dra. Simone Cerqueira Pereira Cruz

Dissertação de Mestrado apresentada ao Programa de Pós-Graduação em Geologia do Instituto de Geociências da Universidade Federal da Bahia como requisito parcial à obtenção do Título de Mestre em Geologia, Área de Concentração: Petrologia, Metalogênese e Exploração Mineral.

SALVADOR-BA
2017

CAROLINE NOVAIS BITENCOURT

"OS RIFTES ESTATERIANO-TONIANO DO SETOR SUL DO AULACÓGENO DO PARAMIRIM, PALEOPLACA SÃO FRANCISCO-CONGO: NOVOS DADOS, CORRELAÇÕES REGIONAIS E INVERSÃO TECTÔNICA"

Dissertação apresentada ao Programa de Pós-Graduação em Geologia da Universidade Federal da Bahia, como requisito para a obtenção do Grau de Mestre em Geologia na área de concentração em Petrologia, Metalogênese e Exploração Mineral, em 13/03/2017.

DISSERTAÇÃO APROVADA PELA BANCA EXAMINADORA:

Dra. Simone Cerqueira Pereira Cruz
Orientadora- UFBA

Dr. Matheus Kuchenbecker
Membro externo – UFVJM

Dr. Luiz César Corrêa Gomes
Membro interno – UFBA

MSc. José Torres Guimarães
Convidado – CPRM

Salvador – BA
2017

"Quero respirar um ar de um novo lar e avistar outras colinas"

(Arrais)

AGRADECIMENTOS

Gratidão a Deus, Criador e Mantenedor da minha vida, pelo seu cuidado e amor incondicional.

Aos meus pais, familiares e amigos, pelo imenso apoio, pelas orações, vibrações positivas... pelo incentivo que deram ao perguntar: “ E aí? Como vai o mestrado? ” ou “ Com o que você trabalha mesmo? ”. Me fazem pensar sobre os inúmeros motivos de ter escolhido geologia.

À professora e orientadora Simone Cerqueira Pereira Cruz, pela dedicação e generosidade sem limites, que certamente me inspiraram a concluir este trabalho e me inspirarão por toda minha caminhada.

Aos professores por regarem esse sentimento de amor que temos a ciência.

A todos os funcionários do Instituto de Geociências da Universidade Federal da Bahia.

Ao meu grupo de pesquisa pela parceria e cumplicidade, por sempre estarem dispostos a ajudar. Em especial a Vanderlúcia pela contribuição mais direta a esta dissertação;

À Coordenação de Pós-Graduação em Geologia-UFBA, pelo apoio e acompanhamento a todo tempo. E pelo excelente trabalho que desenvolvem.

À CPRM, nas pessoas de Cristina Burgos e Rita Menezes, pela disposição, contribuição e apoio de sempre.

Ao Laboratório de Geologia Isotópica do Departamento de Geologia da Universidade Federal de Ouro Preto, na pessoa de Ana Ramalho e Cristiano Lana.

À Fundação de Amparo à Pesquisa do Estado da Bahia (FAPESB).

Enfim! A todas as pessoas que contribuíram, das mais diversas formas, para a realização deste trabalho, o meu MUITO OBRIGADA!

RESUMO

O Aulacógeno do Paramirim tem sua história evolutiva marcada pela superposição de riftes sucessivos que se desenvolveram desde 1770 a 675 Ma. A sua inversão parcial ocorreu no Ediacarano, durante estruturação do Orógeno Araçuaí-Oeste Congo. Dentre os seus compartimentos, tem-se o Cinturão de Dobramentos e Cavalgamentos Serra do Espinhaço Setentrional. Nele, afloram unidades do Supergrupo Espinhaço (Formação Algodão), do Grupo Santo Onofre (Formação Serra da Garapa e Boqueirão) e do Grupo Macaúbas (Formação Nova Aurora), além das rochas da Suíte Intrusiva Lagoa Real e do embasamento. Predominam rochas siliciclásticas metamorfisadas em fácies xisto verde, com feições primárias parcialmente preservadas, mas obliteradas em zonas de cisalhamento. Destaca-se uma litofácie de quartzito e de xisto aluminoso com biotita, granada e estaurolita na Formação Serra da Garapa, sugerindo condições metamórficas de fácies anfibolito. O arcabouço estrutural apresenta três domínios estruturais distinto, denominados de *Klippe* de Jacaraci, *Nappe* de Caetité e Transpressional. A análise estrutural regional permitiu identificar seis fases deformacionais ediacaranas e relacionadas com a inversão do Aulacógeno do Paramirim. O sigma 1 atuou segundo WSW-ENE e foi resposável por um arcabouço estrutural complexo. Estudos geocronológicos U-Pb (LA-ICPMS) foram realizados em zircões detríticos das formações Algodão, Serra da Garapa e Boqueirão, tendo sido encontrado idades variando de 1958 ± 18 a 2870 ± 17 Ma, 894 ± 38 a 2662 ± 19 Ma e 899 ± 76 a 3177 ± 42 Ma, respectivamente. As fontes primárias principais e interpretadas estão relacionadas com as rochas do embasamento dos orógenos Itabuna-Salvador-Curaçá e do Oeste da Bahia, bem como pelas rochas geradas por suas estruturações, além de vulcanitos e plutonitos, máficos e felsicos, de idades entre 1.7 a 0.8 Ga, relacionados com a evolução das bacias precursoras do Orógeno Araçuaí-Oeste Congo. Como fontes secundárias para o Grupo Santo Onofre sugere-se as Sequências Metavulcanossedimentares e *Greenstone Belts* de idades arqueanas e paleoproterozoicas, bem como as rochas do Supergrupo Espinhaço. A continuidade física entre unidades do Grupo Santo Onofre e Macaúbas, assim como a presença de zircões tonianos em ambas, permitem sugerir uma correlação entre as unidades do primeiro grupo com as pré-glaciais do segundo grupo.

Palavras-chave: Aulacógeno do Paramirim, Grupo Santo Onofre; arcabouço estrutural, geocronologia.

ABSTRACT

The evolutionary history of the Paramirim Aulacogen is characterized by the superposition of successive rifts that developed from 1,770 to 675 Ma. The partial inversion of this feature occurred during the Ediacaran with the structuring of the Araçuaí-West Congo Orogen. Among its compartments, is the Northern Serra do Espinhaço Fold Thrust Belt. Units from the Espinhaço Supergroup (Algodão Formation), Santo Onofre Group (Serra da Garapa and Boqueirão Formation) and Macaúbas Group (Nova Aurora Formation) outcrop in this feature, as well as rocks from the Lagoa Real Intrusive Suite and from the basement. Metamorphic siliciclastic rocks predominate in greenschist facies, with partially preserved primary features that suffered obliteration in shear zones. The quartzite and aluminous schist with biotite, garnet and staurolite lithofacies of the Serra da Garapa Formation is an expressive feature that suggests metamorphic conditions of amphibolite facies. The structural framework present three different structural domains called: Jacaraci Klippe, Catetité Nappe and Transpression. Based on the regional structural analysis, six deformational ediacarans phases were identified, which were related to the inversion of the Paramirim Aulacogen. The sigma 1 acted according to a WSW-ENE orientation and was responsible for a complex structural framework. U-Pb geochronological studies (LA-ICPMS) were performed on detrital zircons from the Algodão, Serra da Garapa and Boqueirão formations. Ages ranging from 1,958 ± 18 to 2,870 ± 17 Ma, 894 ± 38 to 2,662 ± 19 Ma, and 899 ± 76 to 3,177 ± 42 Ma were found, respectively. The main primary sources and interpreted sources were related to rocks from the basement of the Itabuna-Salvador-Curaçá and Western Bahia orogens. They were also related to rocks generated by their structuring, as well as vulcanites and plutonites, both mafic and felsic, with ages between 1.7 and 0.8 Ga, related to the evolution of the precursor basins of the Araçuaí-West Congo Orogen. As secondary sources for Santo Onofre Group, results suggest Metavolcanosedimentary sequences and Greenstone Belts of Archean and Paleoproterozoic ages, as well as rocks from the Espinhaço Supergroup. The physical continuity between units of the Santo Onofre and Macaúbas groups, as well as the presence of zircons from the Tonian period in both units, suggest a correlation between units of the first group and pre-glacial units of the latter.

Keywords: Paramirim Aulacogen, Santo Onofre Group, structural framework, geochronology.

SUMÁRIO

CAPÍTULO 1
INTRODUÇÃO GERAL

O Aulacógeno do Paramirim é uma das estruturas da paleoplaca São Francisco-Congo, cuja evolução ocorreu de 1.775 ± 7 Ma (Danderfer Filho et al., 2015) até ca. de 675 Ma (Santana, 2016). Em seu interior, duas bacias podem ser identificadas, separadas pelo Horst Paramirim (Alkmim et al., 1993, Guimarães et al., 2008), denominadas de gráben ou ramo oriental, que corresponde à porção oeste da atual Chapada Diamantina, e gráben ocidental, que corresponde à atual parte leste da Serra do Espinhaço Setentrional (Fig. 1) (Guimarães et al., 2008, 2012). Ambas bacias estão separadas pelo Alto do Paramirim (Cruz et al., 2012). Essas bacias abrigam rochas dos supergrupos Espinhaço e São Francisco (Danderfer e Dardenne, 2002: Alkmim e Martins Neto 2012**;** Souza et al., 2014; e este trabalho). Granitoides anorogênicos da Suíte Intrusiva Lagoa Real (Arcanjo et al., 2000) e diques máficos (Pereira, 2007; Brito, 2008; Guimarães et al., 2008; Teixeira, 2008; Damasceno, 2009, 2013; Danderfer Filho et al., 2009; Menezes Leal et al., 2012) integram o conjunto litológico. O embasamento desse aulacógeno é constituído por metagranitoides, ortognaisses, por vezes migmatíticos, com enclaves metamáficos e metaultramáficos arqueanos, *Greenstone Belts* e Sequências metavulcanossedimentares de idades arqueanas e paleoproterozoicas, respectivamente (Cruz et al., 2017), além de rochas plutônicas ácidas intrusivas de idades sideriana, riaciana e orosiriana (Cordani et al., 1985, 1992; Martin et al., 1991; Marinho, 1991; Nutman e Cordani, 1994; Santos Pinto et al., 1998, 2012; Bastos Leal et al., 1998, 2000; Rosa et al., 2000; Peucat et al., 2002; Barbosa et al., 2012; Medeiros, 2013; Barbosa et al., 2013; Cruz et al., 2012, 2016; Paquette et al., 2015). A sua inversão ocorreu no Ediacarano (Cruz and Alkmim, 2006), durante as deformações que culminaram com a edificação de Gondwana Ocidental (Alkmim et al., 2006, 2007). No setor parcialmente invertido desse aulacógeno, o Corredor do Paramirim (Alkmim et al., 1993), dois cinturões de dobramentos e cavalgamentos foram nucleados, denominados de Serra do Espinhaço Setentrional, a oeste, e Chapada Diamantina, a leste (Cruz et al., 2012) (Fig. 1). Os domínios de deformações endodérmicas desses cinturões integram o setor intracontinental do Orógeno Araçuaí-Oeste Congo (Borges et al., 2015).

A área de estudo localiza-se no centro-sudoeste do Estado da Bahia, entre os municípios de Caetité e Licínio de Almeida (Fig. 2). O principal acesso a partir da capital

baiana se faz pela BR – 324 até Feira de Santana, de onde segue pela BR-116 até o entroncamento com a BA-250 por 130 km. Neste ponto segue pela BA-250 e, posteriormente, pela BA-026 e pela BR-407 até a BA-262. A partir daí, segue-se para a cidade de Brumado pela BA–940 e pela BR-030 até a cidade de Caetité. A distância total de Salvador até Caetité é 635 km.

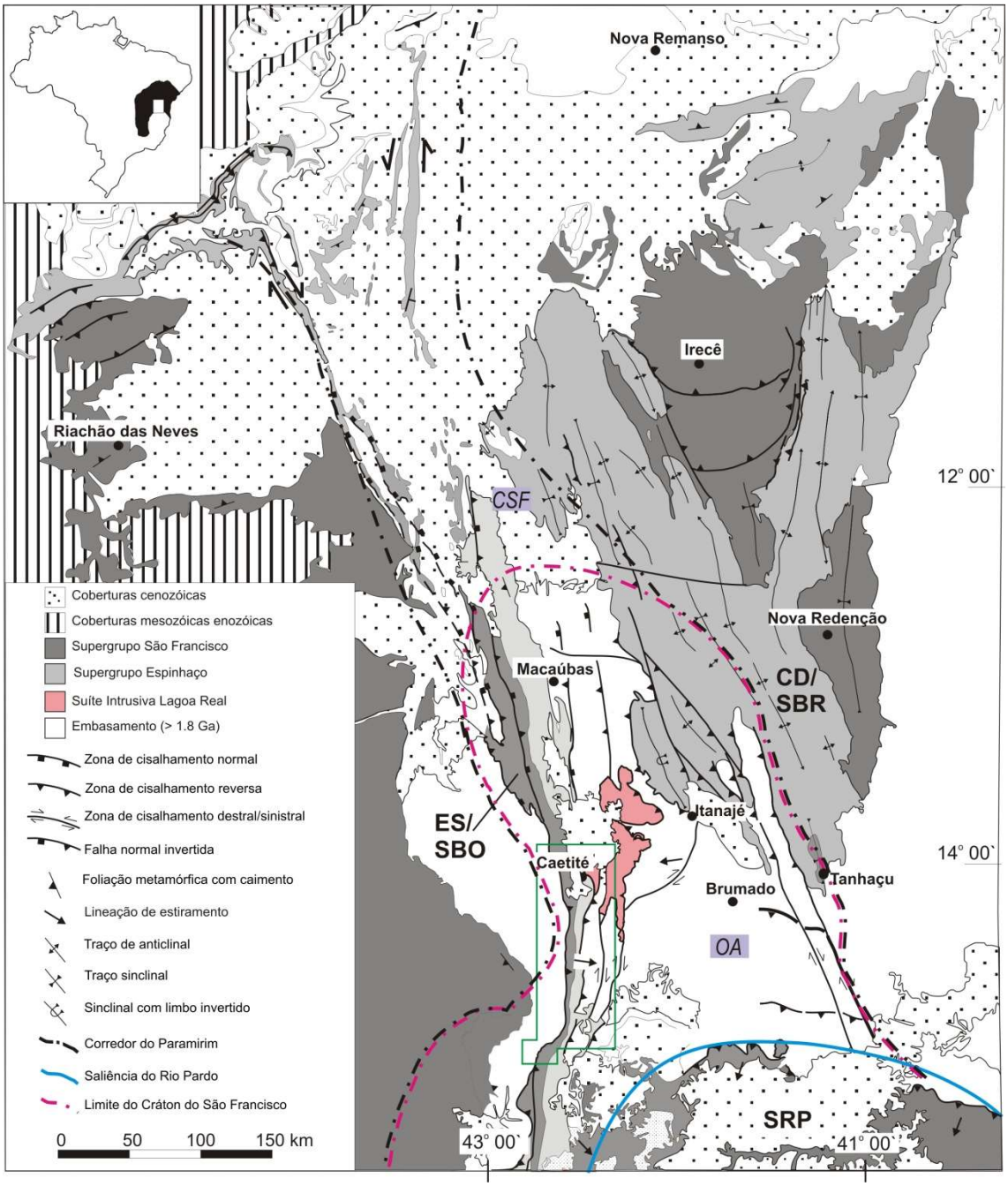

Fig. 1. Mapa Geológico simplificado do Aulacógeno do Paramirim, enfatizando as principais unidades geológicas e estruturas tectônicas de idade brasiliana. ES- Cinturão de Dobramentos e Cavalgamentos Serra do Espinhaço Setentrional, CD- Cinturão de Dobramentos e Cavalgamentos da Chapada Diamantina, SRP- Saliência do Rio Pardo, SBO- Bacia Ocidental, SBR- Bacia Oriental, CSF – Cráton do São Francisco, OA- Orógeno Araçuaí. A área de trabalho está indicada pelo polígono verde. Fonte: Cruz (2004).

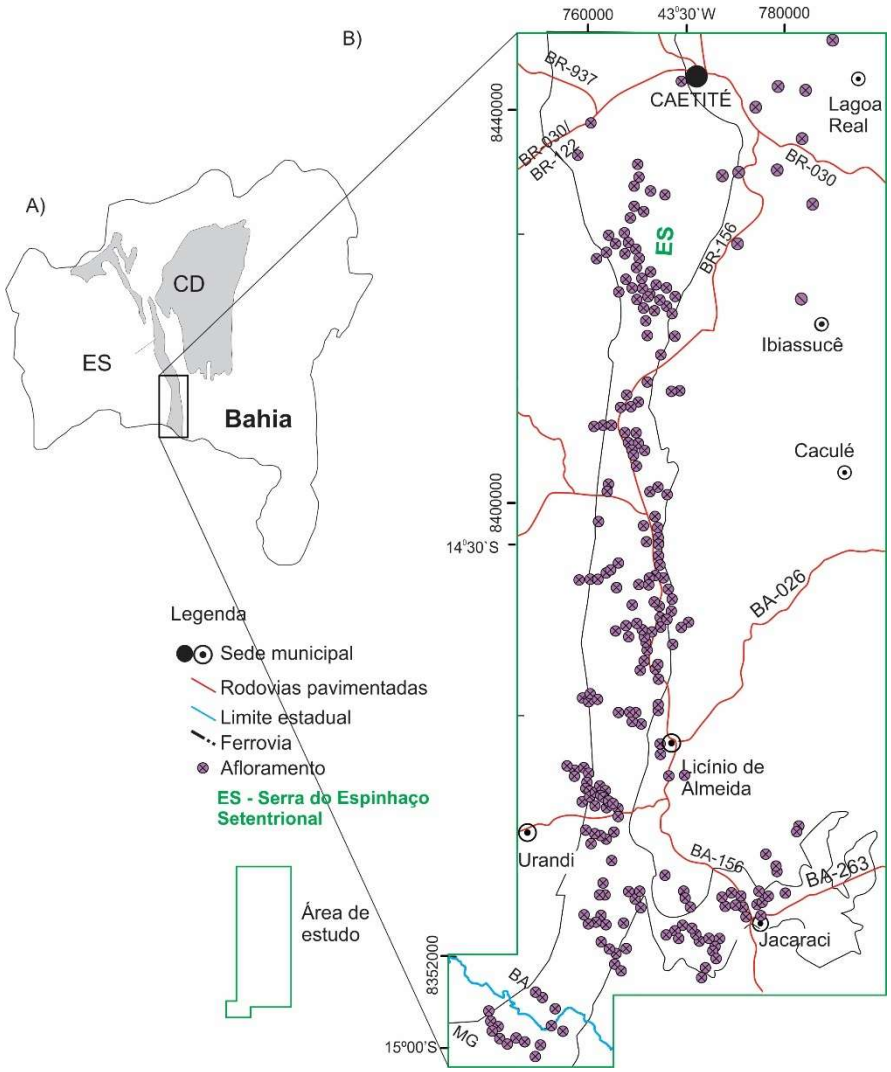

Fig. 2. Mapa de situação (A) e de localização (B) da área de estudo com os pontos de afloramentos visitados. Os afloramentos estão, predominantemente inserido na serra do Espinhaço Setentrional. ES- serra do Espinhaço Setentrional, CD- Chapada Diamantina. Fonte: A) Cruz (2004), B) SEI (2010,2016).

O Cinturão de Dobramentos e Cavalgamentos Serra do Espinhaço Setentrional compreende rochas do Supergrupo Espinhaço e do Grupo Santo Onofre (Supergrupo São Francisco). Na área de estudo, com o foco dado na área de ocorrência na serra do Espinhaço Setentrional a sul da cidade de Caetité (Fig. 2), afloram a Formação Algodão, como unidade do Supergrupo Espinhaço, e as formações Serra da Vereda e Boqueirão do Grupo Santo Onofre. A Formação Algodão foi primeiramente descrita por Danderfer Filho (2000) e pode alcançar em alguns lugares 1600 m de espessura (Guimarães et al., 2012). De acordo com esses autores, essa formação compreende:

- Associação de litofácies composta por metaconglomerado polimítico de aspecto desorganizado e maciço (clastos de granitoide, metarenito, quartzo, quartzito, itabirito),

metabrecha sedimentar monomítica intraformacional (fragmentos de metarenito) e de metarenito feldspático mal selecionado com estratificação paralela e cruzada tangencial à base de grande porte, acanalada e planar;

- Associação de litofácies constituída por metarenito feldspático maciço, metaquartzarenito com estratificação cruzada tangencial de grande porte e do tipo *hummocky*, metaconglomerado polimítico (clastos de metarenito, quartzito, quartzo e granitoide), metapelitos maciço e laminado e metabrecha sedimentar;

- Associação de litofácies formada de metarenito feldspático com estratificação cruzada tangencial de grande porte e níveis de metaconglomerado.

As associações de litofácies discriminadas foram interpretadas por Danderfer Filho (2000), como acumuladas em ambiente continental, através de leques aluviais. Esses leques teriam evoluídos para um sistema fluvial entrelaçado com retrabalhamento eólico, associados a depósitos lacustres que foram afetados por eventos de tempestade. Essa deposição culmina com sedimentação eólica associada a fluxos gravitacionais subaéreos esporádicos.

Recentemente, na região de Botuporã, Danderfer Filho et al. (2015), encontraram rochas metavulcânicas félsicas nessa formação, com idades de cristalização em 1775 ± 7 Ma. Uma idade próxima a essa, 1777 ± 11 Ma, foi obtida por Cruz et al. (em preparação) na região de Licínio de Almeida.

Quanto às unidades do Grupo Santo Onofre, desde a sua primeira descrição por Kaul (1970) até os tempos atuais, passando pelos trabalhos publicados por Costa e Silva (1980), Barbosa e Dominguez (1996), Schobbenhaus (1996), Danderfer Filho (2000), Danderfer e Dardenne (2002), Souza et al. (2003), Loureiro et al. (2009), Guimarães et al. (2008, 2012), por exemplo, vem sendo alvo de grande controvérsia quanto a sua estratigrafia e seu posicionamento estratigráfico. Com relação às unidades constituintes, será adotada a proposta de Guimarães et al. (2012), apresentada na Figura 3. De acordo com esses autores, o Grupo Santo Onofre é subdividido da base para o topo nas formações Fazendinha, Serra da Vereda, Serra da Garapa e Boqueirão, separadas por contatos gradacionais.

Com relação ao posicionamento estratigráfico do Grupo Santo Onofre, Barbosa e Domingues (1996), Souza et al. (2003), Loureiro et al. (2009), Guimarães et al. (2008, 2012) sugerem que este grupo seja uma unidade do Supergrupo Espinhaço.

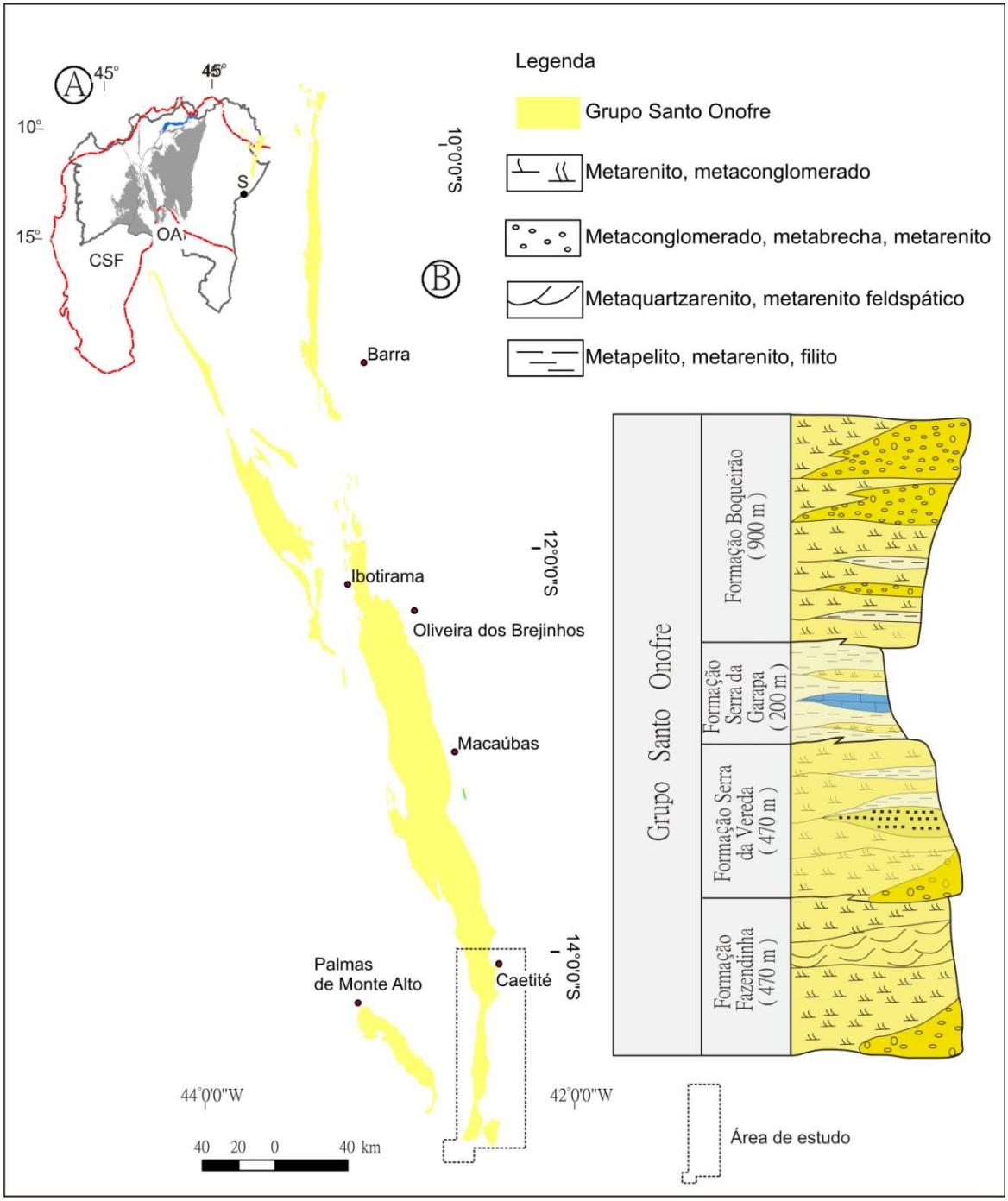

Fig. 3. A) Mapa de situação tectônica da área de estudo; B) distribuição espacial do Grupo Santo Onofre no Cinturão de Dobramentos e Cavalgamentos Serra do Espinhaço Setentrional; c) Perfil esquemáticos das unidades do Grupo Santo Onofre. Modificado de Guimarães et al. (2012).

Por sua vez, Schobbenhaus (1996), Dandefer Filho (2000), Danderfer Filho e Dardenne (2002), Uhlein et al. (2007), Alkmim e Martins Neto (2012) e Alkmim (2014) fizeram correlações regionais entre os grupos Macaúbas e Santo Onofre. Entretanto, poucos eram os estudos geocronológicos publicados em zircões detríticos nessa unidade que comprovem essa suposição. Além disso, apesar dos estudos realizados por Bitencourt (2014)

e Cruz et al. (2014), lacunas existem sobre a contribuição litológica e o arcabouço estrutural desse setor do Cinturão de Dobramentos e Cavalgamentos Serra do Espinhaço Setentrional. Somando-se a isso na bacia oriental existem rochas diamictíticas da Formação Bebedouro (Supergrupo São Francisco) que foram correlacionadas por Babinski et al. (2012) às unidades glaciais do Grupo Macaúbas.

Diante do exposto, algumas questões nortearam este trabalho: quais as unidades que afloram no Cinturão de Dobramentos e Cavalgamentos Serra do Espinhaço Setentrional, especificamente no setor sul à cidade de Caetité? Qual a assinatura geocronológica dos zircões detríticos das formações Algodão (Supergrupo Espinhaço), Serra da Garapa e Boqueirão (Grupo Santo Onofre)? Existe correlação, física e temporal, entre as rochas do Grupo Santo Onofre com as do Grupo Macaúbas e da Formação Bebedouro? Quais os domínios e estruturas deformacionais encontradas neste setor do Cinturão de Dobramentos e Cavalgamentos Serra do Espinhaço Setentrional? Existem relações tectônicas entre as rochas do Grupo Santo Onofre e as rochas anorogênicas tonianas da Suíte Salto da Divisa estudadas por Silva et al. (2008), Menezes et al. (2012) e Victoria et al. (2015)?

Responder essas perguntas representa dar um passo importante na caracterização do Cinturão de Dobramentos e Cavalgamentos Serra do Espinhaço Setentrional, suas rochas e deformações, bem como resolver um dos maiores problemas de cartografia da literatura baiana e mineira, que é a correlação, ou não, das unidades do Grupo Santo Onofre com as do Grupo Macaúbas.

O objetivo geral deste trabalho é contribuir com o entendimento da evolução das bacias precursoras, estateriana e toniana, do Orógeno Araçuaí no cenário de Gondwana Ocidental e sua inversão. Como objetivos específicos, têm-se: a) verificar as litologias aflorantes na área de estudo; b) obter idades de zircões detríticos, inferir sobre áreas fontes e determinar a idade máxima de deposição das unidades aflorantes; c) verificar a posição estratigráfica e correlações regionais do Grupo Santo Onofre com o Grupo Macaúbas e com a Formação Bebedouro, ambas do Supergrupo São Francisco; d) levantar dados sobre o arcabouço estrutural, nas escalas meso e microscópica; e) discutir as implicações tectônicas associadas com a evolução deste setor do Orógeno Araçuaí e elaborar um modelo evolutivo, verificando possíveis correlações regionais com o magmatismo toniano e anorogênico que ocorre na Suíte Salto da Divisa.

Para que esses objetivos fossem alcançados, foram realizados:

(i) Levantamento bibliográfico: nessa fase procedeu-se à leitura de livros, monografias, dissertações, teses, artigos e resumos científicos que versem sobre a área de estudo e sobre aspectos relacionados com Grupo Santo Onofre, Grupo Macaúbas, sistemas glaciais, magmatismo toniano, sistemas orogênicos e bacias precursoras, bem como sobre o Orógeno Araçuaí-Oeste Congo e proveniência de zircões detríticos.

(ii) Trabalho de campo: esses trabalhos totalizaram 57 dias efetivos, durante os quais foram realizadas: (a) seções geológicas regionais, transversais ao *trend*, para reconhecimento das unidades de cobertura do Cinturão de Dobramentos e Cavalgamentos Serra do Espinhaço Setentrional e do seu embasamento; (b) mapeamento geológico, na escala 1:60.000, visando o estudo e a cartografia das unidades estratigráficas, com ênfase nas unidades da serra do Espinhaço Setentrional (Fig. 2). Alguns pontos fora da serra do Espinhaço Setentrional foram realizados com o objetivo de realizar o reconhecimento do embasamento das rochas metassedimentares da Formação Algodão e do Grupo Santo Onofre; (c) levantamento do arcabouço estrutural, em *dip direction*; e (d) coleta de amostras para petrografia/análise microestrutural e geocronologia. Para o mapeamento geológico foram utilizadas fotos aéreas (escala 1:60000) e mapa topográficos (escala 1:100.000), das Folhas Guanambi (IBGE, 1974), Espinosa (IBGE, 1974) e Caculé (IBGE, 1980), imagens de satélite obtidas através do programa Google Pro Earth versão 7.1.2.2041, além de dados geofísicos de levantamento aerogravimétrico e aeromagnético. Em campo foram usados carro traçado, lupa, martelo, caderneta de campo, estereoscópio OPTO EM-2 e bússola Brunton Geo Pocket Transit 5009. Um total de 196 pontos foram descritos e a sua distribuição encontra-se apresentada na Figura 3. As coordenadas dos pontos estão apresentadas no Apêndice B.

(iii) Análises petrográfica e microestrutural: essas análises foram realizadas em 19 lâminas delgadas, dentre simples e polidas. Os estudos foram desenvolvidos no Laboratório Mineralogia Ótica e Petrografia do Instituto de Geociências da Universidade Federal da Bahia. O microscópio utilizado foi o binocular da marca Olympus (Modelo BX41).

(iv) Análise estrutural: essa atividade foi realizada através da coleta de dados em campo, com determinação do posicionamento espacial e integração tridimensional das estruturas. Os dados foram plotados no mapa geológico e organizados em planilhas Excel. O tratamento estatístico foi realizado através do *software* STEREONET 9.5 (Allmendinger et al., 2012; Cardozo e Allmendinger, 2013).

(v) Estudo geocronológico: as análises foram realizadas em zircão detrítico de 5 amostras, sendo duas na Formação Algodão (amostras Salto e CNB 64) e três no grupo Santo

Onofre (amostras MPA, MPC e TR01) (Tab. 1). Após coletadas, as amostras foram submetidas as seguintes etapas (i) britagem e moagem; (ii) utilização do *shatterbox*; (iii) peneiramento; (iv) separação dos minerais magnéticos no *Frantz* modelo L-1; (v) utilização de microbatéia; e, por fim, (vi) análise e seleção óptica dos grãos. Essas etapas foram realizadas no Laboratório de Preparação de Amostras do Serviço Geológico do Brasil (CPRM-SUREG Salvador). No Laboratório de Preparação de Amostras do Departamento de Geologia da Universidade Federal de Ouro Preto, os grãos foram imageados por catodoluminescência no Microscópio Eletrônico de Varredura (JEOL 6510) visando verificar a presença de inclusões e sobrecrescimentos. As montagens foram realizadas em uma resina epoxy (Specifix) com 25 mm de espessura. A Tabela 1 apresenta o número de grãos analisados por amostra. No Laboratório de Geologia Isotópica do Departamento de Geologia da Universidade Federal de Ouro Preto, as análises U-Pb das amostras Salto, CNB 64, MPA e MPC foram realizadas usando um Thermo-Scientific Element 2 Sector Field (SF) ICP-MS acoplado a um laser CETAC LSX-213 G2 + (λ = 213 nm) Nd: YAG. As razões isotópicas ($^{207}Pb/^{206}Pb$, $^{208}Pb/^{206}Pb$, $^{208}Pb/^{232}Th$, $^{206}Pb/^{238}U$ e $^{207}Pb/^{235}U$) foram calculadas usando o *software* de redução de dados Glitter (Van Achterbergh et al., 2001). O valor de ^{235}U foi calculado a partir da razão da abundância natural ($^{235}U = {}^{238}U/137.88$). Os dados foram organizados em tabelas e diagramas utilizando o programa Isoplot (Ludwig, 2012). A amostra TR-01 foi analisada na Universidade de Clermont Ferrand (França) e os procedimentos estão apresentados no Anexo B Detalhes dessas análises encontram-se no artigo do capítulo 2 dessa dissertação.

Tabela 1 – Numero de grãos de zircão detríticos analisados por amostra.

Amostras	Coordenada	Unidade	Número de grãos analisados
SCP Salto	23L, 769059/8444083	Formação Algodão/Supergrupo Espinhaço	40
CNB-64	23L, 761416/8368232		113
MPA	23L, 767211/8432119	Formação Serra da Garapa / Grupo Santo Onofre	70
MPC	23L, 766621/8432139		64
TR-01	23L, 758749/8370741	Formação Boqueirão/ Grupo Santo Onofre	91

O Cinturão de Dobramentos e Cavalgamentos Serra do Espinhaço Setentrional vem sendo alvo de pesquisa desde a década de 1970 e inúmeros trabalhos já foram realizados com foco na cartografia e na análise estratigráfica. No entanto, com relação às idades máximas de deposição do Grupo Santo Onofre, bem como sobre a assinatura de zircões detríticos das unidades constituintes dessa unidade, poucos estudos haviam sido realizados, podendo ser

mencionados Franz et al. (2014) e Sousa et al. (2014). Além disso, o entendimento da extensão, evolução e conexões das bacias precursoras do Orógeno Aracuaí é uma questão que suscita grande interesse da comunidade científica.

Esta dissertação está organizada em três capítulos. No capítulo 1 apresenta-se a Introdução Geral, com a apresentação do tema, problemas, objetivos, materiais e métodos e justificativa. No capítulo 2 apresenta-se o artigo científico a ser submetido e no capítulo 3 têm-se as Conclusões da Dissertação, com algumas recomendações. Um total de 2 apêndices e 1 anexos encontram-se no final do trabalho.

Referências

Alkmim, F.F., 2014. Serra do Espinhaço e Chapada Diamantina. In: Hasui, Y., Carneira, C. D. R., Almeida, F. F., Bartorelli, A. (Eds.), Geologia do Brasil, Beca, São Paulo, 236-244.

Alkmim, F.F., Brito Neves, B.B., Alves, J.A.C., 1993. Arcabouço tectônico do Cráton do São Francisco – uma revisão. In: Dominguez, J.M. e Misi, A. (Eds.), o Cráton do São Francisco. Reunião Preparatória do II Simpósio sobre o Cráton do São Francisco, SBG/ Núcleo BA/SE/SGM/CNPq, Salvador, 45-62.

Alkmim, F.F., Marshak, S., Pedrosa-Soares, A.C., Peres, G.G., Cruz, S.C.P., Whittington, A., 2006. Kinematic evolution of the Araçuaí–West Congo orogen in Brazil and Africa: Nutcracker tectonics during the Neoproterozoic assembly of Gondwana. Precambrian Research 149, 43-63.

Alkmim, F.F., Martins-Neto, M.A., 2012. Proterozoic First-order sedimentary sequences of the São Francisco craton, eastern Brazil, Marine and Petroleum Geology 33, 127-139.

Alkmim, F.F., Pedrosa-Soares, A.C, Noce, C.M., Cruz, S.C.P., 2007. Sobre a Evolução Tectônica do Orógeno Araçuaí-Congo Ocidental. Geonomos 15, 25–43.

Allmendinger, R.W., Cardozo, N., Fisher, D., 2012. Structural geology algorithms: Vectors and tensors in structural geology: Cambridge University Press, 100 pp.

Arcanjo, J.B., Marques-Martins, A.A., Loureiro, H.S.C., Varela, P.H.L., 2000. Projeto vale do Paramirim, escala 1:100.000. Programa de Levantamentos Geológicos Básicos do Brasil, CD-ROOM.

Babinski, M., Pedrosa-Soares, A.C., Trindade, R.I.F., Martins M., C.M. Noce, Liu D., 2012. Neoproterozoic glacial deposits from the Araçuaí orogen, Brazil: Age, provenance and correlations with the São Francisco craton and West Congo belt. Gondwana Research 21, 451-465.

Barbosa, J.S.F. and Dominguez J.M.L., 1996. Mapa Geológico do Estado da Bahia. Escala: 1.000.000. Texto explicativo. Salvador, BA, 382 pp.

Barbosa, J.S.F., Santos-Pinto, M., Cruz, S.C.P., Souza, J.S., 2012. Granitóides. In: Barbosa, J. S. (Eds.) Geologia da Bahia, Pesquisa e Atualização, CBPM Série Publicações especiais, Salvador, 327–394.

Barbosa, N.S., Teixeira, W., Bastos Leal, L.R., Leal, A.B.M., 2013. Evolução crustal do setor ocidental do Bloco Arqueano Gavião, Cráton do São Francisco, com base em evidências U-Pb, Sm-Nd e Rb-Sr. Geologia USP, Série Científica 13, 6-88.

Bastos Leal L.R.B., Teixeira W., Cunha J.C., Leal A.B.M., Macambira M.J.B., Rosa M.L.S., 2000. Isotopic signatures of paleoproterozoica granitoids of the Gavião block and implications for the evolution of the São Francisco craton, Bahia, Brazil. Revista Brasileira de Geociências 30, 66-69.

Bastos Leal, L R., Teixeira, W., Cunha, J.C., Macambira, M.J.B., 1998. Archean tonalitic-trondhjemitic and granitic plutonism in the Gavião block, São Francisco Craton, Bahia, Brazil: Geochemical and geochronology characteristics. Revista Brasileira de Geociência 2, 209-220.

Bittencourt C.N., 2014. Petrologia e análise estrutural multiescalar da Formação Serra da Garapa (Grupo Santo Onofre) na porção sul do Cinturão de Dobramentos e Cavalgamentos Serra do Espinhaço setentrional. Corredor do Paramirim, Caetité, Bahia. (Undergraduate Thesis) Universidade Federal da Bahia, Salvador, 118 pp.

Borges, J.O., Cruz, S.C.P., Barbosa, J.S.F., 2015. Structural framework of the the Lagoa D'Anta mine area, iron-manganese Urandi-Caetité- Licínio de Almeida District, Bahia, Brasil. Brazilian Journal of Geology 45, 173-192.

Brito, D.C., 2008. Geologia, petrografia e litogeoquímica dos diques máficos que ocorrem na porção sudoeste da Chapada Diamantina, Bahia, Brasil. (M. Sc. Thesis) Universidade Federal da Bahia, Salvador, 77pp.

Cardozo, N., Allmendinger, R.W., 2013, Spherical projections with OSX Stereonet: Computers and Geosciences 51, 193 – 205.

Cordani U.G., Sato K., Marinho M.M., 1985. The geologic evolution of the ancient granite-greenstone terrane of central-southern Bahia, Brazil. Precambrian Research 27, 187-213.

Cordani, U.G., Iyer, S.S., Taylor, P.N., Kawashita, K., Sato, K., Mcreath, I., 1992. Pb-Pb, Rb-Sr, and K-Ar sistematic of the Lagoa Real uranium province (south-central Bahia, Brazil) and the Espinhaço Cycle (ca. 1.5-1.0 Ga). Journal of South American Earth Sciences 1, 33-46.

Costa L.A.M. and Silva W.G., 1980. Projeto Santo Onofre, mapeamento. TRISERVICE, convênio DNPM/CPRM, Relatório Final Integrado, Rio de Janeiro, RJ, 374 pp.

Cruz S.C.P., Alkmim F.F., Pedreira A., Teixeira L., Pedrosa-Soares A.C., Gomes L.C.C., Souza J.S., Leal A.B.M., 2012. O Orógeno Araçuaí. In: Barbosa J.S.F., Mascarenhas J.F.; Corrêa-Gomes L.C.; Domingues J.M.L. (Eds.), Geologia da Bahia, Pesquisa e Atualização, CBPM Série Publicações Especiais, Salvador, 131-178.

Cruz, S.C.P., 2004. A interação tectônica entre o Aulacógeno do Paramirim e o Orógeno Araçuaí-Oeste Congo. (Ph.D. Thesis) Universidade Federal de Ouro Preto, Ouro Preto, 505 pp.

Cruz, S.C.P., Alkmim, F.F., 2006. The tectonic interaction between the Paramirim Aulacogen and the Araçuaí Belt, São Francisco Craton region, Easter Brazil. Anais da Academia Brasileira de Ciências 1, 151-173.

Cruz, S.C.P., Barbosa, J. S. F., Barbosa, A.C., Jesus, S.S.G.P., Medeiros, E.L.M., Figueiredo, B.S., Menezes Leal, A.B., Lopes, P., Souza, J.S., 2014. Mapeamento Geológico e Levantamentos de Recursos Minerais das Folhas Espinosa e Guanambi (Escala 1:100.000). Relatório Final, Convênio CPRM-UFBA-FAPEX, Salvador, BA, 253 pp.

Cruz, S.C.P., Barbosa, J.S.F., Marinho M.M., Peucat J.J., Pasquette J.L., 2017. Quantas sequências metavulcanossedimentares pré-estaterianas existem a oeste do lineamento contendas Mirante-Jacobina? Novos dados e correlações regionais. XVII Simpósio Nacional de estudos tectônicos, Salvador. Anais de Resumo Expandidos, p. 120-123.

Cruz, S.C.P., Barbosa, J.S.F., Santos Pinto, M., Peucat J,J, Paquette J.L., Souza, J. S., Martins, V. S., Chemale Júnior, F., Carneiro, M. A., 2016. The Siderian-Orosirian magmatism in the Gavião Paleoplate, Brazil: U-Pb geochronology, geochemistry and tectonic implications. Journal of South American Earth Sciences 69, 43 – 79.

Damasceno, G.C., 2009. Geologia, petrografia e geoquímica preliminar dos diques máficos da porção leste da folha Caetité (SD.23-Z-B-III). (Undergraduate Thesis) Universidade Federal da Bahia, Salvador, 108 pp.

Damasceno, G.C., 2013. Geologia, Petrografia e Geoquímica dos diques máficos da Folha Caetité (SD.23-Z-B-III). (M. Sc. Thesis) Universidade Federal da Bahia, Salvador, 145pp.

Danderfer Filho, A., 2000. Geologia sedimentar e evolução tectônica do Espinhaço Setentrional, Estado da Bahia. (PhD Thesis) Universidade Federal de Brasília, Brasília, 497 pp.

Danderfer Filho, A., Dardenne, M.A., 2002. Tectonoestratigrafia da Bacia Espinhaço na porção centro-norte do Cráton do São Francisco: registro de uma evolução poliistórica descontínua. Revista Brasileira de Geociências 4, 449-460.

Danderfer Filho, A., De Waele, B., Pedreira, A.J., Nalini, H.A., 2009. New geochronological constraints on the geological evolution of Espinhaco basin within the São Francisco Craton-Brazil. Precambrian Research 170, 116–128.

Danderfer Filho, A., Lana, C.C., Nalini Júnior, H.A., Costa, A.F.O., 2015. Constraints on the Statherian evolution of the intraplate rifting in a Paleo-Mesoproterozoic paleocontinent: New stratigraphic and geochronology record from the eastern São Francisco craton. Gondwana Research 28, 668 – 688.

Franz, G., Morteani, G., Gerdes, A., Rhede, D., 2014. Ages of protolith and Neoproterozoic metamorphism of Al-P-bearing quartzites of the Veredas formation (Northern Espinhaco, Brazil): LA-ICP-MS age determinations on relict and recrystallized zircon and geodynamic consequences. Precambrian Research 250, 6-26.

Guimarães, J.T., Alkmim, F. F., Cruz, S.C.P., 2012. Supergrupo Espinhaço e São Francisco. In: Barbosa, J.S.F. (Eds.) Geologia Da Bahia, Pesquisa e Atualização, CBPM Série Publicações Especiais, Salvador, 33–85

Guimarães, J.T., Santos, R.A., Melo, R.C., 2008. Geologia da Chapada Diamantina (Projeto Ibitiara-Rio de Contas). CBPM Série arquivos abertos 31, 68pp.

Jackson S.E., Pearson N.J., Griffin W.L., Belousova E.A., 2004. The application of laser ablation-inductively coupled plasma-mass spectrometry to in situ U–Pb zircon geochronology. Chemical Geology, 211, 47-69.

Kaul, P.F.T., 1970. Geologia da quadrícula Boquira, Bahia. SUDENE/DRN/DG, Relatório interno, Recife, PE, 59 pp.

Loureiro H.S.C., Bahiense I.C., Neves J.P., Guimarães J. T., Teixeira L. R., Santos R. A., Melo R.C., 2009. Geologia e recursos minerais da parte norte do corredor de deformação do Paramirim (Projeto Barra – Oliveira dos Brejinhos). CBPM. Série Arquivos Abertos 33, Salvador, BA, 113 pp.

Ludwig K.R., 2012. Software: Isoplot Version 3.75: a Geochronological Toolkit for Microsoft Excel. Berkeley Geochronology Center, Berkeley, CA, 150 pp.

Marinho, M.M., 1991. La séquence volcano-sédimentaire de Contendas-Mirante et la bordure occidentale du Bloc Jequié (Craton du São Francisco, Brésil): un exemple de transition Archéen-Proterozóïque. (PhD Thesis) Univ. Clemont-Ferrand, Clemont-Ferrand, 388 pp.

Martin, H., Peucat, J.J., Sabaté, P., Cunha, J.C., 1991. Um segment de croûte continentale d'Age archéean ancien (3.5 millards d'années): lê massif de Sete Voltas (Bahia, Brésil). Les Comptes Rendus de l'Académie des Sciences Paris 313, 531-538.

Medeiros E.L.M., 2013. Geologia e Geocronologia do complexo Santa Izabel, na região de Urandi, Bahia., 2013. (M. Sc. Thesis) Universidade Federal da Bahia, Salvador, 96 pp.

Menezes Leal, A.B., Corrêa-Gomes, L.C., Guimarães, J.T., 2012. Diques Máficos. In: Barbosa, J.S.F. (Eds.) Geologia da Bahia. Pesquisa e Atualização, CBPM Série Publicações especiais, Salvador, 199-231.

Menezes, R.C.L., Conceição, H., Rosa, M.L.S., Macambira, M.J.B., Galarza, M.A., Rios, D. C., 2012. Geoquímica e geocronologia de granitos anorogênicos tonianos (c.914–899 Ma) da Faixa Araçuaí no Sul do Estado da Bahia. Geonomos 20, 1–13.

Müller W., Shelley M., Miller P., Broude S., 2009. Initial performance metrics of a new custom-designed ArF excimer LA-ICPMS system coupled to a two-volume laser-ablation cell. Journal of Analytical Atomic Spectrometry 24, 209-214.

Nutman, A.P., Cordani, U.G., 1994. SHRIMP U-Pb zircon geochronology of Archean granitoids from the Contendas Mirante area of the São Francisco Craton, Bahia, Brazil. Journal of South American Earth Sciences 7, 107-114.

Paquette, J.L., Barbosa, J.S.F., Rohais, S. Cruz, S.C.P., Goncalves, P., Peucat, J.J., Leal, A.B.M., Santos-Pinto, M., Martin, H., 2015. The geological roots of South America: 4.1Ga and 3.7 Ga zircon crystals discovered in N.E. Brazil and N.W. Argentina. Precambrian Research 271, 49-55.

Pereira, L.M., 2007. Geologia, Petrografia e Geoquímica dos diques máficos da porção sudeste do Bloco Gavião, Bahia, Brasil. (Undergraduate Thesis) Universidade Federal da Bahia, Salvador, 69 pp.

Peucat, J.J., Mascarenhas, J.F., Barbosa, J.S.F., Souza, F.S., Marinho, M.M., Fanning, C.M., Leite, C.M.M., 2002. 3.3 Ga SHRIMP U-Pb zircon age of a felsic metavolcanic rock from the Mundo Novo greenstone belt in the São Francisco craton, Bahia (NE Brazil). Journal South American Earth Sciences 15, 363-373.

Rosa, A.M.L.S., Conceição, H., Oberli, F., Meier, M., Martin, H., Macambira, M.B., Santos, E.B., Paim, M.M., Leahy, G.A.S., Bastos Leal, L.R., 2000. Geochronology (UPb/Pb-Pb) and isotopic signature (Rb-Sr/Sm-Nd) of the paleoproterozoic Guanambi Batholith, southWestern Bahia State (NE Brazil). Revista Brasileira de Geociências 30, 062-065.

Santana, A.V., 2016. Análise estratigráfica em alta resolução em rampa carbonática dominada por microbiolitos, Formação Salitre, Bacia de Irecê, Bahia. (PhD Thesis) Universidade de Brasília, Brasília, 290 pp.

Santos Pinto, M.A., Peucat, J.J., Martin, H., Barbosa, J.S.F., Fanning, C.M., Cocherie, A., Paquette, J.L., 2012. Crustal evolution between 2.0 and 3.5 Ga in the southern Gavião block (Umburanas-Brumado-Aracatu region), São Francisco Craton, Brazil: A 3.5–3.8 Ga proto-crust in the Gavião block? Journal of South American Earth Sciences 40, 129-142.

Santos Pinto, M.A., Peucat, J.J., Martin, H., Sabaté, P., 1998. Recycling of the Archaean continental crust: the case study of the Gavião Block, Bahia, Brazil. Journal of South American Earth Science 11, 487-498.

Schobbbenhaus, C., 1996. As tafrogêneses superpostas Espinhaço e Santo Onofre, estado da Bahia: Revisão e novas propostas. Revista. Brasileira de Geociências 4, 265-276.

SEI. Superintendência de Estudos Econômicos e Sociais da Bahia, 2010. Sistema de Transporte, escala 1:100.000. Disponível em: < http://www.sei.ba.gov.br>.

SEI. Superintendência de Estudos Econômicos e Sociais da Bahia, 2016. Limite municipal, escala 1:100.000. Disponível em: < http://www.sei.ba.gov.br>.

Silva, L.C., Pedrosa-Soares, A.C., Teixeira, L.R., 2008. Tonian rift-related, A-type continental plutonism in the Araçuaí orogen, Eastern Brazil: new evidences for the breakup stage of the São Francisco–Congo Paleocontinent. Gondwana Research 13, 527–537.

Sousa, F.R., Freitas, M. S., Virgens-Neto, J., 2014. Geologia e Recursos Minerais das Folhas Parnaguá, Rio Paraim e Mansidão - SC.23-Z-A-V, escalas 1:100.000, Programa Geologia do Brasil, CPRM – Serviço Geológico do Brasil, Teresina, PI, 88 pp.

Souza, J.D., 2003. Geologia e Recursos Minerais do Estado da Bahia: Sistema de Informações Geográficas - SIG e Mapas. CPRM, Salvador, BA, CD-ROM.

Texeira, L.R., 2008. Projeto Barra-Oliveira dos Brejinhos. Relatório Temático de Litogeoquímica. Programa Recursos Minerais do Brasil, Salvador, BA, 45pp.

Uhlein A., Trompette R.R., Silva M.E., Vauchez A., 2007. A Glaciação Sturtiana (~750 Ma), a estrutura do rifte Macaúbas Santo Onofre e a estratigrafia do Grupo Macaúbas, Faixa Araçuaí. Geonomos, Belo Horizonte 15, 45–60.

Van Achterbergh, E., Ryan, C.G., Jackson, S.E., Griffin, W., 2001. Appendix III. Data reduction software for LAICP-MS. In: Sylvester, P. (Ed.), Laser-ablation-ICP-MS in the Earth sciences, principles and applications. Mineralogical Association of Canada. Short Course Series 29, 239–243.

Victória A.M., Cruz, S.C.P., Pedrosa-Soares, A., Dussin, I., Borges, R., 2015. New Insights on Rifting Events in the São Francisco-Congo Paleocontinent: The Early tonian Plutonic-Volcanic Province of the Southern Bahia and Nortgeastern Minas Gerais,

Brazil. ATECSUD, Primer Simpósio de Tectónica Sudamericana Santiago Santiago – Chile, Anais, p. 141.

Wiedenbeck M., Allé P., Corfu F., Griffin W.L., Meier M., Oberli F., von Quadt A., Roddick J.C., Spiegel W., 1995. Three natural zircon standards for U-Th-Pb, Lu-Hf, trace element and REE analyses Geostandards Newsletter 19/1, 1-23.

CAPÍTULO 2

STATHERIAN AND TONIAN RIFTS FROM THE SOUTHERN SECTOR OF THE PARAMIRIM AULACOGEN, SÃO FRANCISCO-CONGO PALEO-PLATE: NEW DATA, REGIONAL CORRELATIONS

Caroline Novais Bitencourt[1], Simone Cerqueira Pereira Cruz[1], Vanderlucia dos Anjos Cruz[1], Antônio Carlos Pedrosa-Soares[2] Ana Ramalho Alkmim[3]

1 Universidade Federal da Bahia (UFBA), Pós-Graduação em Geologia. Rua Barão de Geremoabo, s/n, Federação, 40170-209, Salvador, Bahia, Brasil; carolcnb@gmail.com (C.N. Bittencourt), simonecruzufba@gmail.com (S.C. P. Cruz); vanderluciaanjos@yahoo.com.br (V. Anjos Cruz)

2 Universidade Federal de Minas Gerais (UFMG), Instituto de Geociências-Centro de Pesquisa Manoel Teixeira da Costa (IGC–CPMTC), Campus Pampulha, 31270-901, Belo Horizonte, Minas Gerais, Brasil, pedrosasoares@gmail.com (A.C. Pedrosa Soares).

3 Universidade Federal de Ouro Preto (UFOP), Departamento de Geologia-Laboratório de Geoquímica Isotópica. Morro do Cruzeiro, Campus, 35400-000, Ouro Preto, Minas Gerais, Brasil; ana_alkmim@yahoo.com.br (A.R. Alkmim).

ABSTRACT

The evolutionary history of the Paramirim Aulacogen is characterized by the superposition of successive rifts that developed from 1,770 to 675 Ma. In the Northern Serra do Espinhaço Fold Thrust Belt.

Two units of this aulacogen were analyzed in the present study: the Algodão Formation (Espinhaço Supergroup) and the Santo Onofre Group (São Francisco Supergroup).

U-Pb geochronological studies (LA-ICPMS) were performed on detrital zircons these units. Ages ranging were 1,958 ± 18 to 2,870 ± 17 Ma and 894 ± 38 to 3,177 ± 42 Ma, respectively. The main primary sources and interpreted sources were related to rocks from the basement of the Western Bahia orogen. They were also related to rocks generated by their structuring, as well as vulcanites and plutonites, both mafic and felsic, with ages between ca. 1.7 and 0.8 Ga, related to the evolution of the precursor basins of the Araçuaí-West Congo Orogen. As secondary sources, results suggest Metavolcanosedimentary sequences and Greenstone Belts of Archean and Paleoproterozoic ages, as well as rocks from the Espinhaço Supergroup and Macaúbas Group. The physical continuity between units of the Santo Onofre and Macaúbas groups, as well as the presence of zircons from the Tonian period in both units, suggest a correlation between units of the first group and pre-glacial units of the latter.

Keywords: Paramirim Aulacogen, Santo Onofre Group, structural framework, geochronology.

1. Introduction

The Paramirim Aulacogen represents an intracontinental rift system that preceded the Araçuaí-West Congo Orogen (Pedrosa-Soares and Alkmim 2011, Cruz and Alkmim 2017). This feature developed between ca. 1,775 ± 7 Ma (Danderfer Filho et al., 2015) and 675 Ma (Santana, 2016) in the western sector of the São Francisco-Congo paleo-plate (Fig. 1). The lithostratigraphic units of this aulacogen outcrop in the Northern Serra do Espinhaço, in the Paramirim Valley and in Chapada Diamantina, north from parallel 15°S (Figs 1, 2). These units were deposited in the eastern and western basins of this aulacogen (Guimarães et al., 2012, Fig. 2), separated by the Paramirim Horst (Cruz et al. 2012). These subsiding areas were filled predominantly with siliciclastic, felsic metavolcanic and metacarbonate rocks, which are subordinated to the Espinhaço and São Francisco supergroups. Over the past years, various proposals have been suggested to explain the stratigraphic stacking of these supergroups, such as Derby (1906), Schobbenhaus and Kaul (1971), Inda and Barbosa (1978), Costa and Silva (1980), Schobbenhaus (1996), Barbosa and Domingues (1996), Danderfer-Filho (2000), Souza et al. (2003), Guimarães et al. (2008), Loureiro et al. (2009), and Guadganim et al. (2015). The oldest unit of this aulacogen is the Algodão Formation (Danderfer-Filho et al., 2015). The stratigraphic position of this unit, which outcrops at the northernmost area of the aulacogen, was defined according to the presence of Statherian acidic metavolcanic rocks studied by these authors. However, the continuity of this unit southwards has remained an unsolved issue for the literature of the region.

In turn, south from parallel 15°S (Figs 1, 2), Tonian and Cryogenian basins, which preceded the Araçuaí-Western Congo Orogen, evolved into a passive margin, followed by the installation of oceanic crust and the development of a magmatic arc (Pedrosa-Soares et al. 2011, and cited references). Thus, the Macaúbas Group is one of the main Tonian and Cryogenian rift-filling units that developed prior to the oceanization of these basins (Kuchenbecker et al., 2015, Alkmim et al. 2017). Stratigraphic data produced by Guimarães (1996) and Guimarães et al. (2012), and the geochronological data presented by Figueiredo et al. (2009) showed temporal correlation between glacial units from the Bebedouro Formation, in the Paramirim Aulacogen, and glacial units from the Macaúbas Group. Temporal correlations among these glacial units and the Santo Onofre Group, another unit of the

Paramirim Aulacogen, and one of the subjects of the present study was proposed by Schobbenhaus (1996), and Danderfer and Dadernne (2002). However, the lack of geochronological data that could prove this correlation has always been a determinant factor in the controversies regarding the stratigraphic positioning of this group.

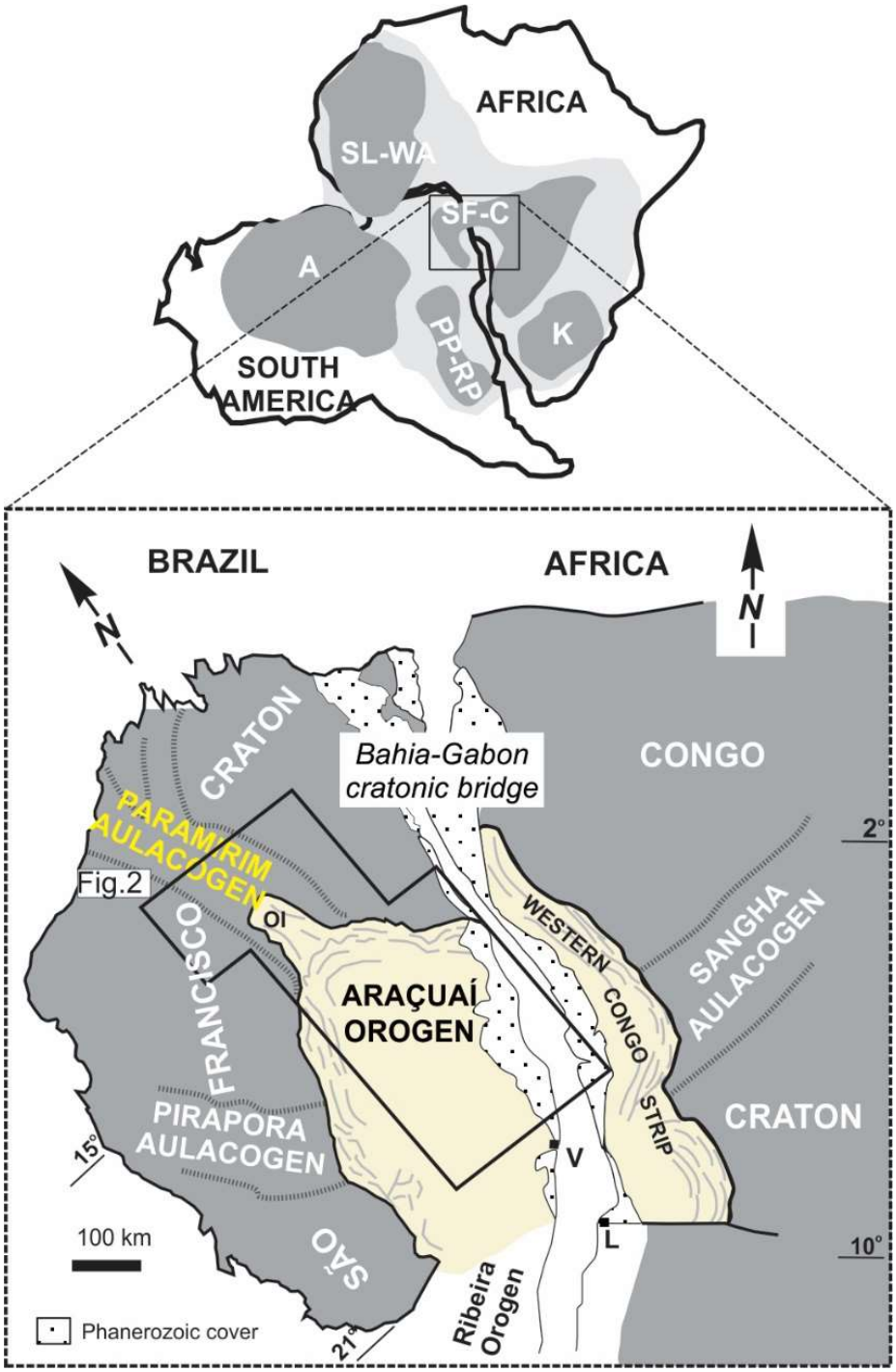

Fig. 1. The Araçuaí-West Congo Orogen and the adjacent São Francisco-Congo craton in the context of West Gondwana (Modificado de Pedrosa Soares et al., 2007). Cratons: A, Amazonian; K, Kalahari; PP-RP, Paranapanema-Rio de la Plata; SF-C, São Francisco-Congo; SL-WA, São Luís-West African.

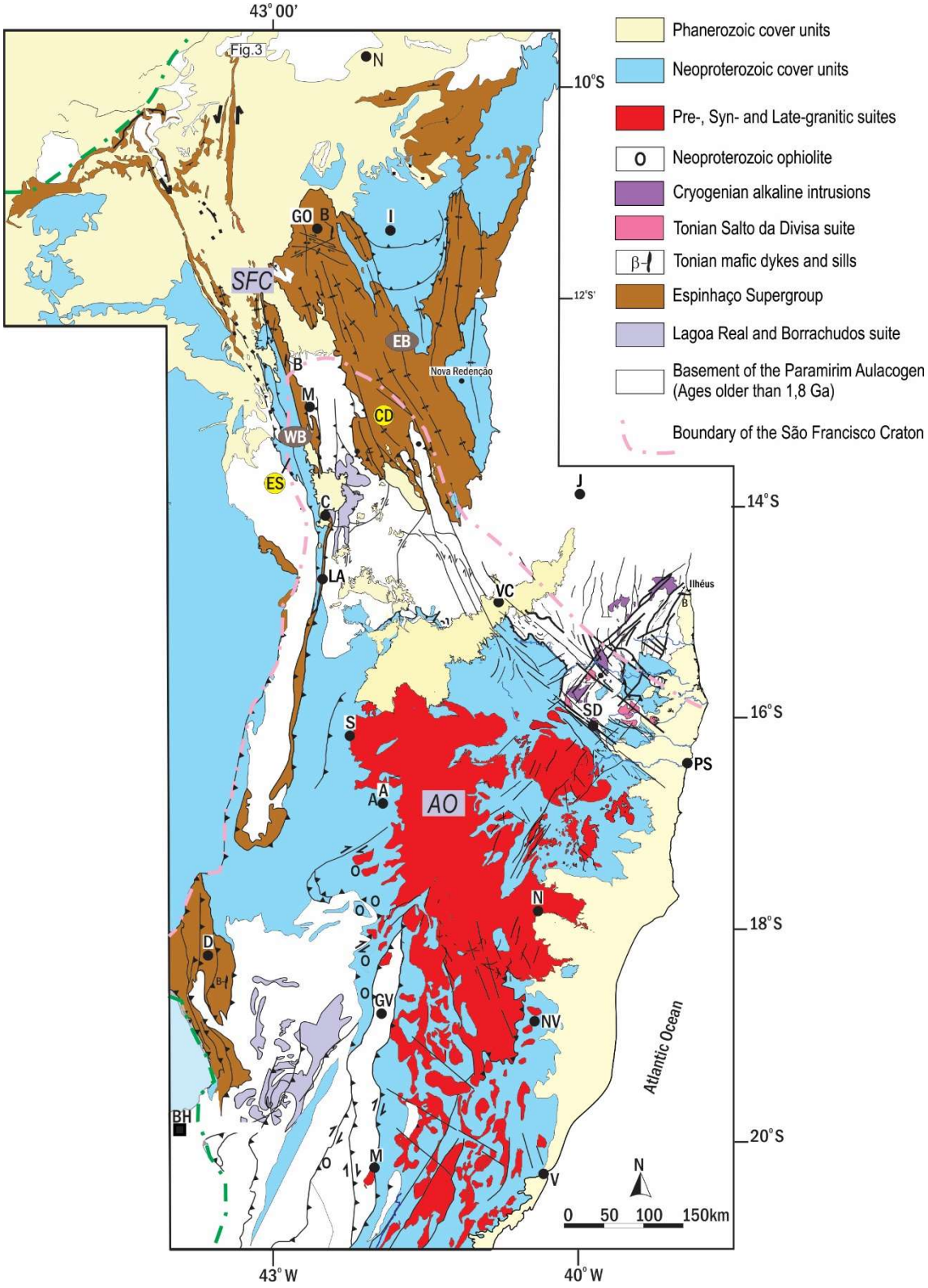

Fig. 2. Simplified geologic map of the Araçuaí Orogen. Modified from Pedrosa-Soares et al. (2007). CD- Chapada Diamantina, NE- Northern Espinhaço. Municipalities (black circles): A- Araçuaí, C- Caetité, D- Diamantina, GO- Gentio do Ouro, I- Irecê, J- Jequié, LA- Licínio de Almeida, M- Macaúbas, MA- Manhuaçu, NA- Nanuque, NR- Nova Remanso, NV- Nova Venécia, PS- Porto Seguro, S- Salinas, SD- Salto da Divisa, V- Vitória da Conquista. Capitals (black squares): BH – Belo Horizonte, V- Vitória. The location of Figure 3 is indicated in this map. Basins of the Paramirim Aulacogen: WB- Western Basin, EB- Eastern Basin.

The Paramirim Aulacogen, as well as the other basins which preceded the Araçuaí-Western Congo Orogen, was partially inverted during the Ediacaran, when the amalgamation of Western Gondwana occurred (Fig. 1). Two thrust and fold belts developed within the sector where the maximum inversion occurred, namely the Northern Serra do Espinhaço and Chapada Diamantina (Danderfer-Filho 1990, 2000; Cruz and Alkmim 2006; Cruz et al., 2012) (Fig. 2).

The objective of the present study was to present new geochronological data obtained from the southern sector of the Northern Serra do Espinhaço Thrust and Fold Belt, within the intracontinental domain of the Araçuaí-Western Congo Orogen, and to proceed with the regional correlations that would contribute to the study of Statherian and Tonian precursor basins from the intracontinental sector of the Araçuaí-Western Congo Orogen, in the area where the Paramirim Aulacogen predominates.

2. Regional Geologic Context

The basement of the Paramirim Aulacogen (Fig. 3) consists of metagranitoids, orthogneisses, often with Archean mafic and ultramafic migmatitic enclaves, greenstone belts, Paleoarchean, Neoarchean and Siderian-Rhyacian metavolcano-sedimentary sequences, and Siderian, Rhyacian and Orosirian acidic intrusive plutonic rocks (Cordani et al., 1985, 1992; Martin et al., 1991; Marinho, 1991; Nutman and Cordani, 1994, Cunha et al., 1996, 2012; Santos-Pinto et al., 1998, 2012; Bastos-Leal et al., 1998, 2000; Rosa et al., 2000; Peucat et al., 2002; Barbosa et al., 2012; Medeiros, 2013; Barbosa et al., 2013; Cruz et al., 2012, 2016).

The alkaline anorogenic magmatism (Machado, 2008) of the Aulacogen is characterized by the metagranitoids of the Lagoa Real Intrusive Suite (Arcanjo et al., 2005). These rocks were crystalized approximately 1,750 Ma ago (Turpin et al., 1988; Cordani et al., 1992; Pimentel et al., 1994; Cruz et al., 2007; Lobato et al., 2015) and were deformed and turned into gneiss in shear zones during the Ediacaran (Cruz and Alkmim, 2006).

Cover units of the Aulacogen encompass rocks from the Espinhaço and São Francisco supergroups. The Espinhaço Supergroup encompasses a succession of siliciclastic rocks (metasandstones, metapelites, and metaconglomerates) with acidic, alkaline, and anorogenic subordinate metavolcanic rocks that outcrop in the Northern Serra do Espinhaço and Chapada Diamantina thrust and fold belts (Fig. 3), measuring 9,300 m and 5,000 m in thickness, respectively (Guimarães et al., 2012).

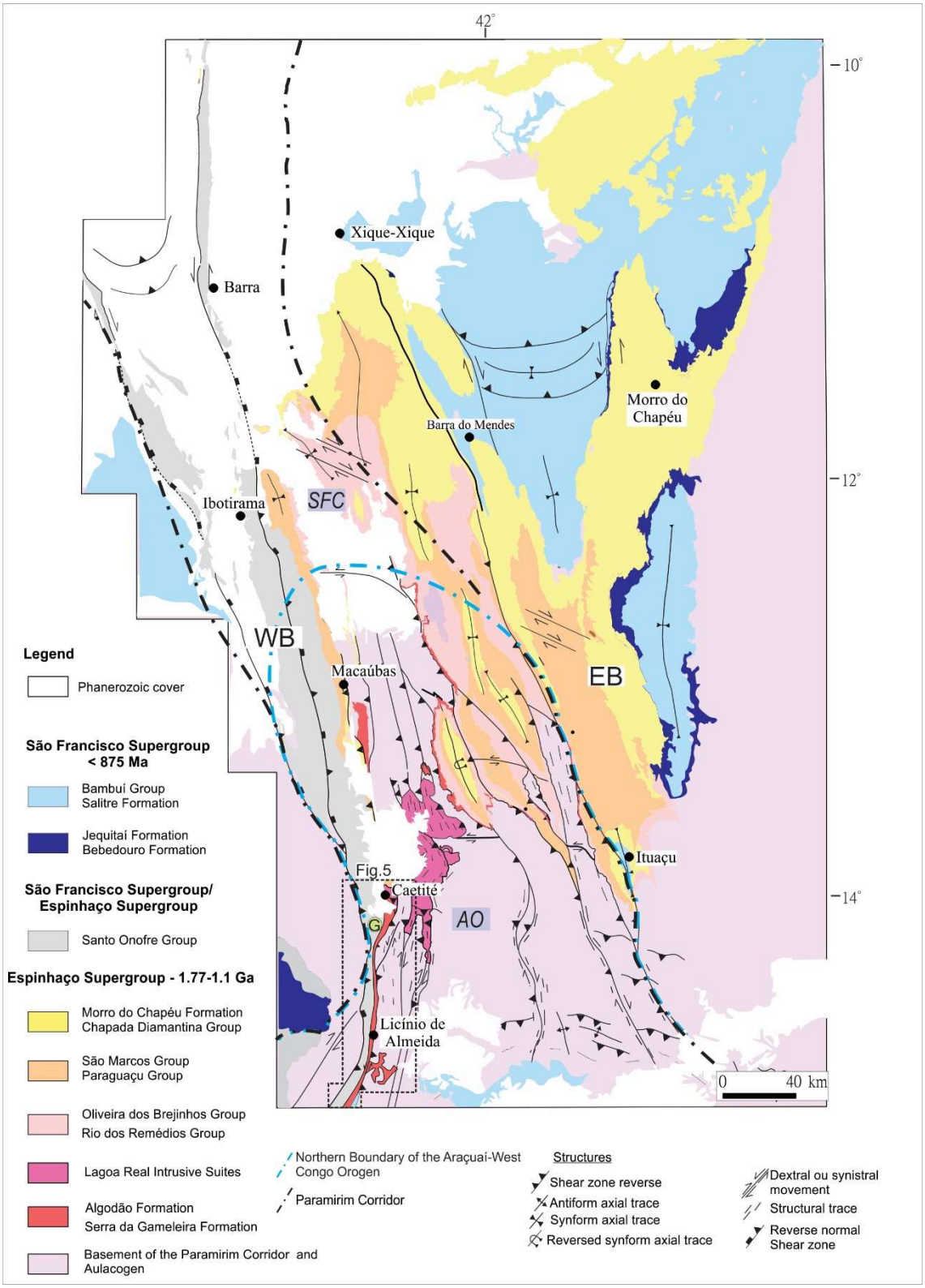

Fig. 3. Simplified geologic map of the Paramirim Aulacogen. Modified from Guimarães et al. (2012). AO – Araçuaí Orogen, SFC – São Francisco Craton. WB- Western Basin, EB – Eastern Basin. Note the location of Figure 5.

Cruz and Alkmim (2017) interpreted six basin-forming events related to the evolution of the Paramirim Aulacogen (Figs. 3, 4), between the Statherian and the Cryogenian, based

on the stacking proposal of Alkmim and Martins-Neto (2012), the ages of acidic metavolcanic rocks obtained by Schobbenhaus et al. (1994), Babinski et al. (1999), Danderfer-Filho et al. (2009, 2015), Guadganim et al. (2015), and Santana (2016), and the ages of mafic dykes obtained by Babinski et al. (1999), Guimarães et al. (2008), Loureiro et al. (2009), and Danderfer-Filho et al. (2009). The Algodão Formation is the oldest of the units (Danderfer-Filho, 2000). It outcrops in the Northern Serra do Espinhaço Thrust and Fold Belt (Fig. 3) and its correlated unit in the Chapada Diamantina Thrust and Fold Belt is the Serra da Gameleira Formation (Guimarães et al., 2008) (Fig. 4). These units are both from the first rift of the Paramirim Aulacogen (Danderfer-Filho et al., 2015).

The São Francisco Supergroup comprises the Santo Onofre Group, one of the investigated subjects of this study, in the Northern Espinhaço Thrust and Fold Belt, as well as the Bebedouro and Salitre formations, in the Chapada Diamantina Thrust and Fold Belt. From the base to the top of this feature, according to Guimarães et al. (2012), the Santo Onofre Group, measuring 2,040 m in thickness, comprises the Fazendinha, Serra da Vereda, Serra da Garapa, and Boqueirão formations, which are separated by very well-exposed gradational contacts located northwards from the municipality of Caetité. In this region, the Santo Onofre Group promotes the structure of two regional synclines. Southwards from Caetité, the contact between the units of this group occurs through transpressional shear zones. In general terms, the Santo Onofre Group consists of feldspathic metasandstones, lithic meta-arkoses, and metaquartz sandstones, either stratified or massive, with oligomictic matrix-supported metaconglomerates (Guimarães et al., 2008). In turn, the Bebedouro Formation consists mainly of massive and stratified clast- and matrix-supported polymictic diamictites, pelites, arkoses, lithic subarkoses, greywackes, and quartz sandstones with subordinated carbonates, which were deposited in a glacial-marine environment (Guimarães, 1996; Guimarães et al., 2012). According to these authors, the Salitre Formation mainly comprises carbonates with calcarenites, dolarenites, and subordinated columnar stromatolites. Recently, Santana (2016) obtained a U-Pb age (zircon, LA-ICP MS) of 669 ± 14 Ma for a felsic metavolcanic rock alternated with carbonates of this formation (Fig. 4).

Dark-grey to greenish diorites and gabbros/diabases (Arcanjo et al., 2005; Brito, 2008; Pereira-Varjão, 2011; Damasceno, 2013) intrude the units of the Espinhaço Supergroup producing sills and dikes (Fig. 4). Dark-grey to greenish diorites and gabbros/diabases predominate (Arcanjo et al., 2005; Brito, 2008; Pereira-Varjão, 2011; Damasceno, 2013). According to these authors, these are tholeiitic rocks from a continental intraplate environment with important crustal contamination. Two crystallization age groups were obtained in zircons

from these mafic rocks: the oldest group, located in the Eastern Basin, indicated ages of 1,514 ± 22 Ma (Babinski et al., 1999, TIMS), 1,496 ± 3.2 Ma and 1,492 ±16 Ma (Guimarães et al., 2008; Loureiro et al., 2009), and 1,507±7 Ma (Silveira et al., 2013). In turn, the youngest group, with representatives in both Western and Eastern basins, was dated as 854 ± 23 Ma (Danderfer-Filho et al., 2009, Shrimp) and 934 ± 14 Ma (Loureiro et al., 2009, LA-ICPMS), respectively.

The inversion of the Paramirim Aulacogen occurred during the Ediacaran with the development of thrust and fold belts, which included the Northern Espinhaço. The dominating structural framework comprises transpressional shear zones and regional folds that were nucleated according to a WSW-ENE tension field (Cruz and Alkmim 2006, Cruz et al. 2012).

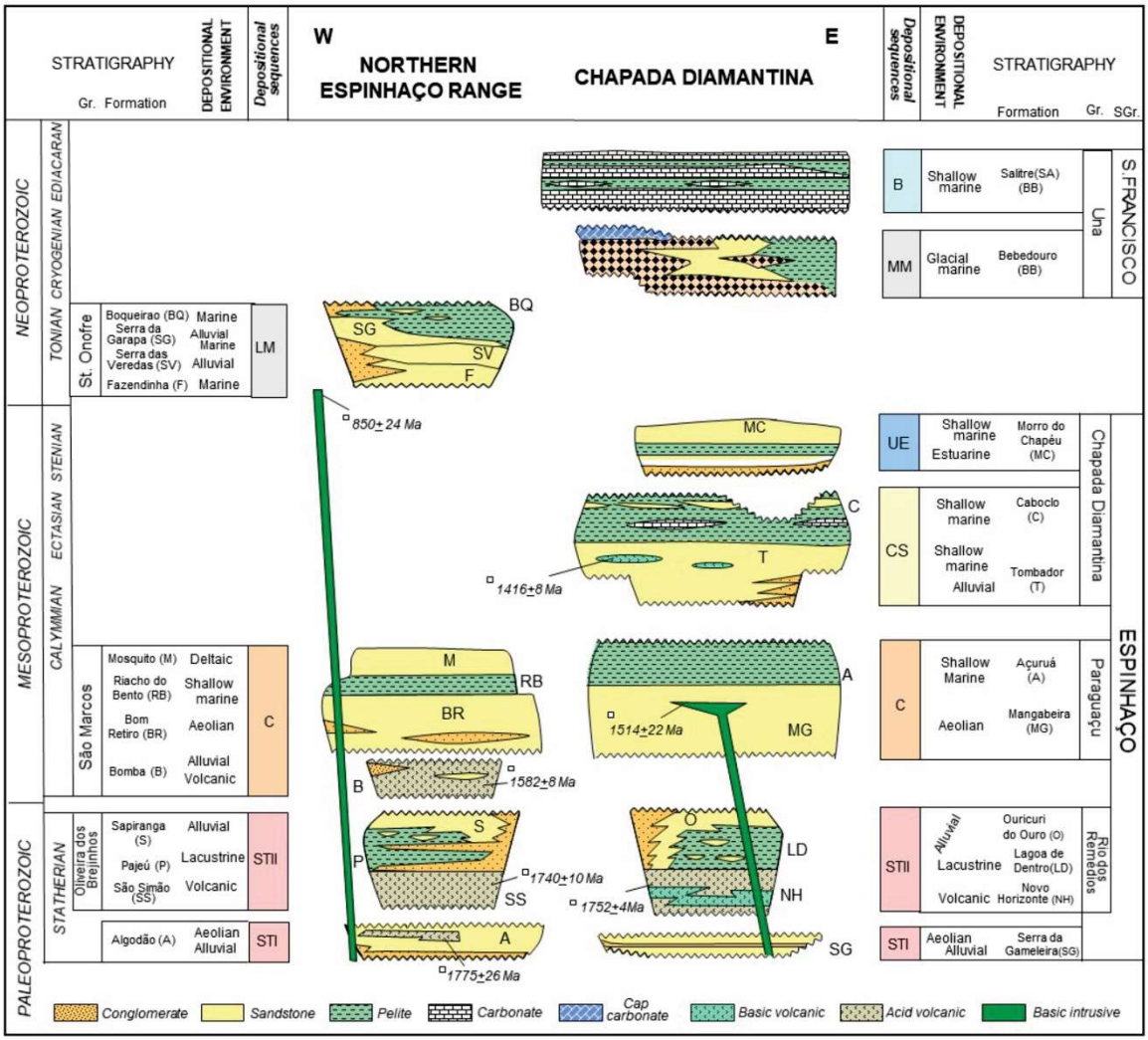

Fig. 4. Stratigraphic chart of the northern Espinhaço and Chapada Diamantina sub-basins of the Paramirim Aulacogen. Depositional sequences: STI Statherian I, STII Statherian II; C Calymmian; CE Calymmian-Stenian; UE Upper Espinhaço; LM Santo Onofre; MM Bebedouro; B Salitre. The numbers denote crystallization or the youngest detrital zircon ages. See text for explanation and references (Cruz and Alkmim 2017, modified from Alkmim and Martins-Neto 2012).

3. Material and Methods

Five samples were selected for geochronological evaluation (U-Pb, LA-ICPMS). Testing was performed on detrital zircons from the Algodão Formation (Samples Salto and CNB 64) and the Santo Onofre Group (Samples MPA, MPC and TR01). Samples were prepared in the Sample Preparation Laboratory of the Geological Survey of Brazil (CPRM, SUREG Salvador). The cathodoluminescence method was used to obtain images of the grains in the Isotope Geochemistry Laboratory of the Department of Geology of the Universidade Federal de Ouro Preto (DEGEO/UFOP) in order to assess the presence of inclusions and overgrowth. The equipment used was a Scanning Electron Microscope JEOL 65. Sample montage was performed using epoxy resin (Specifix) measuring 25 mm in thickness. The U-Pb analyses of samples Salto, CNB 64, MPA, and MPC were performed using a Thermo-Scientific Element 2 Sector Field (SF) ICP-MS coupled to a CETAC LSX-213 G2 + ($\lambda = 213$ nm) Nd:YAG Laser hosted at the Isotope Geochemistry Laboratory of DEGEO/UFOP. The instrumental parameters used in order to perform the analysis in this laboratory are detailed in Appendix A. The data reduction software GLITTER (Van Achterbergh et al., 2001) was used to calculate isotope ratios ($^{207}Pb/^{206}Pb$, $^{208}Pb/^{206}Pb$, $^{208}Pb/^{232}Th$, $^{206}Pb/^{238}U$, and $^{207}Pb/^{235}U$). The value of ^{235}U was calculated from the natural abundance ratio ($^{235}U = {}^{238}U/137.88$). These data were organized in Tables (Appendix B) and diagrams using the software Isoplot (Ludwig, 2012).

U-Pb analyses of sample TR01 were performed in four samples using the LA-ICPMS from Magmas and Volcanoes Laboratory at Clermont-Ferrand, France. Methodology details of the U-Pb analysis are presented in Appendix C.

Maps regarding aerogeophysical analytical signal, total magnetic field, and gamma-spectrometry also assisted in mapping units and interpreting regional structures. Satellite images obtained through the software Google Earth Pro version 7.1.2.2041 were also used in order to draw structural lineaments.

4. Results

4.1. Lithostratigraphic Units

4.1.1. Basement and anorogenic magmatism of the Paramirim Aulacogen

Regarding the basement of the Aulacogen (Figs. 5 and 6), units of the Caetité-Licínio de Almeida metavolcano-sedimentary sequence outcrop (Cunha et al., 2012) in the surroundings of the study area, presenting mostly itabirites, calc-silicate rocks, calcitic an manganese-rich marbles, aluminous schists, and quartzites. The Lagoa Real Intrusive Suite

presents metasyenogranites, meta-alkali-feldspar granite, and mylonitic meta-syenites that have been gneissified in shear zones. These rocks have been less emphasized in the present study. The contact between these units and the Proterozoic metasedimentary rocks analyzed in this study occurred through transpressional shear zones (Fig. 6).

4.1.2. Metasedimentary Units

Considered as that the main focus of the present study, the metasedimentary units analyzed were those of the Algodão Formation and Santo Onofre Group. The Algodão Formation is composed by alternating occurrences of: (i) quartzose to feldspathic metasandstones (Figs. 7A, B), mainly, and subordinated sericitic metasandstones, with medium to large parallel and cross-bedding stratifications (Fig. 7C); (ii) oligomictic metaconglomerates, with, predominantly, sub-rounded clasts of granitoids, metasandstones, quartz, and quartzites, which presented a medium degree of sorting, and, mainly, a sandy quartzose matrix (Fig. 7D); (iii) subordinated laminated metapelites, metarhythmites and metasiltites (Fig. 7E). Levels of quartzites were also observed. Veins of amethysts truncate the rocks of this formation and are economically explored. Cruz et al. (in preparation) found felsic metavolcanic rocks of ca. 1.77 Ga alternating with the metaconglomerates of this formation. These metavolcanic rocks are porphyritic metarhyolites with corrosion microstructures and an aphanitic to very fine phaneritic matrix. Rocks are predominantly composed of quartz, K-feldspar, and sericite. In the field, these volcanites presented preferential magmatic flow orientation.

In the Santo Onofre Group, the Serra da Garapa Formation was subdivided into two lithofacies associations (Figs. 5, 6). The first is composed predominantly by quartzites and hematite-rich (Fig. 8A), graphite-rich (Fig. 8B) and/or manganese-rich metapelites and phyllites, which are sometimes sericitic. Alternating occurrences of quartzose metasandstones and metasubarkoses (Fig. 8C) are less frequent. Parallel bedding is the predominant type of stratification in this first association. The second lithofacies association (Fig. 5) is predominantly composed by staurolite-garnet-quartz-biotite aluminous schist (Figs. 8D, 9A, B) with interleaved quartzites (Fig. 8E). Preserved sedimentary structures were not observed in this association.

Metasubarkoses predominate in the Boqueirão Formation (10A-C, 9C) with intraclasts of graphite-rich phyllites (Fig. 10D), and lithic metasandstones and metasiltites. Metasubarkoses and lithic metasandstones are gray and present fine to medium-sized grains.

Levels of oligomictic metamicroconglomerates, finely laminated rhythmites alternating with fine-grained feldspar metasandstones and metapelites occur subordinately (Fig. 10E). Parallel bedding also predominates in these rocks.

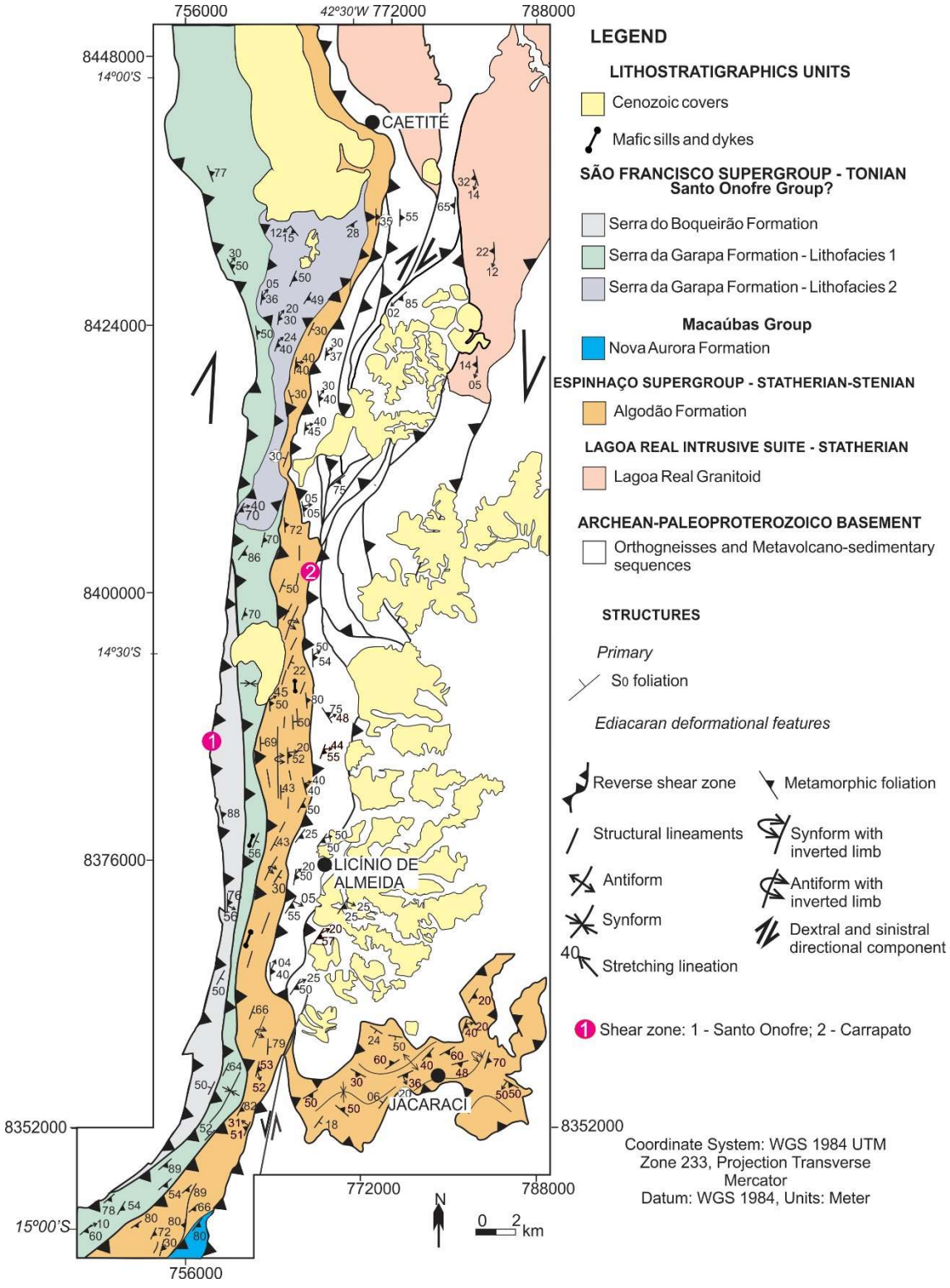

Fig. 5. Geologic map of the study area. Note the location of geological sections of Figure 6, dated samples and location of Figure 15.

The Nova Aurora Formation (Fig. 5) of the Macaúbas Group comprises quartzites of various grain sizes, which are generally micaceous and eventually ferruginous, and also metadiamictites (Fig. 10F). These rocks present a fine to coarse grained sandy matrix that varies from quartzose to micaceous and is locally richer in hematite. The grains of the framework consist of sub-rounded clasts, with sizes ranging between 2 and 4 mm. They are predominantly composed of fragments of hyaline quartz, quartzite, granites, and orthogneisses. Grains presenting bullet-shape geometry are found in these diamictites.

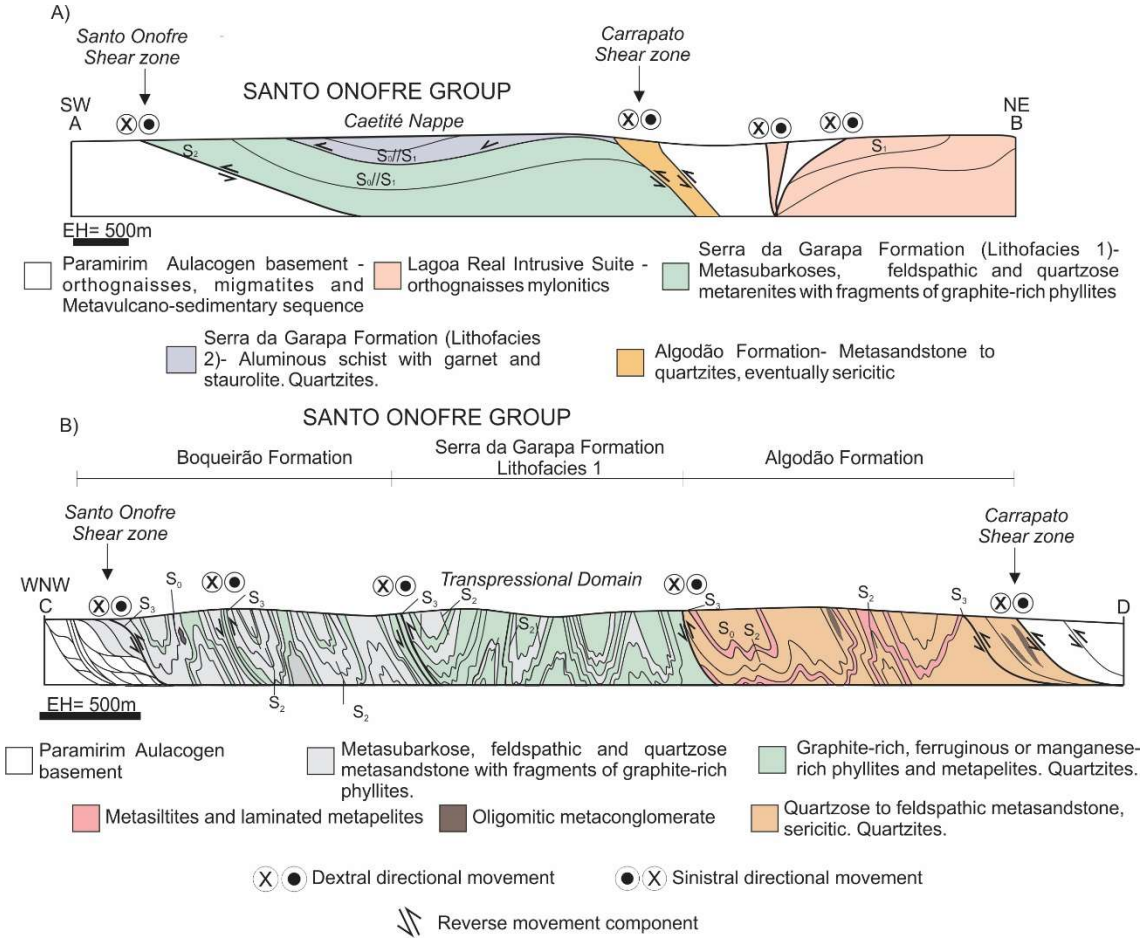

Fig. 6. Geologic sections of the study area. The location of the sections is indicated in Figure 5.

Primary sedimentary bedding predominates among the transpressional shear zones that structure the contacts between the mapped units (Figs. 5 and 6). However, the development of medium to high-dip angle foliation (higher than 60°) and high-rake stretching lineation can be observed in the surrounding areas of these regional deformed structures. Granoblastic microstructures occur in these locations and are often core-mantle and mylonitic, associated with quartz, fragmentation of feldspars, and preferential orientation of phyllosilicates, such as

biotite and muscovite (lepidoblastic microstructure), and quartz (nematoblastic microstructure). The rocks from lithofacies association 2 of the Serra da Garapa Formation are an exception and present continuous foliation, generally at a low angle (Figs. 6, 8E).

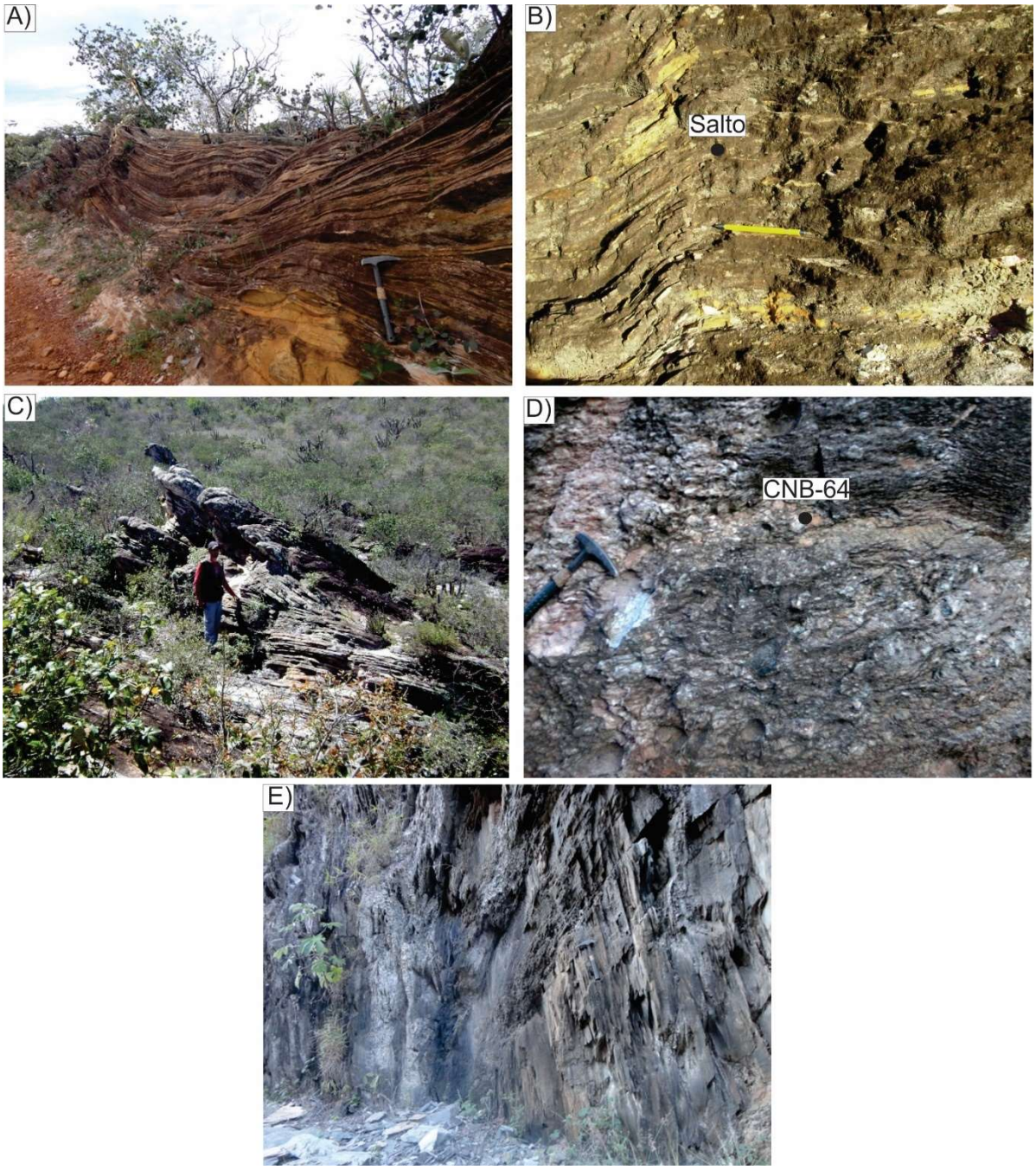

Fig. 7. General aspect of the units mapped with the indication of dated samples. A) The general aspect of metasandstone outcrops of the Algodão Formation (23L, 765026/8385888); B) Quartzose and sericitic metasandstone of the Algodão Formation (Sample Salto, 23L, 769059/8444083); C) Metasandstones of the Algodão Formation with large cross-beddings (23L, 763485/ 8377511); D) Overview of the dated metaconglomerate of the Algodão Formation (Sample CNB-64, 23L, 761416/8368232); E) Laminated metapelite of the Algodão Formation (23L, 760510/8368652). All photos with section view.

Fig. 8. Overall aspect of the Onofre units mapped with the indication of dated samples. A) Hematite-rich phyllites from lithofacies 1 of the Serra da Garapa Formation (23L, 759507/8368497); B) Graphite-rich phyllites from lithofacies 1 of the Serra da Garapa Formation (23L, 763660/8426643); C) Quartzose metasandstones from lithofacies 1 of the Serra da Garapa Formation (23L, 760032/8369353); D) Staurolite-garnet-quartz-biotite aluminous schist from lithofacies 2 of the Serra da Garapa Formation (Santo Onofre Group) (Sample MPA, 23L, 767211/8432119); E) Quartzites from lithofacies 2 of the Serra da Garapa Formation (Sample MPC, 23L, 766621/8432139).

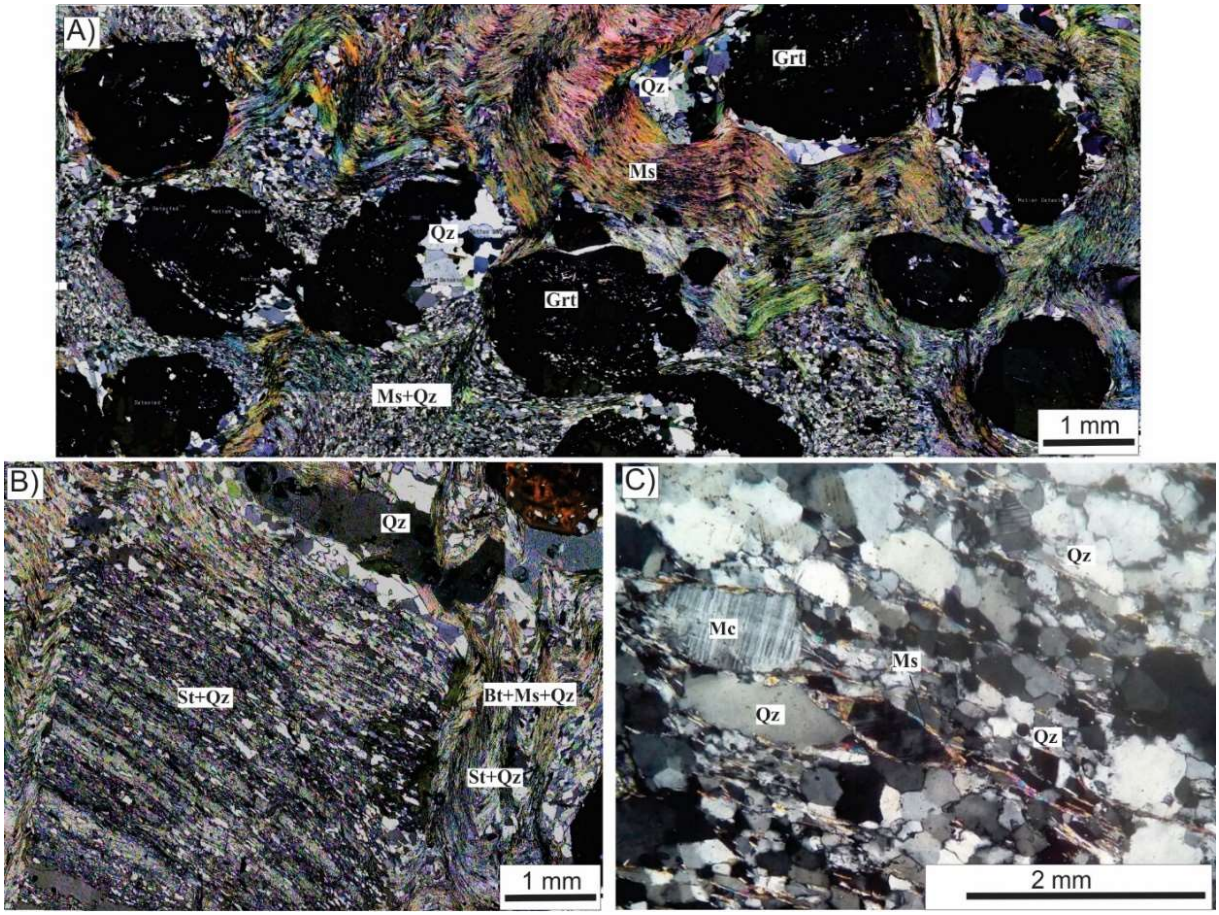

Fig. 9. A, B) Photomicrographs of staurolite-garnet-quartz-biotite aluminous schist (Lithofacies 2) of the Serra da Garapa Formation (Santo Onofre Group) (Sample MPA, 23L, 767211/8432119); (C) Photomicrograph of a metasubarkose from the Boqueirão Formation (Sample TR01, 23L, 758749/8370741). Both samples were dated in the present study. Abbreviations in accordance with Whitney and Evans (2010). Bt – biotite, Gr – garnet, Mc – microcline, Ms – muscovite, Qz – quartz, St – staurolite.

4.2. Geochronology

Five samples of metasedimentary rocks were selected for these analyses: two from the Serra da Garapa Formation (Samples MPA and MPC), one from the Boqueirão Formation (Sample TR-01), both of which belong to the Santo Onofre Group; and two from the Algodão Formation (Samples SALTO and CNB-64) (Fig. 11), of the Espinhaço Supergroup. Data analyzed is available in appendices B and C. A synthesis of the data obtained is presented in Table 1.

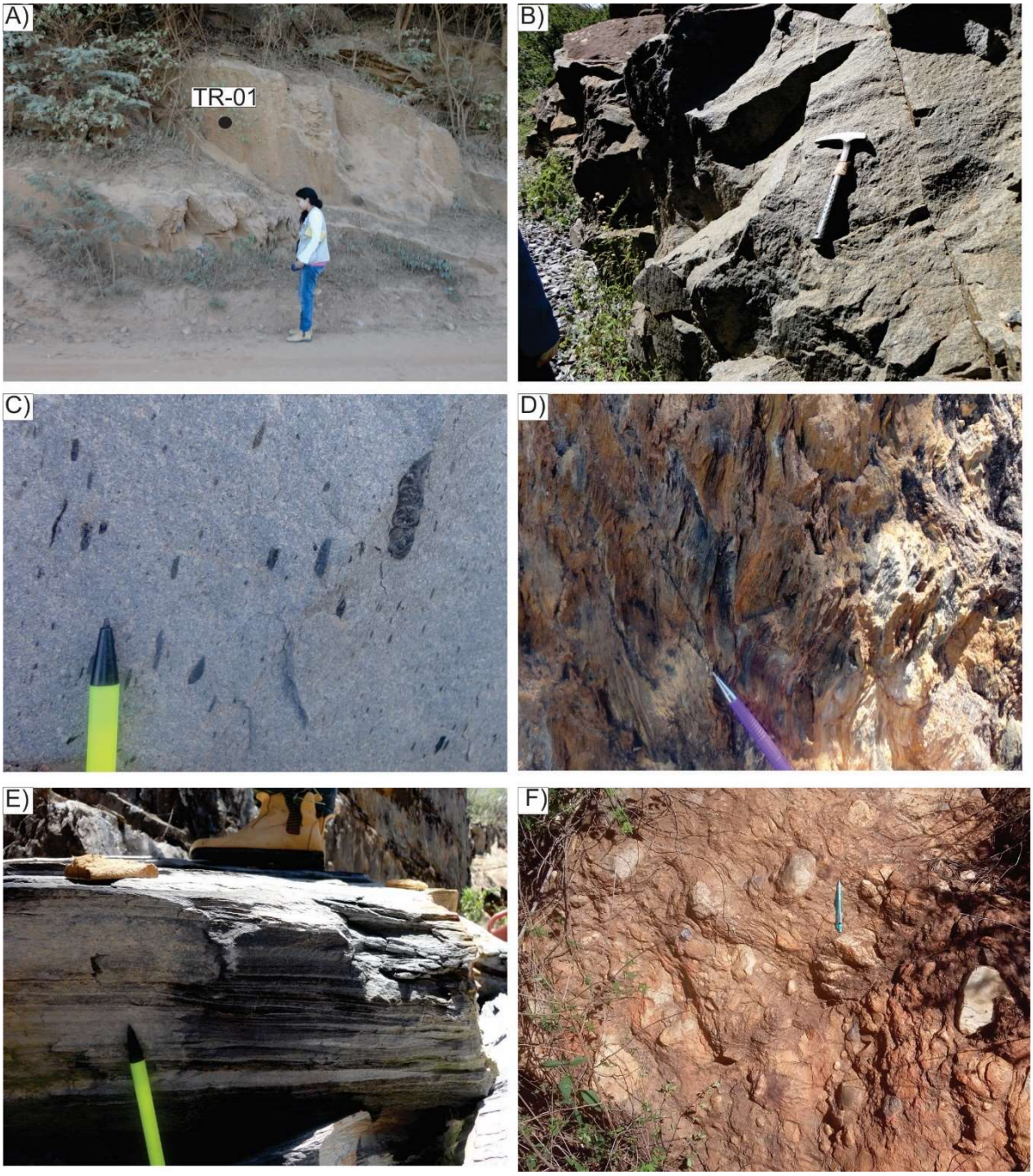

Fig. 10. General aspects of units mapped with indication of dated samples. A) overall view of the outcrop of the Boqueirão Formation (Santo Onofre Group) (Sample TR01, 23L, 758749/8370741); B) feldspathic metasandstone of the Boqueirão Formation (23L, 758665/8370897); C) fragments of graphite-rich phyllite in a metasubarkose of the Boqueirão Formation (23L, 759125/8370167); D) overall aspect of graphite-rich phyllite alternated with metasandstones and metasubarkoses of the Boqueirão Formation (23L, 758854/8370575); E) parallel lamination between metarhythmites (23L, 759125/8370167); F) metadiamictite of the Nova Aurora Formation (Macaúbas Group) (23L, 756819/8344154).

Table 1

Summary of LA-ICPMS U-Pb zircon results. Uncertainties are given at the 1 σ level.

Sample	Coordinate	Formation	Rock	Number of grains analyzed	Number of grains with concordance between 98 and 101%	Age variation (Ma)	Main range (Ma)	Younger grains (Ma)
Espinhaço Supergroup								
SCP Salto	23L, 769059/8444083	Algodão	Metaquartzarenite	40	12	2085 a 2660	1800-2200 (83%)	2085 ± 19
CNB 64	23L, 761416 / 8368232	Algodão	Metaconglomerate	113	27	1958 a 2870	2500-2800 (52%)	1958 ± 18
São Francisco Supergroup – Santo Onofre Group								
MPA	23L, 767211/8432119	Serra da Garapa	Aluminous shale	70	27	938 a 2662	1800-2200 (48%)	938 ± 22
MPC	23L, 766621/8432139	Serra da Garapa	Quartzite	64	50	894 a 2585	1800-2200 (32%)	894 ± 38
TR 01	23L, 758749/8370741	Boqueirão	Metasubarcoseo	91	91	899 a 3177	1800-2200 (75%)	899 ± 79

4.2.1. Algodão Formation

Meta-quartz sandstone of the Algodão Formation (Sample SCP Salto)

The outcrop (Fig. 7B) is located by the highway BA-030, close to the municipality of Caetité (UTM 23L, 769059/8444083) (Fig. 5). Quartz, with subordinated muscovite and chlorite, predominated in the rock sample analyzed. Foliation is mylonitic and presents a maximum dip angle of 30° towards NE. Outcropping chevron folds are observed. The presence of chlorite suggests metamorphism of greenschist facies.

Zircons (Fig. 11A) were brown, transparent, subhedral to anhedral, and some presented inclusions. They were generally rounded, with prismatic habit and sizes ranging between 50 and 200 μm. Grains presented oscillatory zoning and some presented inherited cores. Most of the grains analyzed presented well-defined overgrowth edges. Under cathodoluminescence (CL), lighter-shaded cores are observable, probably presenting low-U. From the 40 grains analyzed, 12 presented U-Pb ages ($^{206}Pb/^{207}Pb$) with agreement between 98% and 101%. Ages ranged between 2,085 Ma and 2,660 Ma (Fig. 12A). Considering all zircon grains analyzed, 83% presented ages between 2,000 and 2,200 Ma, and 7% between 2,500 and 2,800 Ma. The probability of relative density of detrital zircon distribution

presented a main peak at the age of 2,160 Ma, and other less expressive peaks at the ages of 2,290 Ma and 2,650 Ma. The youngest age found was 2,085 ± 19.24 Ma.

Metaconglomerate of the Algodão Formation (Sample CNB-64)

The sample was collected from a cut in the railway (Fig. 7D), southwards from the municipality of Licínio de Almeida (Fig. 5) and eastwards from the Northern Espinhaço Thrust and Fold Belt (UTM 23L, 761416/8368232). These rocks are oligomictic metaconglomerates, with alternating occurrences of metarhythmites (metasiltites, meta-argillites, and metasandstones). The framework is predominantly formed by pebbles composed of quartzites and, subordinately, gneisses. Round and sub-round pebbles predominate. The matrix of this sample was predominantly clayey. The material used for analysis encompassed both pebbles and matrix.

Zircons (Fig. 11B) were transparent, subhedral to anhedral, round to sub-round, prismatic, some were bipyramidal, and sizes ranged between 50 and 300 μm. Some crystals presented micrometric inclusions. Under cathodoluminescence (CL), zircons presented oscillatory zoning. The majority of grains presented a darker overgrowth edge defined by CL. From the total of 113 zircons analyzed, 27 grains presented agreement between 98% and 101% regarding ages ranging between 1,958 Ma and 2,870 Ma (Fig. 12B). Data were grouped into intervals of 1,800 – 2,200 Ma (40%), 2,200 – 2,500 Ma (4%), 2,500 – 2,800 Ma (52%), and 2,800 – 3,200 Ma (4%). The probability of relative density distribution of detrital zircons presented two main peaks, at the ages of 2,500 Ma and 2,600 Ma, and another less expressive peak at approximately 2,200 Ma. The youngest age found was 1,958 ± 18 Ma.

4.2.2. Santo Onofre Group

Staurolite-biotite-quartz-muscovite-garnet aluminous schist of the Serra da Garapa Formation (Santo Onofre Group) (Sample MPA)

The outcrop (Fig. 8D) is located in the northern portion of the study area, at the banks of the Moita dos Porcos stream (UTM 23L, 767211/8432119), southwards from the municipality of Caetité (Fig. 5). The rock presents garnet and staurolite porphyroblasts immersed in a fine to medium-grained matrix composed of quartz, muscovite, biotite, hematite and graphite. Schistosity is parallel in relation to the compositional gneissic banding that hosts lineation stretching and intrafolial isoclinal folds. The dip angle of the foliation

ranges between 0° and 21°. Studies conducted by Bitencourt (2014) suggest that these rocks were metamorphosed in the medium amphibolite facies.

Zircons analyzed (Fig. 11C) were brown to transparent, subhedral to anhedral, rounded, with prismatic habit, and some of them were bipyramidal. Grain size varied between 50 and 150 μm, and some grains presented inclusions. Under cathodoluminescence (CL) they presented oscillatory zoning and the majority of grains presented a darker overgrowth edge. Lighter-shaded zircon grain cores, under CL, probably presented low U. A total of 70 zircons were analyzed, from which 27 grains presented agreement between 98% and 101%. The most concordant U-Pb ages ($^{206}Pb/^{207}Pb$) ranged between 938 Ma and 2,662 Ma (Fig. 12C), and were grouped into intervals of 850 – 1,000 Ma (4%), 1,600 – 1,800 Ma (4%), 1,800 – 2,200 Ma (48%), 2,200 – 2,500 Ma (26%), and 2,500 – 2,800 Ma (18%). The probability of relative density of detrital zircon distribution presented a mean peak at the age of 2,110 Ma, and other less expressive peaks at ages of 1,750 Ma, 1,940 Ma, 2,010 Ma, 2,310 Ma, 2,380 Ma, 2,460 Ma, 2,540 Ma, 2,620 Ma, and 2,650 Ma. The youngest zircon age found was 938 ± 22 Ma.

Quartzite from Serra da Garapa Formation (Santo Onofre Group) (Sample MPC)

The sample (Fig. 8E) was collected in the Moita dos Porcos dam (UTM 23L, 766621/8432139), southwards from the municipality of Caetité (Fig. 5). The rock presents schistosity with a dip angle lower than 30° and occurs alternating with aluminous schists similar to those observed in sample MPA.

Zircons were brown to transparent, ranging between subhedral and anhedral, with prismatic habit and sizes ranging between 50 and 250 μm (Fig. 11D). Some zircons presented oscillatory zoning, but, in general, grains did not present internal structures. A total of 62 zircons were analyzed, from which 50 grains presented agreement between 98% and 101%. The obtained U-Pb ages ($^{206}Pb/^{207}Pb$) ranged between 894 Ma and 2,585 Ma (Fig. 12D). They were grouped into intervals of 850 – 1,000 (4%), 1,000 – 1,200 (12%), 1,200 – 1,400 (20%), 1,400 – 1,600 (4%), 1,600 – 1,800 (24%), 1,800 – 2,200 (32%), and 2,500 – 2,800 (4%). The probability of the relative density distribution of detrital zircons presented a main peak 1,810 Ma ago, and other less expressive peaks at ages of 1,020 Ma, 1,260 Ma, 1,400 Ma, 1,540 Ma, 1,620 Ma, 1,690 Ma, 1,970 Ma, 2,080 Ma, 2,160 Ma, and 2,580 Ma (Fig. 12D). The youngest zircon was dated as 894 ± 38 Ma.

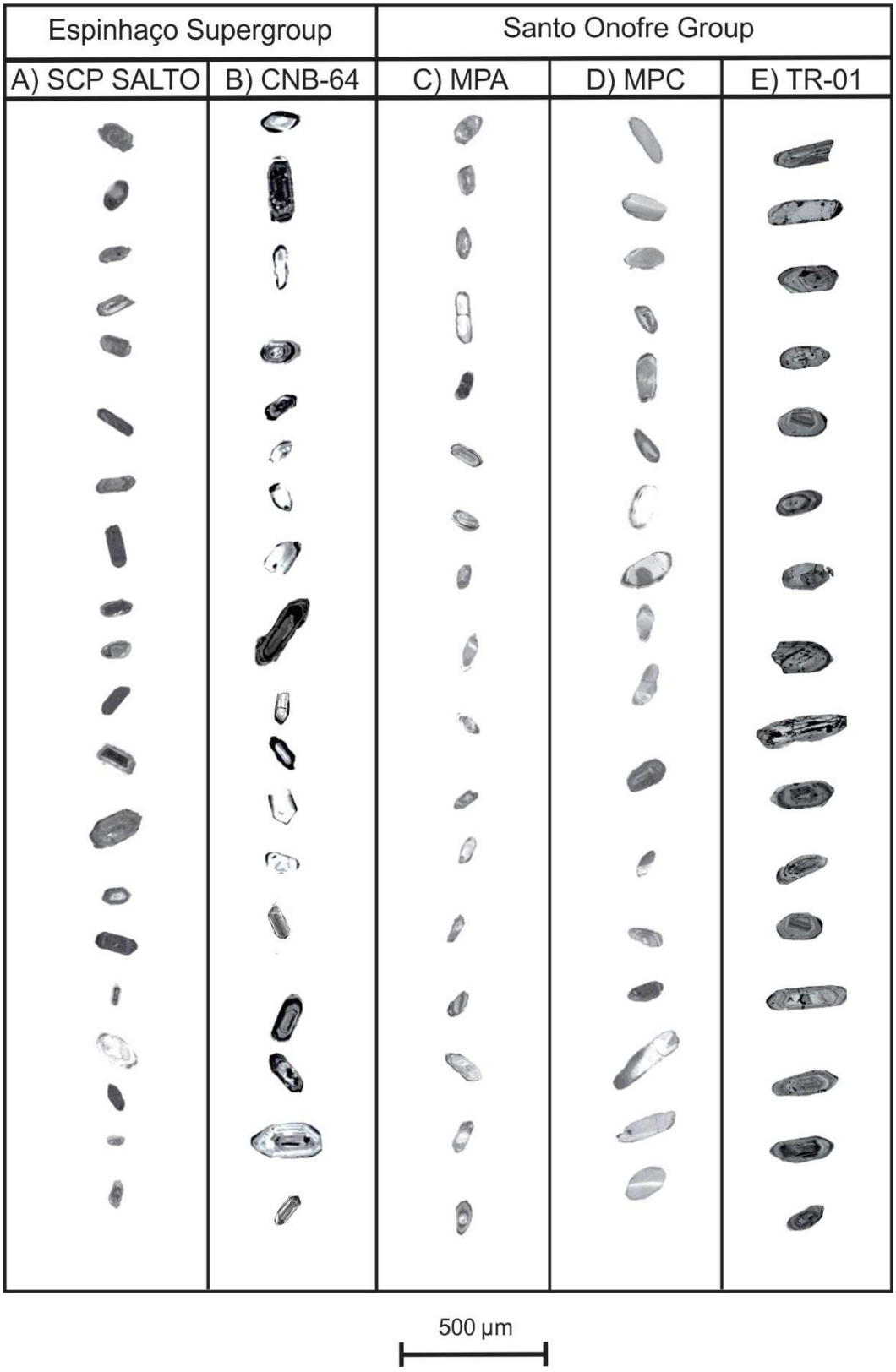

Fig. 11. Cathodoluminescence images of representative detrital zircon crystals from the analyzed samples of the Santo Formation (Espinhaço Supergroup) and Serra da Gapara and Boqueirão formations (Santo Onofre Group).

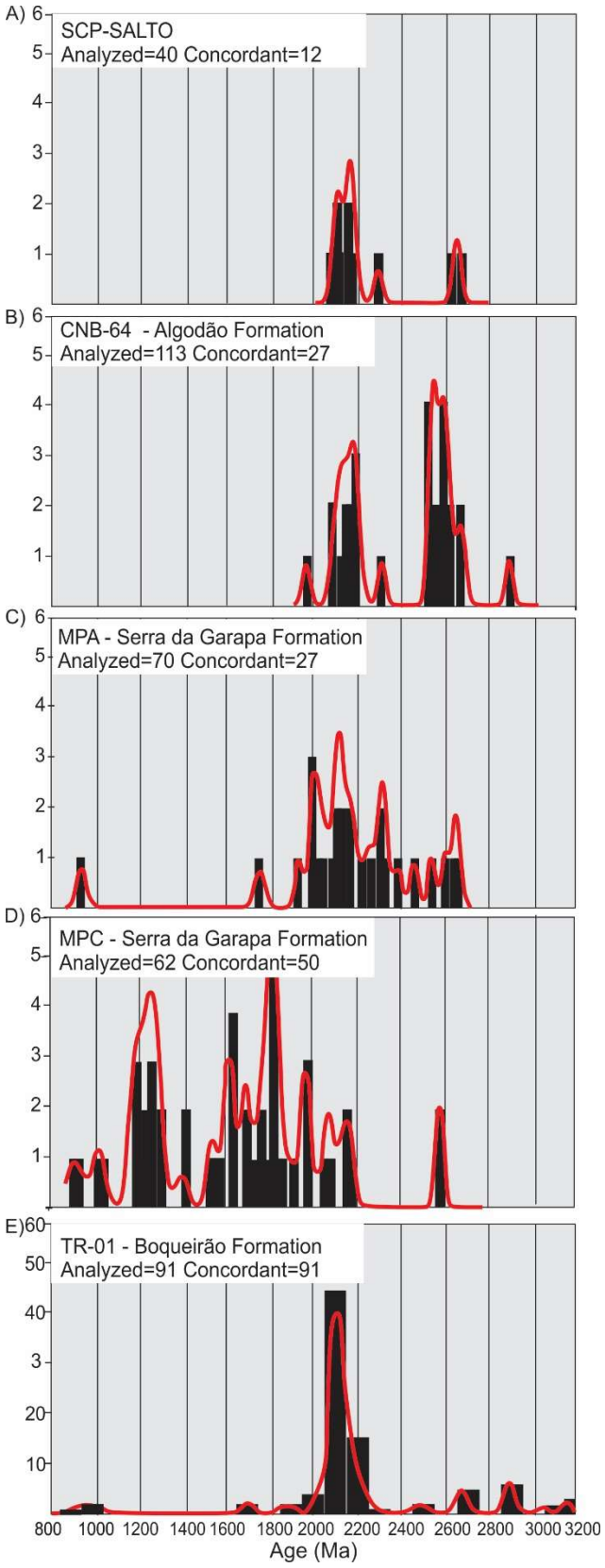

Fig. 12. Frequency histogram and probability curves of U-Pb ages (detritical zircons) for the analyzed samples of the Santo Formation (Espinhaço Supergroup) and Serra da Gapara and Boqueirão formations (Santo Onofre Group) with oncordance ($^{206}Pb/^{207}Pb$) between 98 e 101%**:** A) Sample SCP-Salto, B) Sample CNB-64: Algodão Formation (Espinhaço Supergroup); C) Sample MPA, D) Sample MPC: Serra da Garapa Formation (Santo Onofre Group) E) Sample TR-01: Boqueirão Formation (Santo Onofre Group).

Metasubarkose of the Boqueirão Formation (Santo Onofre Group) (Sample TR-01)

This sample was collected from an unpaved road cut (Fig. 10A, UTM 23L, 758749/8370741) located southwards from the municipality of Licínio de Almeida (Fig. 5) on the western edge of the Northern Espinhaço Thrust and Fold Belt. This rock presents alternating occurrences of graphite-rich phyllites and, eventually, fragments of these phyllites. The sample was predominantly composed of quartz, but also contained K-feldspar, biotite, and muscovite in lower quantities. Moreover, the rock presents mylonitic foliation related to high-dip-angle shear zones and its association with phyllites suggests metamorphism in the greenschist facies.

Zircons presented colors ranging from colorless to dark pink. Crystals were translucent and subhedral (Fig. 11E). Most of the grains were rounded, prismatic, and bipyramidal, with sizes ranging from 100 to 250 μm. Inclusions were rare. All crystallographic phases suffered strong abrasion. A total of 91 zircons were analyzed and concordance ages between 98% and 101% ranged from 899 Ma to 3,177 Ma (Fig. 12E). These ages were grouped into intervals of 850 – 1,000 Ma (3%), 1,600 – 1,800 Ma (2%), 1,800 – 2,200 Ma (75%), 2,200 – 2,500 Ma (3%), 2,500 – 2,800 Ma (6%), and 2,800 – 3,200 Ma (11%). The main peak occurred at the age of 2,070 Ma. All other intervals revealed statistically lower contributions for ages of 1,700 Ma, 1,900 Ma, 2,400 Ma, 2,600 Ma, 2,800-2,900 Ma, 3,000 Ma, and 3,100 Ma. The youngest zircon grain dated presented an age of 899 Ma ± 79.

5. Discussion

5.1. Provenance

5.1.1. Algodão Formation

Summarizing the U-Pb ($^{206}Pb/^{207}Pb$) data obtained for the Algodão Formation in samples SCP Salto and CNB 64, the ages obtained ranged between 1,958 ± 18 Ma and 2,870 ± 17 Ma, divided into the following intervals (Fig. 13A): 1,800 – 2,200 (51%), 2,200 – 2,500 (5%), 2,500 – 2,800 (41%), and 2,800 – 3,200 (3%).

The higher amount of data obtained for the Algodão Formation is related to the interval between 1,800 and 2,200 Ma (Fig. 13A). Adding this set of data to the interval of 2,200 – 2,500 Ma, this represents 56% of the overall obtained data. This result is not surprising and is consistent with the period of higher magmatic and metamorphic activity in the São Francisco

Craton and in the basement of the Araçuaí-West Congo Orogen, represented by the Western Bahia Arc and Orogen (Cruz et al., 2016) and its correlated units in the Mantiqueira and Juiz de Fora complexes (Heilbron and Machado 2003; Noce et al., 2005, 2007), and with the rocks of the Itabuna-Salvador-Curaçá Orogen (Barbosa et al., 2012)

In the Western Bahia Orogen (Cruz et al., 2016), which represents an important area of the basement of the Paramirim Aulacogen, the development of Siderian-Rhyacian-Orosirian magmatism is related to the installation of an arc between 2.38 – 2.1 Ga and collision between 2.1 – 2.09 Ga. The collision produced crustal thickening and fusions of the Archean crust (Santos-Pinto et al., 2012, Cruz et al., 2016), with records of crustal fusions as young as 1,943± 5 Ma (Barbosa et al., 2013). The plutonic bodies produced in this event were intrusive in Greenstone Belts and in Archean gneissic-migmatitic terrains (Bastos-Leal et al., 2003; Arcanjo et al., 2005; Guimarães et al., 2008; Santos-Pinto et al., 2012; Medeiros, 2013; Campos, 2013; Martins 2014; Cruz et al., 2016). The large amount of these plutons in the basement of the Paramirim Aulacogen could be an indication that they may have strongly contributed to the sedimentary input of the Espinhaço Supergroup and, consequently, to the Algodão Formation. Siderian (Barbosa et al., 2013) and Rhyacian (Medeiros, 2013) metamorphic sources may also have contributed by providing zircons to this basin. Rhyacian (2,140 ± 14 Ma, zircon, SHRIMP) and Orosirian (2,039 ± 8 Ma) ages were obtained in Córrego Tingui monzogranitic orthogneisses and in Serra Branca foliated syenites, respectively, by Silva et al. (2016).

The peak between 2,500 and 2,800 Ma found in Figure 13A reflects the influence of the preserved Archean cores in the basement of the Paramirim Aulacogen. This is a group of orthogneisses that comprises the southern portion of the Gavião Paleoplate with U-Pb age ranging mainly between 2,500 and 2,600 Ga, represented by the Caraguataí (2,696 ± 5 Ma, Cruz et al., 2012) and Serra do Eixo massifs (2,524±14 to 2,656±10, Bastos-Leal et al., 2003). In the Santa Isabel Complex, Medeiros (2013) found the age 2,587 ± 10 Ma for a rock whose protolith was correlated to protoliths from the Caraguataí Suite (Cruz et al., 2012). Neoarchean ages (2,657 ± 25) were obtained for orthogneisses of the Barrocão/Rio Itacambiruçu Complex by Silva et al. (2016).

The subordinated peak between 2,800 and 3,200 (Fig. 13A) is probably correlated to rocks from the Santa Isabel and Porteirinha complexes, which are basement units of the Paramirim Aulacogen located in the western and southwestern regions of the Northern Espinhaço Thrust and Fold Belt, respectively. In the Santa Isabel Complex, Medeiros (2013) obtained U-Pb age of 3,136 ± 8 Ma (zircon, LA-ICPMS) in a metatexite migmatite paleosome,

and 3,097 ± 24 Ma in diatexite migmatites. In turn, Barbosa et al. (2013) obtained U-Pb age of 2,954 ± 100 Ma (zircon, LA-ICPMS) in granulite migmatites. In the Porteirinha Complex, Silva et al. (2016) obtained ages of 3,145 ± 24 Ma (zircon, SHRIMP), which was interpreted as related to the metamorphism of orthogneisses in this complex. Other Mesoarchean ages were obtained in the basement of the Paramirim Aulacogen, such as in the orthogneisses from Mariana (3,021 ± 4 Ma, Bastos-Leal et al., 2003), Serra do Eixo (2,970 ± 46 Ma to 3,158±10, Bastos-Leal et al., 2003), and Guajeru (3,191 ± 35, Lopes, 2002). Some of the potential primary and secondary sources that can be related to the age intervals obtained for detrital zircons of the Algodão Formation are presented in Table 2 and Figure 14.

5.1.2. Santo Onofre Group

For the Santo Onofre Group (Fig. 13B), ages ranged between 894 and 3,177 Ma, and eight intervals were recorded: 800 – 1,000 (4%), 1,000 – 1,200 (3%), 1,200 – 1,400 (6%), 1,400 – 1,600 (1%), 1,600 – 1,800 (8%), 1,800 – 2,200 (59%), 2,200 – 2,500 (6%), 2,500 – 2,800 (7%), and 2,800 – 3,200 (6%).

The Tonian magmatism recorded in the Santo Onofre Group samples was responsible for the age peak between 850 and 1,000 Ma (Fig. 13B), and could be associated with the following primary sources: (i) mafic dykes with crystallization ages of 854 ± 23 Ma (Danderfer-Filho et al., 2009) and 934 ± 14 Ma (Loureiro et al., 2009); (ii) Salto da Divisa Felsic Intrusive Suite, with crystallization age between 875 ± 9 Ma (Silva et al., 2008) and 914 ± 9 Ma (Menezes et al., 2012), and metavolcanic rocks that crystallized 913 ± 4 Ma ago (Victória et al., 2015). Rifts that triggered these magmatism events represent the last tensional event that preceded the inversion of the Paramirim Aulacogen and the structuring of the intracontinental sector of the Araçuaí-West Congo Orogen (Cruz and Alkmim, 2006; Borges et al., 2015; Cruz et al., 2015). This rifting process is globally coetaneous to the fragmentation of the Rodinia Supercontinent (Brito Neves, 1999; Fuck et al., 2008).

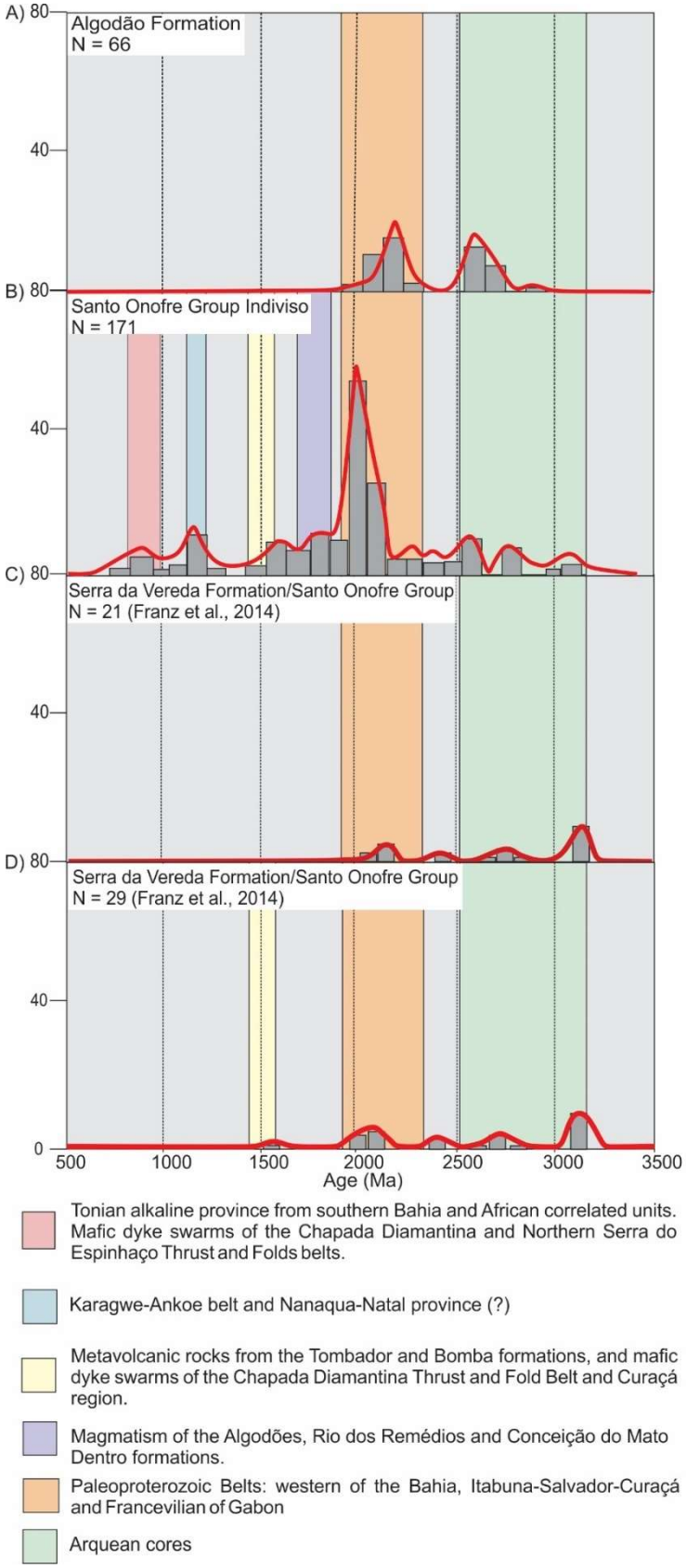

Fig. 13. Frequency histogram and probability curves of U-Pb ages (detrital zircons) for the analyzed samples of the Algodão Formation (Espinhaço Supergroup) (A) and Santo Onofre Group (B-D) with concordance ($^{206}Pb/^{207}Pb$) between 98 e 101%**:** C and D) Data from the Veredinha Formation obtained by Franz et al. (2014) with concordance of 98-101% and 96-104 %, respectively.

Age peaks of 1,000-1,200 and 1,200-1,400 Ma (Fig. 13B) reflect quite scarce sources in the São Francisco-Congo Craton (Kuchenbecker et al., 2015), in the Araçuaí Orogen, and in the Paramirim Aulacogen. This age interval is related to an A-type magmatism similar to that of the Karagwe-Ankole Belt (1,205 ± 19 Ma to 1,383 ± 17 Ma, Tack et al., 1994, 2010; Hanson et al., 1988; Ring et al., 1999; Fernandez-Alonso et al., 2012) and that of the Namaqua-Natal Province (1,286 ± 7 Ma, Evans et al., 2007; Pettersson et al., 2007). For similar records, in units of the Macaúbas Group, Kuchebecker et al. (2015) suggested the existence of a complex and vast fluvial system draining the São Francisco-Congo paleocontinent and flowing into the main grabens of the basins that hosted sediments from this group. This system could bring sediments from the Karagwe-Ankole Belt and Namaqua-Natal Province to feed the basins that hosted rocks from either the Espinhaço Supergroup or the Macaúbas Group. The presence of zircons of this age may either reflect magmatism that has not yet been observed in the Paramirim Aulacogen or suggest that the metasedimentary units of the Espinhaço Supergroup or Macaúbas Group may have acted as secondary sources for the units of the Santo Onofre Group.

The peak of 1,400-1,600 Ma (Fig. 13B) represents a minimum contribution to the samples analyzed in the present study. This peak is likely to be related to the presence of felsic metavolcanic rocks of the Espinhaço Supergroup, and with mafic dykes that truncate the metasedimentary units of this supergroup. For felsic rocks, crystallization ages of 1,528 ± 8 Ma and 1,569 ± 14 Ma were found by Danderfer-Filho et al. (2009) (U-PB, SHRIMP) in the Bomba Formation, and ages of 1,416 ± 28 Ma were found by Guaudagni et al. (2015) (U-Pb, LA-ICPMS) in the Tombador Formation. U-Pb and Pb-Pb ages of mafic rocks ranged between 1,492 ± 16 Ma (Loureiro et al., 2009) and 1,514 ± 22 Ma (Babinski et al., 1999).

The peak between 1,600 and 1,800 Ma (Fig. 13B) is related to the magmatism associated with Statherian taphrogenesis in the Paramirim Aulacogen, represented by anorogenic plutons of the Lagoa Real Intrusive Suite (crystallization in 1,725 ± 10 Ma; Cordani et al., 1992) and by acidic metavolcanic rocks of the Algodão (crystallization in 1,775 ± 7 Ma; Danderfer-Filho et al., 2015), Novo Horizonte (crystallization in 1,752 ± 4 Ma; Schobbenhaus et al., 1994; and 1,748 ± 4 Ma; Babinski et al., 1999), São Simão (crystallization in 1,731 ± 5; Danderfer-Filho et al., 2009 and 1,740 ± 10 Ma; Danderfer-Filho et al., 2015) and Bomba formations (crystallization in 1,528 ± 8 Ma and 1,569 ± 14 Ma; Danderfer Filho et al., 2009).

The potential primary and secondary sources interpreted for detrital zircons found in the Santo Onofre Group are also presented in Table 2 and Figure 14. The primary sources for the interval of 1,800 – 3,200 Ma should be similar to those interpreted for the Algodão Formation. As previously mentioned, a likely secondary source for the Santo Onofre Group is the Espinhaço Supergroup, which was deposited in a Statherian-Stenian rift system that developed in the São Francisco-Congo Paleo-plate (Danderfer-Filho et al., 2009; Chemale-Júnior et al., 2011, 2012; Dussin and Chemale-Júnior, 2012) and presents a thick stack of metasedimentary rocks. In the Espinhaço Supergroup, a large quantity of detrital zircons with ages ranging between 1,100 Ma and 3,600 Ma were dated by Chemale-Júnior et al. (2012), Lopes (2012), Chaves et al. (2013) and Guaudani et al. (2015). The Archean and Paleoproterozoic Metavolcano-sedimentary Sequences and Greenstone Belts from the basement of the Paramirim Aulacogen (Bastos-Leal et al., 1998; Bastos-Leal et al., 2003; Cunha et al., 2012), as well as their African correlated units (Feybesse et al., 1998; Tack et al., 2001; Thieblemont et al., 2009), may also have contributed to the sediment input and collaborated towards the age values found in the Santo Onofre Group, similar to what has been observed for the Algodão Formation.

Table 2
Suggested primary and secondary sources for detrital zircons from the Algodão and Santo Onofre formations analyzed in the present study. References: 1- Cordani et al. (1992), 2- Nutman et al. (1994), 3- Pimentel et al. (1994), 4- Schobbenhaus et al. (1994), 5- Santos-Pinto et al. (1998), 6- Babinski et al. (1999), 7- Lopes (2002), 8- Bastos-Leal et al. (2003), 9- Arcanjo et al. (2005), 10- Cruz et al. (2007), 11- Guimarães et al. (2008), 12 - Silva et al. (2008), 13 – Danderfer-Filho et al. (2009), 14 - Loureiro et al. (2009), 15- Chemale-Júnior et al. (2011), 16- Babinsky et al. (2012), 17- Barbosa et al. (2012), 18- Chemale-Júnior et al. (2012), 19 - Cunha et al. (2012), 20 - Cruz et al. (2012), 21- Menezes et al. (2012), 22 – Santos-Pinto et al. (2012), 23- Barbosa et al. (2013), 24- Medeiros (2013), 25- Franz et al. (2014), 26- Martins et al. (2014), 27- Danderfer-Filho et al. (2015), 28 - Guaudani et al. (2015), 29- Kuchenbecker et al. (2015), 30- Paquete et al. (2015), 31- Victória et al. (2015), 32- Cruz et al. (2016 and cited references), 33- Silva et al. (2016).

Primary Sources	References	Secondary Sources s	References
Tonian Sources			
Santo Onofre Group			
Salto da Divisa Suite	12, 21, 31	-	
Mafic dikes of the western and eastern basins (Paramirim Aulacogen)	13, 14		
Stenian Sources			
Santo Onofre Group			
-	-	Espinhaço Supergroup	-
-	-	Macaúbas Group	16, 29
Ectasian Sources-			
Santo Onofre Group			
-	-	Espinhaço Supergroup (From A-type magmatism of the Karagwe-Ankole belt)	15, 18
		Macaúbas Group (From type-A magmatism of the Namaqua-Natal province)	16, 29
Calymmian Sources-			
Santo Onofre Group			
Bimodal calymmian, plutonic and volcanic, mafic and felsic, anorogenic and alkaline magmatism during evolution of the Paramirim Aulacogen	6, 11, 13, 14, 28	Espinhaço Supergroup	25, 28
		Macaúbas Group	16, 29
Statherian Sources			
Santo Onofre Group and Algodão Formation		**Santo Onofre Group**	
Acid, anorogenic, alkaline and plutonic magmatism of the Lagoa Real Intrusive Suite associated with evolution of the Paramirim Aulacogen	1, 3, 10	Espinhaço Supergroup	15, 18, 25, 28
Anorogenic volcanism of the Espinhaço supergroup (Algodão and Rio dos Remédios formations)	4, 6, 27	Macaúbas Group	16, 29
Siderian, Rhyacian and Orosirian Sources			
Santo Onofre Group and Algodão Formation			
Magmatism of the western Bahia magmatic arc and continental collision between Gavião and Jequié paleoplates	17, 32, 33	Metavolcano-sedimentary Sequences	2, 19, 30
		Espinhaço Supergroup	25, 28
		Macaúbas Group	16, 29
Neoarchean Sources			
Santo Onofre Group and Algodão Formation			
Caraguataí Magmatic Suite and correlate units	8, 20, 24, 26, 33	Metavolcanosedimentary Sequences	2, 19, 30
		Espinhaço Supergroup	25, 28
		Macaúbas Group	16, 29
Mesoarchean Sources			
Santo Onofre Group and Algodão Formation			
Santa Isabel Suite	23, 24	Metavolcano-sedimentary Sequences	2, 19, 30
Gavião Complex	7, 8	Espinhaço Supergroup	25, 28
Porteirinha Complex	33	Macaúbas Group	16, 29

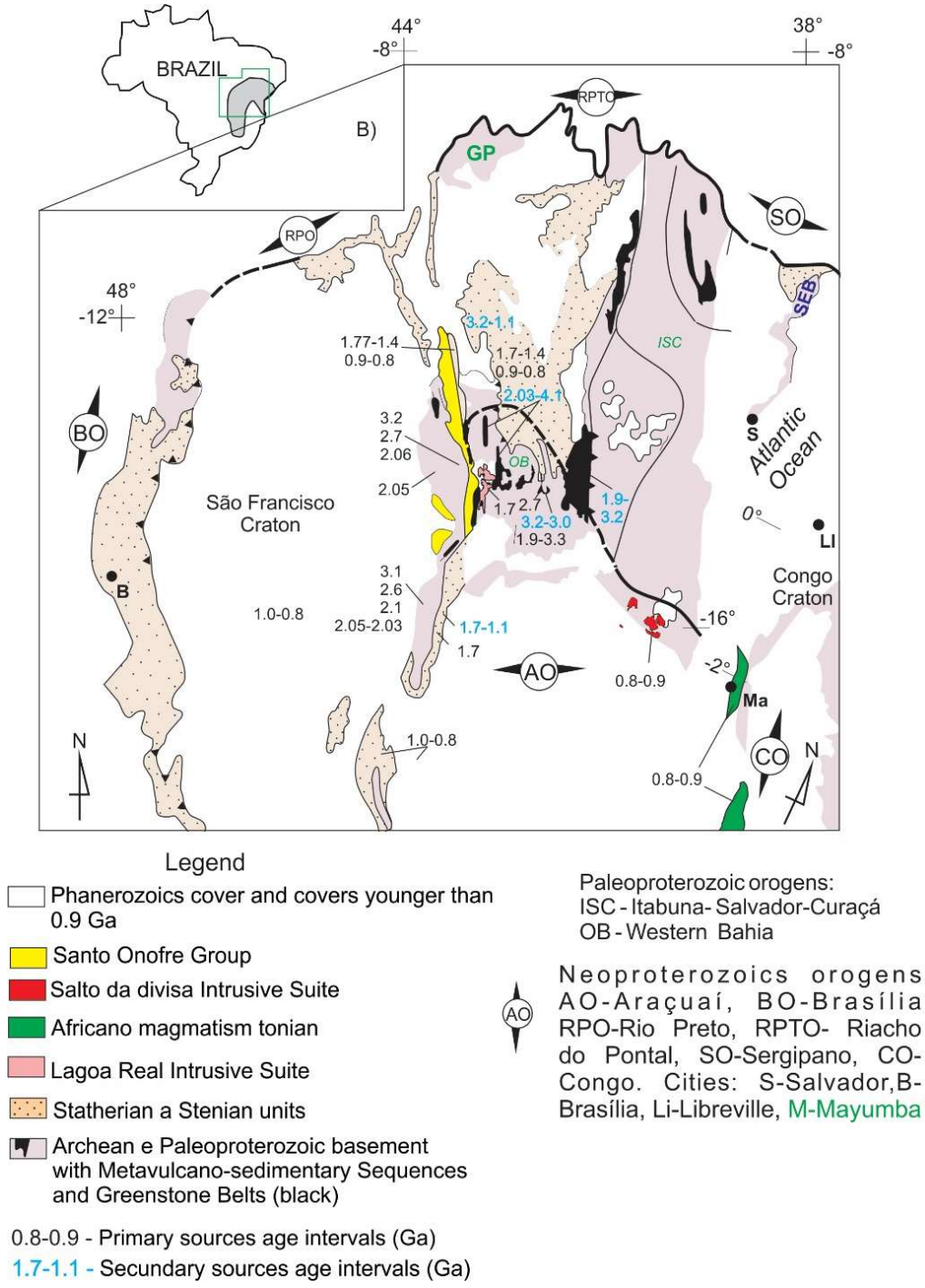

Fig. 14. (A) Situation map, (B) showing the location, within the area of the polygon, of the likely primary and secondary source areas of the analyzed detrital zircons in samples from Santo Onofre Group. Modified from Cruz et al. (2016). In blue, secondary sources; in black, primary sources.

Although there are Paleoarchean rocks in the basement of the Paramirim Aulacogen dated by Santos-Pinto et al. (2012), curiously, no detrital zircons with ages relative to this Era were found in the studied samples from either the Algodão Formation or the Santo Onofre Group.

Considering the result obtained by Franz et al. (2014) and an interval of concordance of 98 and 101%, the detrital zircon spectrum obtained for the Serra da Vereda Formation presented zircons with minimum ages of 1,974 ± 50 Ma (Fig. 13C). On the other hand, when considering the interval used by these authors, in other words, between 96 and 104%, the minimum age found was 1,580 ± 97 Ma (Fig. 13D). This age distribution is quite discrepant when comparing to what was obtained for the Serra da Garapa and Boqueirão formations. Therefore, two hypotheses can be formulated: (i) the Serra da Vereda and Fazendinha formations are not units of the Santo Onofre Group, as also suggested by Guimarães (2014); and/or (ii) the source areas for the zircons of these two formations were predominantly rocks older than 1,580 Ma.

Similarity between geochronological signatures is observable when comparing the summary of geochronological data of the Macaúbas Group integrated by Kuchenbecker et al. (2015) with the data of the present study for the Santo Onofre Group (Fig. 15). The main peak of approximately 2,100 Ma is maintained in both groups. However, regarding source areas, units from the Macaúbas Group presented detrital zircons as old as Paleoarchean, while the maximum age obtained in the Santo Onofre Group was Mesoarchean.

According to Pedrosa-Soares et al. (2011), the Macaúbas Group can be subdivided into three larger successions from its base to its top and from west to east: (i) pre-glacial succession, comprising the Matão, Duas Barras and Rio Peixe Bravo formations; (ii) glacial succession, including the diamictites-rich stack of the Serra do Catuni, Nova Aurora, and Lower Chapada Acauã; and (iii) post-glacial succession, comprised by diamictites from the Upper Chapada Acauã and Ribeirão da Folha formations. The youngest zircon ages in these successions were: 900 ± 21 Ma (U-Pb, SHRIMP in detrital zircons) found in the Duas Barras Formation, obtained by Babinski et al. (2012); 933 ± 9 Ma (U-Pb, SHRIMP, detrital zircon) found in the Serra do Catuni Formation by Babinski et al. (2012); 870 Ma, found in the Lower Chapada Acauã Formation by Kuchenbecker et al. (2015); and between 758 ± 7 Ma and 743 ± 7 Ma (U-Pb, LA-MC-ICP-MS, detrital zircon) found in the Upper Chapada Acauã Formation by Kuchenbecker et al. (2015).

In turn, in the Santo Onofre Group, the youngest zircons found in the Serra da Garapa Formation presented ages between 938 ± 22 Ma and 894 ± 38 Ma (Samples MPA and MPC, respectively), while the minimum age for the Boqueirão Formation obtained in sample TR-01 was 899 Ma ± 79 Ma. These ages were similar to the youngest ages of detrital zircons found in the Duas Barras and Serra do Catuni formations by Babinski et al. (2012). Kuchenbecker

et al. (2015) found similar ages for the Nova Aurora (939 ± 18 Ma, U-Pb, LA-ICP MS, detrital zircon) and Lower Chapada Acauã formations (953 ± 18 Ma, U-Pb, LA-ICP MS, detrital zircon), both belonging to the glacial succession of the Macaúbas Group. These data demonstrate the similarity between geochronological signatures of the Macaúbas and Santo Onofre groups.

Figure 16 shows an integrated map for the Macaúbas and Santo Onofre groups, encompassing the data obtained in the present study, as well as from Pedrosa et al. (2007), Guimarães et al. (2012), Babinski el al. (2012), and Kuchenbecker et al. (2015). Similarities are observed when comparing the lithological composition of rocks from the Serra da Garapa Formation and from the Santo Onofre Group with the rocks from the Rio Peixe Bravo Formation and from the pre-glacial succession of the Macaúbas Group (Knauer et al., 2007). Cartographically, longitudinal continuity can be observed among them and, therefore, a chronocorrelation is proposed between these formations.

The lower unit of the Boqueirão Formation outcrops in the study area southwards from the municipality of Caetité (Figs. 5, 16), presenting metasubarkoses with fragments of graphite-rick phyllite, lithic metasandstones, metasiltites, and metarhythmites. These metarhythmites are quite similar to varves. The geochronological signature found in the Boqueirão Formation was similar to what was obtained in the integration performed by Kuchenbecker et al. (2015) (Fig. 15) for glacial and post-glacial units of the Macaúbas Group, considering that Tonian zircons were only found in these units. However, the correlation proposal presented in Figure 16 includes the Boqueirão Formation in pre-glacial units, since more detailed studies should be conducted in order to verify the existence or not of varves in this unit.

Figueiredo et al. (2009) obtained detrital zircon ages for rocks from the Bebedouro Formation in the Chapada Diamantina Thrust and Fold Belt. The data obtained by these authors were organized in Figures 15F, G considering concordance values between 85 and 115%, and between 98 and 101%, respectively. Some aspects of the detrital geochronological signature of these rocks were similar to those found in the Santo Onofre Formation, which were: (i) maximum zircon age found was Mesoarchean, with ages of 3,177 ± 42 Ma in the Santo Onofre Formation and 3,047 ± 32 Ma in the Bebedouro Formation (concordance between 98 and 101%); and (ii) in the Bebedouro Formation, the youngest detrital zircon obtained presented age of 892 ± 64 Ma, while in the Santo Onofre Group, the youngest age obtained was 894 ± 38 Ma. Regarding frequency peaks, both units presented a strong

contribution of sources with ages between 1,800 and 2,200 Ma. In the Bebedouro Formation, the contribution of sources with ages between 1,600 and 1,800 Ma was also significant.

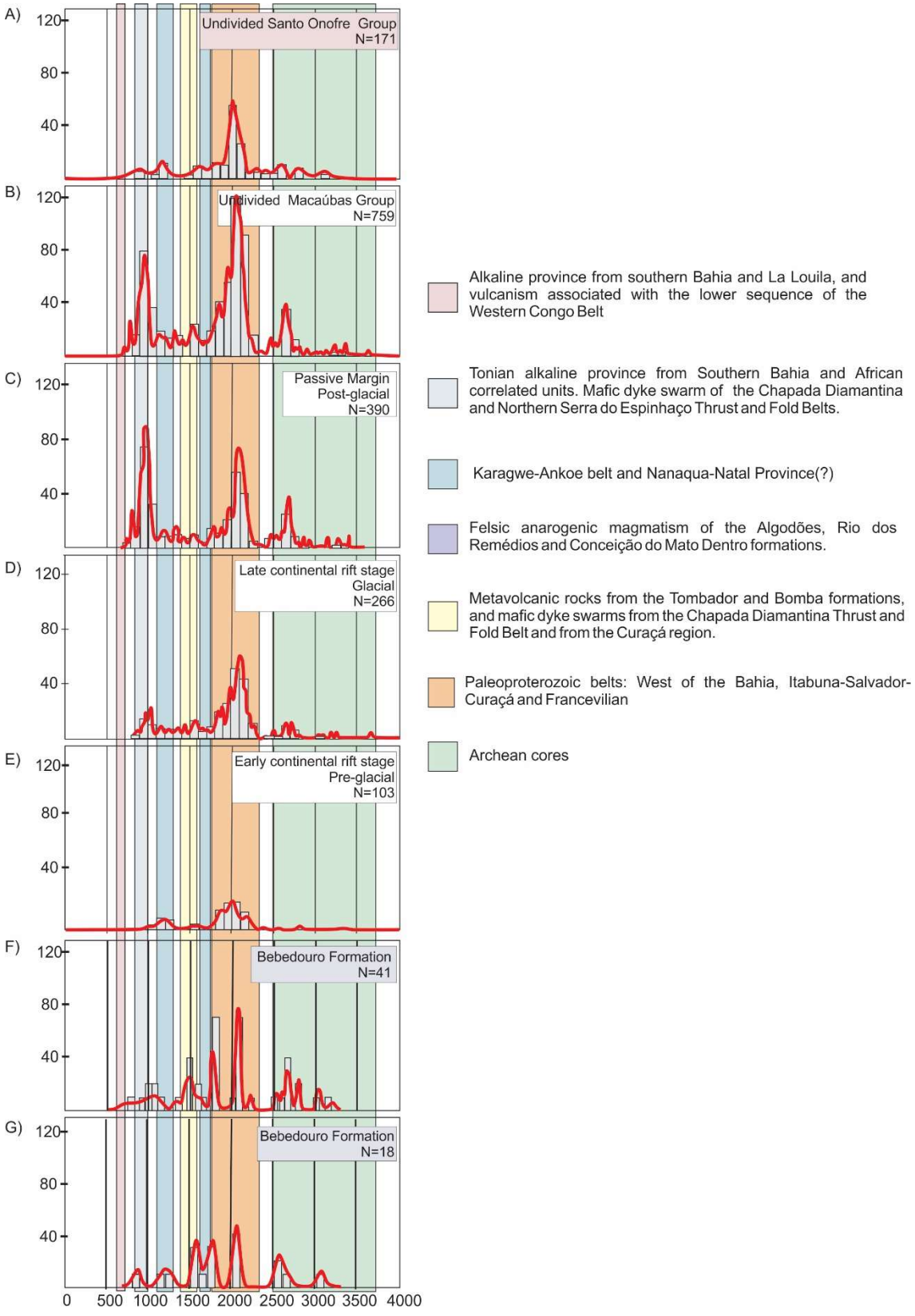

Fig. 15. Frequency histogram and probability curves of U-Pb ages (detrital zircons, $^{206}Pb/^{207}Pb$) for the analyzed samples of the of the Santo Onofre (A, concordance between 98-101%) and Macaúbas groups (B-E, concordance

higher than 89%) and the Bebedouro Formation (F- Concordance between 85 and 115%, and G- Recalculating for the concordance between 98 and 101%). Data from the Macaúbas Group from Kuchenbecker et al. (2015) and from the Bebedouro Formation (from Figueiredo et al. 2009).

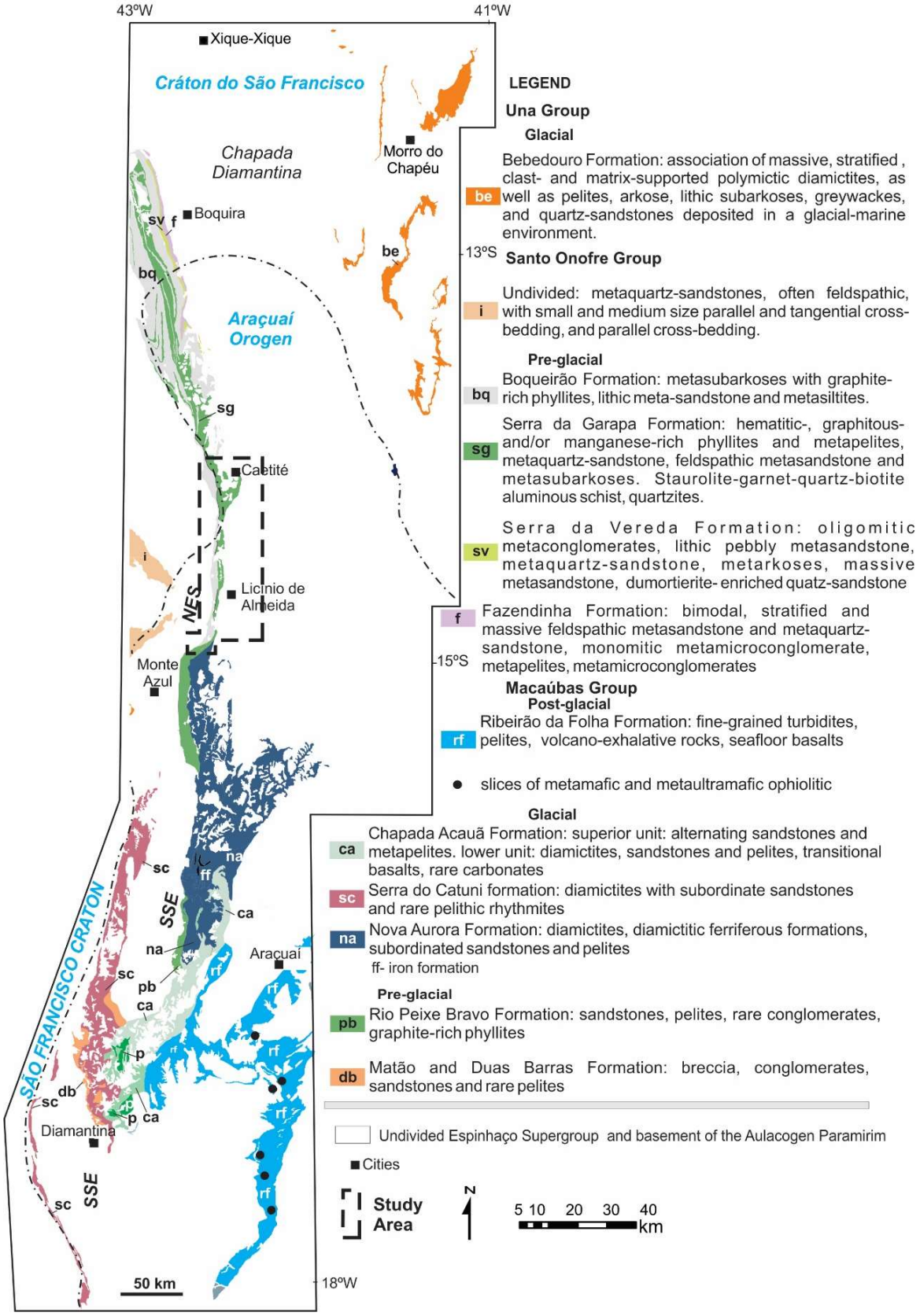

Fig. 16. Geologic map integrating the western sector of occurrence of the Macaúbas Group (from Pedrosa-Soares et al, 2007 and Kuchenbecker et al., 2015), the Santo Onofre Group (from the present study and Guimarães et al., 2012), and the Bebedouro Group. Modified from Kuchenbecker et al. (2015). Acronyms: NES-Northern Serra do Espinhaço, SSE – Southern Serra do Espinhaço.

Over the past decades, the stratigraphic positioning of the Santo Onofre Group was the target of several divergences. Authors have at times interpreted the group as an intermediate unit of the Espinhaço Supergroup (Costa and Silva, 1980), other times as an upper unit of this supergroup (Barbosa and Dominguez, 1996; Danderfer-Filho, 2000; Souza et al., 2003; Loreiro et al., 2009; Guimarães et al., 2012), or even as a unit that belongs to the São Francisco Supergroup (Danderfer-Filho and Dardenne 2002, Pedrosa-Soares and Alkmim, 2011, Alkmim and Martins-Neto, 2012, Alkmim, 2014, and Cruz and Alkmim, 2017). The new data found in the present study allow the classification of this group with greater precision as a unit of the São Francisco Supergroup, whose deposition is related to the evolution of a rift of probably Tonian age.

5.2 Statherian and Tonian rifts: their context in the evolution of precursor basins of the Araçuaí-West Congo Orogen and tectonic inversion

According to Pedrosa-Soares and Alkmim (2011), several attempts of breaking the São Francisco-Congo paleo-plate occurred since the Statherian until the Cryogenian. The first of these attempts occurred during the Statherian and led to the development of two overlapped intracontinental rifts, the first of which is recorded in the siliciclastic and acidic, anorogenic, metavolcanic rocks of the Algodão Formation (Fig. 17A) (Danderfer-Filho et al., 2015).

In the Paramirim Aulacogen, between 1,750 and 1,000 Ma (Fig. 17B), the Eastern Basin, located within the Chapada Diamantina region (Fig. 3), and only part of the Western Basin, located northwards from the municipality of Caetité (Fig. 5), presented a more complete section of the units of the Espinhaço Supergroup, whose acidic metavolcanic rock deposition and records allow to interpret the existence of at least three intracontinental rifts (Pedrosa-Soares and Alkmim 2011; Cruz and Alkmim, 2017). Within this context of rift opening, felsic, acidic, alkaline and anorogenic metavolcanic rocks, with ages between approximately 1,750 and 1,420 Ma, and mafic dykes with ages approximately between 1,600 and 850 Ma (Schobbenhaus et al., 1994; Babinski et al., 1999; Guimarães et al., 2008; Loureiro et al., 2009; Danderfer-Filho et al., 2009, 2015; Guaudani et al., 2015) characterize a continuous evolution of this basin, since the Statherian until the Tonian. Cryogenian felsic volcanic rocks were found by Santana (2016) in the Chapada Diamantina region.

To Alkmim et al. (2006, 2017) and Kuchenbecker et al. (2015), the evolution of the Macaúbas basin occurred between 930 and 630 Ma (Fig. 17C). Two sequences were interpreted by these authors: (i) the oldest one is pre-glacial, Tonian, and encompasses the Capelinha, Matão, Duas Barras, Domingas, and Rio Peixe Bravo formations; and (ii) the youngest one, with glacial and deep marine records, is Cryogenian, comprised by the Serra do Catuni, Nova Aurora, Chapada Acauã, and Ribeirão da Folha formations. The oceanization of this basin occurred between 600 and 660 Ma, and is revealed by the presence of ophiolites (Queiroga et al., 2007; Queiroga, 2010). Based on data obtained in this study, the deposition of the Santo Onofre Group is suggested to be chronocorrelated to the deposition of Tonian pre-glacial rocks of the Macaúbas Group, though with deposition between 934 and 850 Ma. The Santo Onofre-Macaúbas Tonian rift system was installed upon the tectonic inheritance of Statherian and Calymmian rifts (Kuchenbecker et al., 2015; Alkmim et al., 2006, 2017; Cruz and Alkmim, 2017) that developed within the scenario of the Paramirim Aulacogen and in the region that currently comprises the largest Brazilian expression of the Araçuaí-West Congo Orogen.

The deposition of the Santo Onofre Group would also be contemporary with: (i) fissure mafic magmatism of the Gentio do Ouro, dated as 934 ± 14 Ma (Loureiro et al., 2009), and of the Pedro Lessa Suite, dated as 902 ± 2 Ma (Machado et al., 1989; Dussin and Chemale-Júnior, 2012); (ii) mafic dykes from Salvador, Ilhéus and Olivença, with crystallization ages between 926 ± 5 and 918 ± 7 Ma (Evans et al., 2015); (iii) basaltic greenschists of the Terra Branca Plateau that crystallized 889 ± 10 Ma ago (Souza, 2016); (iv) mafic dykes of the Formiga Suite, with ages of 984 ± 110 Ma (Chaves and Correia-Neves, 2005) and 940 ± 50 Ma (Carneiro and Oliveira, 2005); (v) basaltic-subordinated greenschists of the Rio Preto valley, with maximum age of 1.1 Ga (Babinski et al., 2012); (vi) anorogenic magmatism of the Salto da Divisa Suite, with ages ranging between 914 ± 3 Ma and 875 ± 9 Ma (Silva et al., 2008; Menezes et al., 2012); and (vii) volcanic pile of the Zandinian-Mayumbian succession within the Western Congo Belt, with ages of 912 and 920 ± 8 Ma (Tack et al., 2001). The set of existing data, which are preserved in several regions of the São Francisco Craton and in the Araçuaí-West Congo Orogen, show an important rupture event of the Rodinia continent during the transition between the Stenian and Tonian.

Although in the northern area of the municipality of Caetité (Fig. 5) a more complete exposure of the units of the Espinhaço Supergroup can be observed, in the study area there is a gap of at least 900 Ma between the deposition ages of the units of this supergroup and the

metasedimentary rocks of the Santo Onofre Group, which presented a maximum Tonian age. Chemale-Júnior et al. (2011, 2012) also observed the existence of a gap of this same magnitude in the region of Diamantina, state of Minas Gerais, within the Southern Espinhaço Basin.

Approximately 630 Ma ago, the Rio Doce magmatic arc was installed with the deposition of correlated sedimentary units (Gradim et al., 2014) (Fig. 17D). According to Alkmim et al. (2006, 2007), the closing (Fig. 17E) of this last rift, which was a precursor of the Araçuaí-West Congo Orogen, occurred in four stages: (i) initial convergence; (ii) collision; (iii) lateral escape; and (iv) gravitational collapse. According to these authors, the closing of this rift was induced at a distance, as a consequence of collisions involving the São Francisco-Congo, Rio de La Plata, and Amazon paleo-plates. Thus, the convergence of the opposite margins of the Macaúbas Basin began, in a way that was comparable by the authors to the functioning of a nutcracker (nutcracker model) (Fig. 17E). Reflex tectonics would have led to the development of the Rio Pardo Salience (Cruz and Alkmim, 2006) followed by the installation of a regional transpressional system identified by Cruz and Alkmim (2006), Cruz et al. (2007, 2015), Borges et al. (2015), and Silva (2010). The Northern Espinhaço Thrust and Fold Belt developed in this context.

6. Conclusion

Based on what was presented and discussed in the present study, the analysis of detrital zircons performed in the Algodão, Serra da Garapa and Boqueirão formations revealed ages between 1,958 ± 18 and 2,870 ± 17 Ma, 894 ± 38 and 2,662 ± 19 Ma, and 899 ± 76 and 3,177 ± 42 Ma, respectively. Zircon sources were basement rocks and rocks from the structuring of the Itabuna-Salvador-Curaçá and the Western Bahia orogens, in addition to volcanic and plutonic, metamafic and metafelsic rocks, with ages generally between 1,800 and 800 Ma, related to the evolution of basins which were precursors to the Araçuaí-West Congo Orogen.

Geochronological data suggested deposition for the Algodão Formation with a maximum age of 1,958 ± 18 Ma. The presence of metavolcanic rocks of approximately 1.77 Ga, observed by other authors, shows that these are the oldest units of the Paramirim Aulacogen. In turn, zircon spectra identified in the Santo Onofre Group ranged from the Archean until the Tonian, and were similar to those found in glacial units of the Macaúbas Group and the Bebedouro Formation (São Francisco Supergroup). However, since the rocks

of the Santo Onofre Group did not present safe evidences associated with glacial environments, they were correlated with the pre-glacial units of the Macaúbas Group and African correlated units. More detailed studies should be performed in order to better understand the facies associations of this unit, especially regarding the Boqueirão Formation. Temporally, the deposition of the units of the Santo Onofre Group relate to the structuring of rifts that hosted the Salto da Divisa Suite, and with other magmatic rocks associated with Tonian basins that were precursor to the Araçuaí-West Congo Orogen.

The tectonic evolution interpreted suggested the existence of a sedimentation gap of at least 900 Ma between the deposition of rocks of the Algodão and Serra da Garapa formations (Santo Onofre Group). The sedimentation of the Macaúbas Group, younger than 850 Ma, provided continuity to the filling of this basin. Oceanization and the later installation of a magmatic arc occurred 660 Ma ago. Approximately 560 Ma ago, the Santo Onofre-Macaúbas basins suffered complete inversion in the context of Western Gondwana.

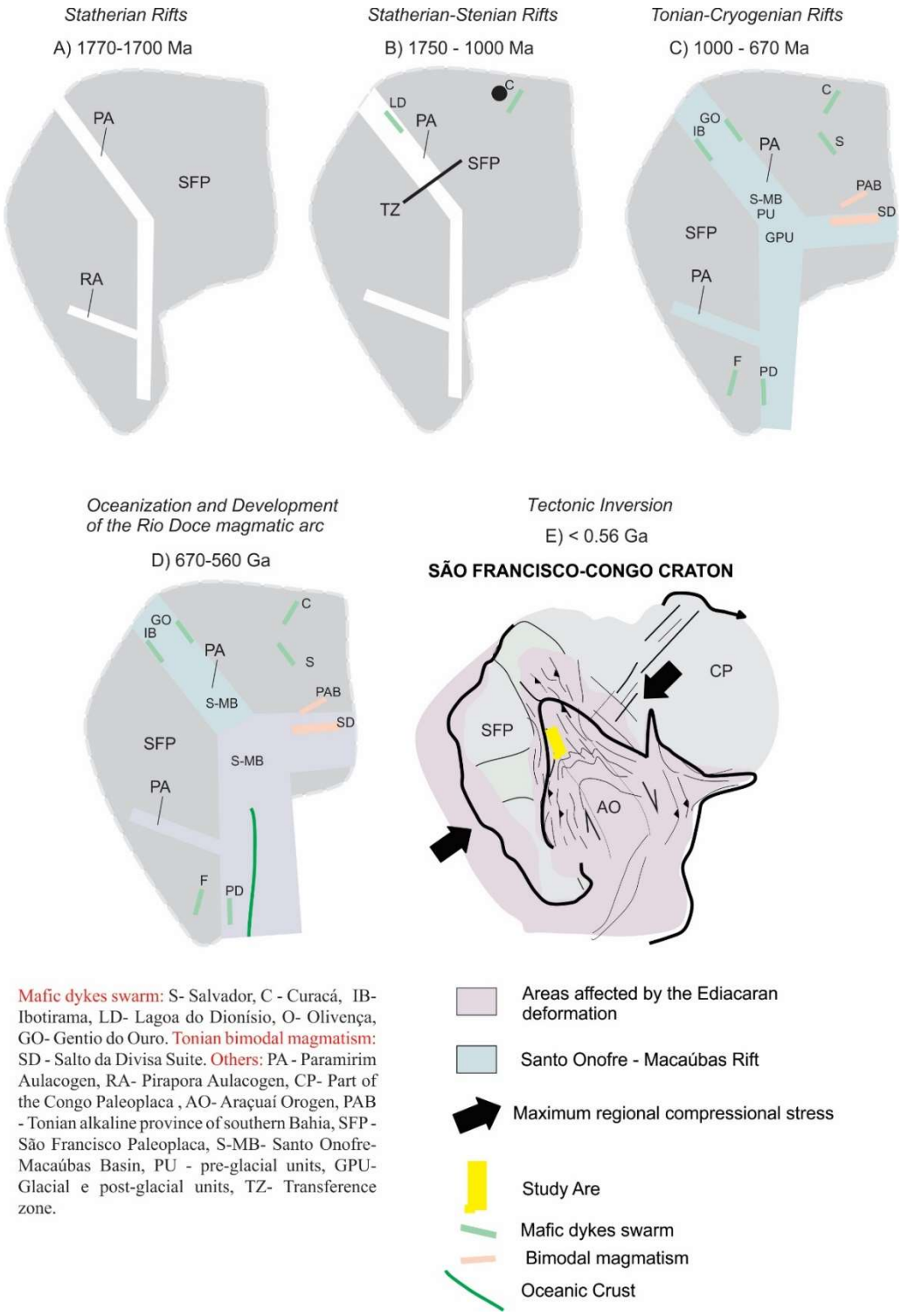

Fig. 17. Tectonic evolution model proposal since the opening of the precursor basins of the Araçuaí Orogen (A-C), until the inversion of basins. (D) Mafic dyke swarms: S- Salvador, C - Curaçá, I - Ilhéus, IB- Ibotirama, LD- Lagoa do Dionísio, O- Olivença, GO- Gentio do Ouro. Bimodal magmatism: SD - Salto da Divisa Suite. PA - Paramirim Aulacogen, AR- Pirapora Aulacogen, CP- Part of the Congo Paleo-plate, AO- Araçuaí Orogen, SFP - São Francisco Paleo-plate, PU- Pre-glacial units, GPU- Glacial and post-glacial units, TZ- Transference zone.

Acknowledgments

The authors wish to express their gratitude to CNPq for the scholarships and the research grants for Simone Cerqueira Pereira Cruz (Proc. 307590/2009-7 and 303451/2015-7) and Fundação de Amparo à Pesquisa do Estado da Bahia for the scholarship for Caroline Novais Bitencourt. The authors also thank the anonymous reviewers and editor of the article for their contributions to the improvement.

References

Alkmim, F.F., Marshak, S., Pedrosa-Soares, A.C., Peres, G.G., Cruz, S.C.P., Whittington, A., 2006. Kinematic evolution of the Araçuaí–West Congo orogen in Brazil and Africa: Nutcracker tectonics during the Neoproterozoic assembly of Gondwana. Precambrian Research 149, 43-63.

Alkmim, F.F., Pedrosa-Soares, A.C, Noce, C. M., Cruz, S.C.P., 2007. Sobre a Evolução Tectônica do Orógeno Araçuaí-Congo Ocidental. Geonomos 15, 25–43.

Alkmim, F.F. and Martins-Neto, M.A., 2012. Proterozoic First-order sedimentary sequences of the São Francisco craton, eastern Brazil, Marine and Petroleum Geology 33, 127-139.

Alkmim, F.F., Kuchenbecker, M., Reis, H.L.S., Pedrosa-soares, A.C., 2017. The Araçuaí Belt. In: Heilbron, M., Cordani, U.G., Alkmim, F.F. (Eds.). São Francisco Craton Eastern Brazil: Tectonic Genealogy of a Miniature Continet. Regional Geology Reviews. 1ed.: Springer International Publishing, 255-276.

Allmendinger, R.W., Cardozo, N., Fisher, D., 2012. Structural geology algorithms: Vectors and tensors in structural geology: Cambridge University Press, 302 pp.

Almeida F.F., 1977. O Cráton do São Francisco. Revista Brasileira de Geociências 4, 349-364.

Arcanjo, J.B., Martins, A.A.M., Loureiro, H.S.C., Varela, P.H.L., 2005. Projeto Vale do Paramirim, Bahia: geologia e recursos minerais. CBPM. Série Arq. Abertos 22, Salvador, BA, 82pp.

Babinski, M., Pedrosa Soares, A.C., Trindade, R.I.F., Martins M., C.M. Noce, Liu D., 2012. Neoproterozoic glacial deposits from the Araçuaí orogen, Brazil: Age, provenance and

correlations with the São Francisco craton and West Congo belt. Gondwana Research 21 (2-3), 451-465.

Babinski, M., Pedreira, A., Brito-Neves, B.B., Van-Schmus, W.R., 1999. Contribuição à geocronologia da Chapada Diamantina. In: SBG/ BA-SE, Simpósio Nacional de Estudos Tectônicos, 7, Anais, pp. 118-121.

Barbosa, J.S.F. and Dominguez J.M.L., 1996. Mapa Geológico do Estado da Bahia. Escala: 1.000.000. Texto explicativo. Salvador, BA, 382pp.

Barbosa J.S.F., Sabaté P., 2002. Geological features and the Paleoproterozoic collision of four Archean crustal segments of the São Francisco Craton, Bahia, Brazil. A synthesis. Anais Academia Brasileira de Ciencias 2, 343-359.

Barbosa, J.S.F., Santos-Pinto, M., Cruz, S.C.P., Souza, J.S., 2012. Granitóides. In: Barbosa, J.S.F. (Eds.) Geologia da Bahia, Pesquisa e Atualização, CBPM Série Publicações especiais, Salvador, 327–394.

Barbosa, N.S., Teixeira, W., Bastos Leal, L.R., Leal, A.B.M., 2013. Evolução crustal do setor ocidental do Bloco Arqueano Gavião, Cráton do São Francisco, com base em evidências U-Pb, Sm-Nd e Rb-Sr. Revista do Instituto de Geociências - USP 13, 6-88.

Barbosa, R.G., Souza, J.S., Barbosa, J.S.F., Hamilton, M.A., 2015. The post-tectonic granites of the Gavião Block: the exemple of Salinhinha Monzogranite, Brumado, Bahia, Brazil. In: The 8th Hutton Symposium on Granites and Related Rocks, Anais, Florianópolis, Brasil, CD-ROM.

Bastos-Leal, L.R., Teixeira, W., Cunha, J.C., Macambira, M.J.B., 1998. Archean tonalitic-trondhjemitic and granitic plutonism in the Gavião block, São Francisco Craton, Bahia, Brazil: Geochemical and geochronology characteristics. Revista Brasileira de Geociência 2, 209-220.

Bastos-Leal L.R., Teixeira W., Cunha J.C., Leal A.B.M., Macambira M.J.B., Rosa M.L.S., 2000. Isotopic signatures of paleoproterozoica granitoids of the Gavião block and implications for the evolution of the São Francisco craton, Bahia, Brazil. Revista Brasileira de Geociências 30, 66-69.

Bastos-Leal L.R., Cunha J.C., Cordani U.G., Teixeira W., Nutman A.P., Menezes Leal A.B., Macambira M.J.B., 2003. SHRIMP U–Pb, $^{207}Pb/^{206}Pb$ zircon dating, and Nd isotopic

signature of the Umburanas greenstone belt, northern São Francisco craton, Brazil. Journal South American Earth Science 15, 775–785.

Bitencourt C.N., 2014. Petrologia e análise estrutural multiescalar da Serra da Garapa Formation (Santo Onofre Group) na porção sul do Cinturão de Dobramentos e Cavalgamentos Espinhaço Setentrional. Corredor do Paramirim, Caetité, Bahia. (Undergraduate Thesis) Universidade Federal da Bahia, Salvador, 118 pp.

Borges, J.O., Cruz, S.C.P., Barbosa, J.S.F., 2015. Structural framework of the the Lagoa D'Anta mine area, iron-manganese Urandi-Caetité- Licínio de Almeida District, Bahia, Brasil. Brazilian Journal of Geology 45, 173-192.

Brito-Neves, B.B., 1999. América do Sul: quatro fusões, quatro fissões e o processo acrescionário andino. Revista Brasileira de Geociências 29, 379-392.

Brito, D.C., 2008. Geologia, petrografia e litogeoquímica dos diques máficos que ocorrem na porção sudoeste da Chapada Diamantina, Bahia, Brasil. (M. Sc. Thesis) Universidade Federal da Bahia, Salvador, 77pp.

Campos, L.D., 2013. O depósito de Au-Cu Lavra Velha, Chapada Diamantina Ocidental: um exemplo de depósito da classe IOCG associado aos terrenos paleoproterozoicos do Bloco Gavião. (M. Sc. Thesis) Universidade Federal da Bahia, Salvador, 113 pp.

Carneiro, M.A. and Oliveira, A.H., 2005. Tectonic evolution of southern São Francisco Craton: three tectonothermal events based on 40Ar/39Ar isotopic data. III Simpósio do Craton São Francisco, Seção técnica St5-05, Salvador, CD-ROM.

Chaves, A.O. and Correia Neves, J.M., 2005. Radiometric ages, aeromagnetic expression, and general geology of mafic dykes from southeastern Brazil and implications for African-South American correlations. Journal of South American Earth Sciences 19, 387-397.

Chaves, M.L.S.C., Babinski, M., Silva, M.C.R., Scholz, R., 2013. Idades U–Pb em zircão do conglomerado diamantífero de Grão Mogol (Espinhaço Supergroup): implicações para a origem dos diamantes da Serra do Espinhaço em Minas Gerais. Brazilian Journal Geology 43, 139–151.

Chemale-Júnior, F., Dussin, I.A., Alkmim, F.F., Martins, M.S., Queiroga, G., Armstrong, R., Santos, M.N., 2012. Unravelling a Proterozoic basin history through detrital zircon

geochronology: the case of the Espinhaço Supergroup, Minas Gerais, Brazil. Gondwana Research 22, 200–206.

Chemale-Júnior, F., Dussin I.A., Martins, M., Santos, M.N., 2011. Nova abordagem tectono-estratigráfica do Espinhaço Supergroup em sua porção meridional (MG). Geonomos 19, 173-41.

Cordani U.G., Sato K., Marinho M.M., 1985. The geologic evolution of the ancient granite-greenstone terrane of central-southern Bahia, Brazil. Precambrian Research 27, 187-213.

Cordani, U.G., Iyer, S.S., Taylor, P.N., Kawashita, K., Sato, K., Mcreath, I., 1992. Pb-Pb, Rb-Sr, and K-Ar sistematic of the Lagoa Real uranium province (south-central Bahia, Brazil) and the Espinhaço Cycle (ca. 1.5-1.0 Ga). Journal of South American Earth Sciences 1, 33-46.

Costa L.A.M. and Silva W.G., 1980. Projeto Santo Onofre, mapeamento. TRISERVICE, convênio DNPM/CPRM, Relatório Final Integrado, Rio de Janeiro, RJ, 374 pp.

Cruz, S.C.P. and Alkmim, F.F., 2006. The tectonic interaction between the Paramirim Aulacogen and the Araçuaí Belt, São Francisco Craton region, Easter Brazil. Anais da Academia Brasileira de Ciências 1, 151-173.

Cruz, S.C.P., Alkmim, F.F., Leite, C.M.M., Evangelista, H.J. Cunha, J.C., Matos, E.C., Noce, C.M., Marinho, M.M., 2007. Geologia e arcabouço estrutural do Complexo Lagoa Real, Vale do Paramirim, Centro-Oeste da Bahia. Revista Brasileira de geociências 37 (4, suplemento), 28-146.

Cruz S.C.P., Alkmim F.F., Pedreira A., Teixeira L., Pedrosa-Soares A.C., Gomes L.C.C., Souza J.S., Leal A.B.M., 2012. O Orógeno Araçuaí. In: Barbosa J.S.F (Eds.), Geologia da Bahia, Pesquisa e Atualização, CBPM Série Publicações Especiais, Salvador, 131-178.

Cruz, S.C.P., Alkmim, F.F., Barbosa, J.S.F., Dussin, I., Gomes, L.C.C., 2015. Tectonic inversion of compressional structures in the Southern portion of the Paramirim Corridor, Bahia, Brazil. Brazilian Journal of Geology 45, 541-567.

Cruz, S.C.P., Barbosa, J.S.F., Santos Pinto, M., Peucat, J.J., Paquette J.L., Souza, J.S., Martins, V.S., Chemale Júnior, F., Carneiro, M.A., 2016. The Siderian-Orosirian

magmatism in the Gavião Paleoplate, Brazil: U-Pb geochronology, geochemistry and tectonic implications. Journal of South American Earth Sciences 69, 43 – 79.

Cruz, S.C. P., Alkmim, F.F., 2017. The Paramirim Aulacogen. In: Heilbron. M., Cordani, U.G., Alkmim, F.F. (Eds.). São Francisco Craton Eastern Brazil: Tectonic Genealogy of a Miniature Continet. Regional Geology Reviews. Springer International Publishing, 97-115.

Cunha, J.C., Bastos Leal, L.R., Fróes, R.J.B., Teixeira, W., Macambira, M.J.B., 1996. Idade dos greenstone belts e dos terrenos TTG's associados da região de Brumado, centro oeste do Cráton do São Francisco (Bahia-Brasil). In: SBG, Congresso Brasileiro de Geologia, 39, Anais, pp. 67-70.

Cunha J.C., Barbosa J.S.F., Mascarenhas J.F., 2012. Greenstones Belts e Sequências Similares. In: Barbosa, J. S. (Eds.), Geologia da Bahia, Pesquisa e Atualização, CBPM Série Publicações especiais, Salvador, 203–325.

Damasceno, G.C., 2013. Geologia, Petrografia e Geoquímica dos diques máficos da Folha Caetité (SD.23-Z-B-III). (M. Sc. Thesis) Universidade Federal da Bahia, Salvador, 145pp.

Danderfer-Filho, A., 1990. Análise estrutural descritiva e cinemática do Espinhaço Supergroup na região da Chapada Diamantina (BA). (M. Sc. Thesis) Universidade Federal de Ouro Preto, Ouro Preto, 99pp.

Danderfer-Filho, A., 2000. Geologia sedimentar e evolução tectônica do Espinhaço Setentrional, Estado da Bahia. (Ph.D. Thesis) Universidade Federal de Brasília, Brasília 497 pp.

Danderfer-Filho, A. and Dardenne, M.A., 2002. Tectonoestratigrafia da Bacia Espinhaço na porção centro-norte do Cráton do São Francisco: registro de uma evolução poliistórica descontínua. Revista Brasileira de Geociências 4, 449-460.

Danderfer-Filho, A., De Waele, B., Pedreira, A.J., Nalini, H.A., 2009. New geochronological constraints on the geological evolution of Espinhaco basin within the São Francisco Craton-Brazil. Precambrian Research 170, 116–128.

Danderfer-Filho, A., Lana, C.C., Nalini Júnior, H.A., Costa, A.F.O., 2015. Constraints on the Statherian evolution of the intraplate rifting in a Paleo-Mesoproterozoic paleocontinent:

New stratigraphic and geochronology record from the eastern São Francisco craton. Gondwana Research 28, 668 – 688.

Derby, O.A., 1906. The Serra do Espinhaço. Brazilian Journal Geology 14, 374-401.

Dussin, I.A., Chemale Júnior, F., 2012. Geologia estrutural e estratigrafia do sistema Espinhaço – Chapada Diamantina e sua aplicação nas bacias mesozóico-cenózoicas da margem passiva brasileira. PETROBRAS, Rio de Janeiro, RJ, 218 pp.

Evans, D.A.D., Trindade, R.I.F., Catelani, E.L., D'agrella-Filho, M.S., Heaman, L.M., Oliveira, E.P., Söderlund, U., Ernst, R.E., Smirnov, A.V., Salminen, J.M., 2015. Return to Rodinia? Moderate to High Palaeolatitude of the São Francisco/Congo Craton at 920 Ma. Geological Society of London Special Publication 424, 1-24.

Evans, D.M., Windrim, D.P., Armstrong, R.A., 2007. Age of metavolcanic rocks at the northern margin of the Namaqua–Natal Metamorphic Province in the Karas Mountains, Namibia, defined by SHRIMP U–Pb dating of zircons. South African Journal Geology 110, 47–54.

Fernandez-Alonso, M., Cutten, H., De Waele, B., Tack, L., Tahon, A., Baudet, D., Barritt, S.D., 2012. The Mesoproterozoic Karagwe-Ankole Belt (formerly the NE KibaraBelt): the result of prolonged extensional intracratonic basin development punc-tuated by two short-lived far-field compressional events. Precambrian Research 216–219, 63–86.

Feybesse, J.L., Johan, V., Triboulet, C., Guerrot, C., Mayaga-Mikolo, F., Bouchot, V., EkoNdong, J., 1998. The West Central African belt: a model of 2.5–2.0 Ga accretion and two-phase orogenic evolution. Precambrian Research 87, 161–216.

Figueiredo, F.T., Almeida R.P., Tohver E., Babinski M., Liu D., Fanning C.M., 2009. Neoproterozoic glacial dynamics revealed by provenance of diamictites of the Bebedouro Formation, São Francisco Craton, Central Eastern Brazil. Terra Nova 21, 375-385.

Franz, G., Morteani, G., Gerdes, A., Rhede, D., 2014. Ages of protolith and Neoproterozoic metamorphism of Al-P-bearing quartzites of the Veredas formation (Northern Espinhaço, Brazil): LA-ICP-MS age determinations on relict and recrystallized zircon and geodynamic consequences. Precambrian Research 250, 6–26.

Fuck, R.A., Brito Neves, B.B., Schobbenhaus, C., 2008. Rodinia descendants in South America. Precambrian Research 160, 108-126.

Gradim, C., Roncato, J., Pedrosa-Soares, A.C., Cordani, U.G., Dussin, I.A., Alkmim, F.F., Queiroga, G., Jacobsohn, T., Silva, L.C., Babinski, M., 2014. The hot back-arc zone of the Araçuaí orogen, Eastern Brazil: from sedimentation to granite generation. Brazilian Journal Geology 44, 155–180.

Guadagnin F., Chemale Júnior. F., Magalhães A.J.C., Santana A., Dussin I., Takehara L., 2015. Age constraints on crystal-tuff from the Espinhaço Supergroup - insight into the Paleoproterozoic to Mesoproterozoic intracratonic basin cycles of the Congo - São Francisco Craton. Gondwana Research 7, 363-376.

Guimarães, J.T., 1996. A Bebedouro Formation no Estado da Bahia: Faciologia, Estratigrafia e Ambiente de Sedimentação. (M. Sc. Thesis) Universidade Federal da Bahia, Salvador, 155 pp.

Guimarães, J.T., Santos, R.A., Melo, R.C., 2008. Geologia da Chapada Diamantina (Projeto Ibitiara-Rio de Contas). CBPM Série arquivos abertos 31, Salvador, BA, 68 pp.

Guimarães, J.T., Alkmim, F.F., Cruz, S.C.P., 2012. Espinhaço Supergroup e São Francisco. In: Barbosa, J.S.F. (Eds.) Geologia Da Bahia, Pesquisa e Atualização, CBPM Série Publicações Especiais, Salvador, 33–85.

Guimarães, J.T., 2014. O Espinhaço Supergroup Baiano: paradoxo, correlação e evolução tectônica. In: SBG, Anais, 47 Congresso Brasileiro de Geologia, Salvador – BA, pp. 1061.

Hanson, R.E., Wilson, T.J., Brueckner, H.K., Onstott, T.C., Wardlaw, M.S., Johnd, C.C., Hardcastle, K.C., 1988. Reconnaissance geochronology, tectonothermalevolution, and regional significance of the middle Proterozoic Choma-Kalomo Block, Southern Zambia. Precambrian Reserach 42, 39–61.

Heilbron, M. and Machado, N., 2003. Timing of terrane accretion in the Neoproterozoic-Eopaleozoic Ribeira orogen (SE Brazil). Precambrian Research 125, 87-112.

Inda H.A.V., Barbosa, J.F., 1978. Texto explicativo para o Mapa Geológico do Estado da Bahia, Escala 1:1.000.000. CPM-SME BA/CBPM, Salvador, BA, 137pp.

Kaul, P.F.T., 1970. Geologia da quadrícula Boquira, Bahia. SUDENE/DRN/DG, Relatório interno, Recife, PE, 59 pp.

Knauer, L.G., Lopes-Silva, L., Souza, F.B., Silva, L.R., Carmo, R.C., 2007. Nota explicativa da Folha Monte Azul, SD.23-Z-D-II, escala 1:100.000. CPRM-PRONAGEO.

Kuchenbecker, M., Pedrosa-Soares, A.C., Babinski, M., Fanning, M., 2015. Detrital zircon age patterns and provenance assessment for pre-glacial to post-glacial successions of the Neoproterozoic Macaúbas Group, Araçuaí orogen, Brazil. Precambrian Research 266, 12-26.

Lobato, L.M., Pimentel, M., Cruz, S.C.P., Machado, N., Noce, C.M., Alkmim, F.F., 2015. U-Pb Geochronology of the Lagoa Real Uranium District, Brazil: Implications for the age of the uranium mineralization. Journal of South American Earth Sciences 58, 129-140.

Lopes, G.A.C., 2002. Projeto Guajeru, 1. CBPM, Salvador, 408 pp.

Lopes, T.C., 2012. O Espinhaço Supergroup na Serra do Cabral, Minas Gerais: contribuição ao estudo de proveniência sedimentar. (M.Sc. thesis) Universidade Federal de Minas Gerais, Belo Horizonte, 116 pp.

Loureiro H.S.C., Bahiense I.C., Neves J.P., Guimarães J.T., Teixeira L.R., Santos R.A., Melo R.C., 2009. Geologia e recursos minerais da parte norte do corredor de deformação do Paramirim (Projeto Barra – Oliveira dos Brejinhos). CBPM. Série Arquivos Abertos 33, Salvador, BA, 113 pp.

Ludwig K.R., 2012. Software: Isoplot Version 3.75: a Geochronological Toolkit for Microsoft Excel. Berkeley Geochronology Center, Berkeley, CA, 150 pp.

Machado, G.S., 2008. Geologia da porção sul do complexo Lagoa Real, Caetité, Bahia. (Undergraduate Thesis) Universidade Federal da Bahia, Salvador, 90pp.

Machado, N., Schrank, A., Abreu, F.R., Knauer, L.G., Almeida-Abreu, P.A., 1989. Resultados preliminares da geocronologia U–Pb na Serra do Espinhaço Meridional. Boletim Núcleo Minas Gerais-Sociedade Brasileira de Geologia 10, 171–174.

Marinho, M.M., 1991. La séquence volcano-sédimentaire de Contendas-Mirante et la bordure occidentale du Bloc Jequié (Craton du São Francisco, Brésil): un exemple de transition Archéen-Proterozóïque. (Ph.D. Thesis) Univ. Clemont-Ferrand, Clemont-Ferrand, 388 pp.

Martin, H., Peucat, J.J., Sabaté, P., Cunha, J.C., 1991. Um segment de croûte continentale d'Age archéean ancien (3.5 millards d'années): lê massif de Sete Voltas (Bahia, Brésil). Les Comptes Rendus de l'Académie des Sciences Paris 313, 531-538.

Martins, A.A.M., 2014. Projeto Brumado-Condeúba. Salvador, CPRM (No prelo, Programa Geologia do Brasil- PGB).

Medeiros E.L.M., 2013. Geologia e Geocronologia do Complexo Santa Izabel, na região de Urandi, Bahia., 2013. (M. Sc. Thesis) Universidade Federal da Bahia, Salvador, 96 pp.

Menezes, R.C.L., Conceição, H., Rosa, M.L.S., Macambira, M.J.B., Galarza, M.A., Rios, D. C., 2012. Geoquímica e geocronologia de granitos anorogênicos tonianos (c.914–899 Ma) da Faixa Araçuaí no Sul do Estado da Bahia. Geonomos 20, 1–13.

Noce C.M., Zucchetti M., Baltazar O.F., Armstrong R., Dantas E.L., Renger F.E., Lobato L. M., 2005. Age of felsic volcanism and the role of ancient continental crust in the evolution of the Neoarchean Rio das Velhas greenstone belt (Quadrilátero Ferrífero, Brazil): U-Pb zircon dating of volcaniclastic graywackes. Precambrian Research 141, 67-82.

Noce, C.M., Pedrosa-Soares, A.C., Silva, L.C., Armstrong, R., Piuzana, D., 2007. Evolution of polycyclic basement complexes in the Araçuaí Orogen, based on U-Pb SHRIMP data: Implications for Brazil-Africa links in Paleoproterozoic time. Precambrian Research 159, 60-78.

Nutman, A.P., Cordani, U.G., Sabaté, P., 1994. SHRIMP U-Pb ages of detrital zircons from the early Proterozoic Contendas-Mirante supracrustal belt, Francisco Craton, Bahia, Brazil. Journal South American Earth Sciences 7, 109-114.

Paquette, J.L., Barbosa, J.S.F., Rohais, S. Cruz, S.C.P., Goncalves, P., Peucat, J.J., Leal, A.B.M., Santos-Pinto, M., Martin, H., 2015. The geological roots of South America: 4.1Ga and 3.7Ga zircon crystals discovered in NE Brazil and NW, Argentina. Precambrian Research 271, 49-55.

Pedrosa-Soares, A.C., Noce, C.M., Alkmim, F.F., Silva, L.C., Babinski, M., Cordani, U., Castañeda, C., 2007. Orógeno Araçuaí: síntese do conhecimento 30 anos após Almeida 1977. Geonomos 15, 1–16.

Pedrosa-Soares, A.C., Alkmim, F.F., 2011. How many rifting events preceded the development of the Araçuaí-West Congo orogen? Geonomos 12, 244-251.

Pedrosa-Soares A.C., Babinski M., Noce C., Martins M., Queiroga G., Vilela F., 2011. The Neoproterozoic Macaúbas Group (Araçuaí orogen, SE Brazil) with emphasis on the diamictite formations. In: Arnaud, E., Halverson, G. P. Shields-Zhou, G. (Eds.), The Geological Record of Neoproterozoic Glaciations. Geological Society London, 523–534.

Pereira-Varjão L.M., 2011. Geologia, Petrografia e Litogeoquímica dos Diques Máficos da Porção Sudeste do Bloco Gavião, Bahia, Brasil. (M. Sc. Thesis) Universidade Federal da Bahia, Salvador, 114 pp.

Pettersson, Å, Cornell, D.H., Moen, H.F.G., Reddy, S., Evans, D., 2007. Ion-probe datingof 1.2 Ga collision and crustal architecture in the Namaqua-Natal Province ofsouthern Africa. Precambrian Research. 158, 79–92.

Peucat, J.J., Mascarenhas, J.F., Barbosa, J.S., Souza, F.S., Marinho, M.M., Fanning, C.M. Leite, C.M.M., 2002. 3.3 Ga SHRIMP U-Pb zircon age of a felsic metavolcanic rock from the Mundo Novo greenstone belt in the São Francisco craton, Bahia (NE Brazil). Journal South American Earth Sciences 15, 363-373.

Pimentel, M.M., Machado, N., Lobato, L.M., 1994. Geocronologia U/Pb de rochas graníticas e gnáissicas da região de Lagoa Real, Bahia, e implicações para a idade da mineralização de urânio. In: Congresso Brasileiro de Geologia, 38, Boletim de Resumos Expandidos, pp. 389-390.

Queiroga, G.N., 2010. Caracterização de restos de litosfera oceânica do Orógeno Araçuaí entre os paralelos 17◦ e 21◦S. (Ph.D. thesis) Universidade Federal de Minas Gerais, Belo Horizonte, 180 pp.

Queiroga, G.N., Pedrosa-Soares, A.C., Noce, C.M., Alkmim, F.F., Pimentel, M.M., Dantas, E., Martins, M., Castañeda, C., Suita, M.T.F. & Prichard, H. 2007. Age of the Ribeirão da Folha ophiolite, Araçuaí Orogen: The U-Pb Zircon (la-icpms) dating of a plagiogranite. Geonomos 15, 61-65.

Ring, U., Kröner, A., Layer, P., Buchwaldt, R., Toulkeredis, T., 1999. Deformed A-typegranites in northern Malawi, east-central Africa: pre- or syntectonic. Journal Geology Society London 156, 695–714.

Rosa, A.M.L.S., Conceição, H., Oberli, F., Meier, M., Martin, H., Macambira, M.B., Santos, E.B., Paim, M.M., Leahy, G.A.S., Bastos Leal, L.R., 2000. Geochronology (U-Pb/Pb-Pb) and isotopic signature (Rb-Sr/Sm-Nd) of the paleoproterozoic Guanambi Batholith, southWestern Bahia State (NE Brazil). Revista Brasileira de Geociências 30, 062-065.

Santana, A.V., 2016. Análise estratigráfica em alta resolução em rampa carbonática dominada por microbiolitos, Formação Salitre, Bacia de Irecê, Bahia. (Ph.D. Thesis) Universidade de Brasília, Brasília, pp.

Santos-Pinto, M.A., Peucat, J.J., Martin, H., Sabaté, P., 1998. Recycling of the Archaean continental crust: the case study of the Gavião Block, Bahia, Brazil. Journal of South American Earth Science 11, 487-498.

Santos-Pinto, M.A.S., Peucat, J.J., Martin, H., Barbosa, J.S.F., Fanning, C.M., Cocherie, A., Paquette, J.L., 2012. Crustal evolution between 2.0 and 3.5 Ga in the southern Gavião block (Umburanas-Brumado-Aracatu region), São Francisco Craton, Brazil: A 3.5–3.8 Ga proto-crust in the Gavião block? Journal of South American Earth Sciences 40, 129-142.

Schobbenhaus, C., Hoppe, A., Baumann, A., Lork, A., 1994. Idade U/Pb do vulcanismo Rio dos Remédios, Chapada Diamantina, Bahia. In: SBG, Congresso Brasileiro de Geologia, 38, Anais, pp. 397-399.

Schobbenhaus, C., 1996. As tafrogêneses superpostas Espinhaço e Santo Onofre, estado da Bahia: Revisão e novas propostas. Revista. Brasileira de Geociências 4, 265-276.

Schobbenhaus, C., Kaul, P.F.T., 1971. Contribuição à estratigrafia da Chapada Diamantina - Bahia - Central. Minerário e Metalurgia 53, 116-120.

Silva, L.C., Pedrosa-Soares, A.C., Teixeira, L.R., 2008. Tonian rift-related, A-type continental plutonism in the Araçuaí orogen, Eastern Brazil: new evidences for the breakup stage of the São Francisco–Congo Paleocontinent. Gondwana Research 13, 527–537.

Silva, L.C., Pedrosa-Soares, A.C., Armstrong, R.P., Piva, C., Reis T.M.J., Piacentini M. A. P., Santos, G. G.., 2016. Disclosing the Paleoarchean to Ediacaran history of the São Francisco craton basement: The Porteirinha domain (northern Araçuaí orogen, Brazil). Journal of South American Earth Sciences 68, 50-67.

Silva, C.M.T., 2010. O Sistema Transcorrente da Porção Sudeste do Orógeno Araçuaí e Norte da Faixa Ribeira: Geometria e Significado Tectônico. (Ph. D. Thesis) Universidade Federal de Ouro Preto, Ouro Preto, 249 pp.

Silveira, E.P., Söderlund, U., Oliveira, E.P., Ernst, R., Menezes Leal, A.B., 2013. First precise U-Pb baddeleyite ages of 1500 Ma mafic dykes from the São Francisco Craton, Brazil, and tectonic implications. Lithos 174, 144-156.

Sousa, F. R., Freitas, M.S., Virgens-Neto, J., 2014. Geologia e Recursos Minerais das Folhas Parnaguá, Rio Paraim e Mansidão - SC.23-Z-A-V, escalas 1:100.000, Programa Geologia do Brasil, CPRM – Serviço Geológico do Brasil, Teresina, PI, 88 pp.

Souza, M.E.S., 2016. Caracterização Litoestrutural e Geocronológica dos Metagabros e Xistos Verdes do Macaúbas Group na Faixa Terra Branca-Planalto de Minas, Minas Gerais. (M. Sc. Thesis) Universidade Federal de Ouro Preto, Ouro Preto, 245 pp.

Souza, J.D., 2003. Geologia e Recursos Minerais do Estado da Bahia: Sistema de Informações Geográficas - SIG e Mapas. CPRM, Salvador, BA, CD-ROM.

Tack, L., Liégeois, J.P., Deblond, A., Duchesne, J.C., 1994. Kibaran A-type granitoidsand mafic rocks generated by two mantle sources in a late orogenic setting (Burundi). Precambrian Research 68, 323–356.

Tack, L., Wingate, M.T.D., De Waele, B., Meert, J., Belousova, E., Griffin, B., Tahon,A., Fernandez-Alonso, M., 2010. The 1375 Ma Kibaran Event in Central Africa: prominent emplacement of bimodal magmatism under extensional regime. Precambrian Research 180, 63–84.

Tack, L., Wingate, M.T.D., Liégeois, J.P., Fernandez-Alonso, M., Deblond, A., 2001. Early Neoproterozoic magmatism (1000–910 Ma) of the Zadinian and Mayumbian Groups (Bas-Congo): onset of Rodinian rifting at the western edge of the Congo Craton. Precambrian Reserach 110, 277–306.

Thiéblemont, P., Castaing, C., Billa, M., Bouton, P., Préat, A., 2009. Notice explicative de la carte géologique et des ressources minérales de la République Gabonaise à 1/1000000. Editions DGMG, Ministère des Mines, du Pétrole, des Hydrocarbures, Libreville, Gabon.

Turpin, L., Maruèjol, P., Cuney, M., 1988. U-Pb, Rb-Sr and Sm-Nd chronology of granitic basement, hydrotermal albitites and uranium mineralization, Lagoa Real, South Bahia, Brazil. Contribution to Mineralogy and Petrology 98, 139-147.

Van Achterbergh, E., Ryan, C.G., Jackson, S.E., Griffin, W., 2001. Appendix III. Data reduction software for LAICP-MS. In: Sylvester, P. (Eds.), Laser-ablation-ICP-MS in the Earth sciences, principles and applications. Mineralogical Association of Canada. Short Course Series 29, 239–243.

Victória A.M., Cruz, S.C.P., Pedrosa-Soares, A., Dussin, I., Borges, R., 2015. New Insights on Rifting Events in the São Francisco-Congo Paleocontinent: The Early tonian Plutonic-Volcanic Province of the Southern Bahia and Nortgeastern Minas Gerais, Brazil. ATECSUD, Simpósio de Tectónica Sudamericana em Santiago-Chile, 1, Anais, p

Appendix A- Analytical techniques in the Ouro Preto Laboratory

Instrument	Element 2
Scan mode	E-Scan
Scanned masses	202, 204, 206, 207, 208, 232, 238
Mass resolution	300
Dwell time	4 (202), 4 (204), 14 (206), 20 (207), 10 (208), 10 (232), 14 (238) ms
Integration time	0.9 s
Background	15 s
Ablation time	30 s
Carrier Gas	0,5 L/min He (+ 1,0 L/min Ar)
Laser	CETAC LSX-213 G2 +
Spot size	20 μ
Laser settings	10 Hz, 3,5 J/cm³
Cell volume	Low (teardrop)

Appendix B- Zircon U-Pb data of samples from Algodão Formation and Santo Onofre Grup (Serra da Garapa and Boqueirão Formation) obtained through in situ Laser Ablation ICP-MS. 1: concentration uncertainty c. 20%; 2: data not corrected for common-Pb; The decay constants of Jaffrey et al. (1971) were used.

Sample SCP SALTO	Isotopic Ratios						ρ	Age (Ma)						Disc (%)
	$^{207}Pb/^{235}U$	Error 1σ	$^{206}Pb/^{238}U$	Error 1σ	$^{207}Pb/^{206}Pb$	Error 1σ		$^{206}Pb/^{238}U$	Error 1σ	$^{207}Pb/^{235}U$	Error 1σ	$^{207}Pb/^{206}Pb$	Error 1σ	
4.sSMPABC020	14.97559	0.13341	0.57041	0.00479	0.19043	0.00203	0.942635823	2909.5	19.67	2813.7	8.48	2745.878883	17.45	-3.3
4.sSMPABC058	7.39853	0.06765	0.39894	0.00308	0.1345	0.00159	0.844346624	2164.1	14.21	2160.8	8.18	2157.540633	20.53	-0.2
4.sSMPABC050	7.49831	0.0728	0.40152	0.00321	0.13544	0.00168	0.823436022	2176	14.77	2172.8	8.7	2169.685353	21.45	-0.1
4.sSMPABC045	7.53335	0.07677	0.40127	0.00329	0.13617	0.00175	0.804555134	2174.9	15.12	2177	9.13	2179.047778	22.17	0.1
4.sSMPABC054	8.50446	0.07465	0.42486	0.00325	0.14518	0.00166	0.871474025	2282.5	14.68	2286.4	7.98	2289.912468	19.5	0.2
4.sSMPABC026	7.29717	0.0648	0.39465	0.00307	0.13412	0.00153	0.876003268	2144.4	14.2	2148.5	7.93	2152.602295	19.84	0.2
4.sSMPABC035	12.44728	0.09744	0.50444	0.00355	0.17897	0.00194	0.898992399	2632.9	15.2	2638.8	7.36	2643.348848	17.86	0.2
4.sSMPABC017	12.67503	0.10474	0.5083	0.00401	0.18086	0.0019	0.954686298	2649.4	17.16	2655.8	7.78	2660.772229	17.34	0.2
4.sSMPABC049	7.37196	0.06517	0.39635	0.00313	0.1349	0.00151	0.893306973	2152.2	14.46	2157.6	7.9	2162.720933	19.45	0.3
4.sSMPABC027	6.7141	0.05801	0.3773	0.00296	0.12908	0.00142	0.908008357	2063.7	13.86	2074.5	7.64	2085.478463	19.24	0.5
4.sSMPABC060	6.75013	0.07124	0.37424	0.00307	0.13084	0.00169	0.777278038	2049.3	14.41	2079.2	9.33	2109.269518	22.5	1.5
4.sSMPABC041	6.71866	0.06201	0.37305	0.00309	0.13063	0.00146	0.897454352	2043.7	14.49	2075.1	8.16	2106.45101	19.52	1.5
4.sSMPABC018	6.75208	0.06399	0.37371	0.00305	0.13106	0.00154	0.861173365	2046.8	14.33	2079.5	8.38	2112.216438	20.48	1.6

Sample CNB 64	Isotopic Ratios				ρ	Age (Ma)					Disc (%)
	$^{207}Pb/^{235}U$	Error 1σ	$^{206}Pb/^{238}U$	Error 1σ		$^{206}Pb/^{238}U$	Error 1σ	$^{207}Pb/^{235}U$	Error 1σ	$^{207}Pb/^{206}Pb$	Error 1σ	
5.sSMPABC022	7.52116	0.06824	0.40042	0.00361	0.993659	2170.973	16.6	2174.6	8.13	2178.02468	17.67	0.2
5.sSMPABC023	10.91152	0.10098	0.47602	0.00422	0.957937	2509.907	18.42	2514.392	8.61	2518.015411	17.92	0.2
5.sSMPABC026	12.55619	0.11115	0.50667	0.00422	0.940883	2642.398	18.04	2646.241	8.33	2649.180214	17.87	0.1
5.sSMPABC033	7.29529	0.06873	0.39818	0.00335	0.893021	2160.654	15.44	2147.691	8.41	2135.317391	19.88	-0.6
5.sSMPABC038	7.42953	0.07102	0.39868	0.00341	0.894768	2162.958	15.7	2163.964	8.55	2164.917016	19.96	0.0
5.sSMPABC039	11.68244	0.10238	0.48969	0.00428	0.997335	2569.335	18.53	2578.235	8.2	2585.23907	16.84	0.3
5.sSMPABC040	11.97235	0.12881	0.49671	0.00444	0.830826	2599.641	19.14	2602.6	10.08	2604.903353	21.2	0.1
5.sSMPABC042	15.75502	0.14058	0.55522	0.00481	0.970902	2846.846	19.95	2860.835	8.52	2870.701735	17.06	0.5
5.sSMPABC043	7.52975	0.08971	0.39732	0.00372	0.785855	2156.687	17.15	2176.742	10.68	2195.699869	24.03	0.9
5.sSMPABC045	11.17479	0.10988	0.48228	0.00463	0.976343	2537.189	20.13	2536.705	9.16	2536.317658	17.78	0.0
5.sSMPABC047	12.72485	0.12134	0.50918	0.00425	0.875319	2653.128	18.15	2659.235	8.98	2663.884228	19.2	0.2
5.sSMPABC055	6.72299	0.0799	0.37714	0.00384	0.856731	2062.91	17.98	2074.908	10.5	2086.840617	22.75	0.6
5.sSMPABC058	11.33541	0.10676	0.48388	0.00437	0.958898	2544.144	18.98	2550.289	8.79	2555.179319	17.74	0.2
5.sSMPABC062	11.63142	0.1045	0.48888	0.00418	0.951679	2565.829	18.09	2573.761	8.4	2580.014097	17.71	0.3
5.sSMPABC064	8.64703	0.07309	0.4294	0.00354	0.975327	2303.012	15.95	2300.391	7.69	2298.064686	17.57	-0.1
5.sSMPABC065	10.92379	0.10163	0.47506	0.00404	0.91408	2505.713	17.64	2516.037	8.65	2524.377163	18.78	0.4
5.sSMPABC076	11.37513	0.11311	0.48168	0.00413	0.862277	2534.579	17.97	2554.083	9.28	2569.604453	19.95	0.8
5.sSMPABC077	7.49305	0.06594	0.39916	0.00347	0.987853	2165.17	15.98	2171.184	7.88	2176.872838	17.66	0.3
5.sSMPABC081	7.43089	0.06592	0.40237	0.00353	0.988946	2179.943	16.22	2163.687	7.94	2148.300171	17.73	-0.7
5.sSMPABC085	11.33916	0.10262	0.48091	0.004	0.919063	2531.228	17.39	2550.462	8.44	2565.791459	18.37	0.8
5.sSMPABC096	6.71374	0.07132	0.3764	0.00324	0.810305	2059.445	15.17	2074.266	9.39	2089.017437	22.23	0.7
5.sSMPABC098	11.04474	0.11089	0.47878	0.00472	0.981904	2521.95	20.56	2526.028	9.35	2529.305836	17.95	0.2
5.sSMPABC133	11.02824	0.10295	0.47947	0.00433	0.967401	2524.957	18.88	2524.691	8.69	2524.477917	17.46	0.0
5.sSMPABC135	11.99536	0.13713	0.49669	0.00496	0.873528	2599.555	21.38	2602.991	10.71	2605.665307	21.29	0.1
5.sSMPABC137	5.83239	0.05674	0.35187	0.00337	0.984475	1943.522	16.07	1950.542	8.43	1958.002152	18.71	0.36
5.sSMPABC140	7.08822	0.07142	0.38993	0.0037	0.941743	2122.504	17.16	2121.616	8.97	2120.755755	19.12	-0.04
5.sSMPABC145	7.09219	0.07271	0.39222	0.00358	0.890306	2133.116	16.59	2122.016	9.12	2111.279424	20.39	-0.52

Sample MPA	Isotopic Ratios						ρ	Age (Ma)						Disc (%)
	$^{207}Pb/^{235}U$	Error 1σ	$^{206}Pb/^{238}U$	Error 1σ	$^{207}Pb/^{206}Pb$	Error 1σ		$^{206}Pb/^{238}U$	Error 1σ	$^{207}Pb/^{235}U$	Error 1σ	$^{207}Pb/^{206}Pb$	Error 1σ	
4.sSMPABC089	7.03815	0.06733	0.38933	0.00317	0.13112	0.00153	0.851121	2119.7	14.71	2116.3	8.51	2113.019116	20.39	-0.2
4.sSMPABC043	7.50471	0.06369	0.40159	0.00318	0.13552	0.00146	0.933054	2176.4	14.61	2173.5	7.6	2170.714303	18.65	-0.1
4.sSMPABC057	5.74816	0.05341	0.3512	0.00293	0.1187	0.00133	0.897882	1940.3	14	1938.6	8.04	1936.747151	19.94	-0.1
4.sSMPABC044	6.21777	0.05628	0.36559	0.0029	0.12335	0.00141	0.876363	2008.6	13.68	2007	7.92	2005.238782	20.15	-0.1
4.sSMPABC059	8.8234	0.07357	0.43351	0.0034	0.14761	0.00157	0.940622	2321.5	15.31	2319.9	7.6	2318.421682	18.11	-0.1
4.sSMPABC037	8.88397	0.07605	0.43482	0.00346	0.14817	0.00161	0.929554	2327.4	15.55	2326.2	7.81	2324.913143	18.52	-0.1
4.sSMPABC079	12.77081	0.12207	0.51164	0.00436	0.18103	0.00211	0.891521	2663.6	18.59	2662.9	9	2662.329074	19.16	0.0
4.sSMPABC056	6.19239	0.05726	0.36434	0.00304	0.12326	0.00137	0.902347	2002.7	14.38	2003.4	8.08	2003.942891	19.63	0.0
4.sSMPABC035	7.17011	0.07083	0.39186	0.00337	0.1327	0.00158	0.870578	2131.4	15.63	2132.8	8.8	2133.999573	20.68	0.1
4.sSMPABC061	12.03269	0.10184	0.49792	0.00398	0.17525	0.00186	0.944426	2604.8	17.11	2607	7.93	2608.424003	17.61	0.1
4.sSMPABC080	12.59669	0.11244	0.5077	0.00421	0.17994	0.00198	0.928989	2646.8	17.99	2650	8.4	2652.317469	18.11	0.1
4.sSMPABC062	11.24197	0.09176	0.48291	0.00376	0.16883	0.00176	0.953917	2539.9	16.35	2543.4	7.61	2546.077175	17.4	0.1
4.sSMPABC058	4.62117	0.05163	0.31198	0.00275	0.10742	0.0014	0.788961	1750.5	13.52	1753.1	9.33	1756.104383	23.62	0.1
4.sSMPABC064	8.61722	0.08125	0.42747	0.00348	0.1462	0.00172	0.863411	2294.3	15.71	2298.4	8.58	2301.947472	20.08	0.2
4.sSMPABC083	7.50306	0.0967	0.39988	0.00401	0.13607	0.002	0.778084	2168.5	18.46	2173.4	11.55	2177.768794	25.39	0.2
4.sSMPABC065	6.39314	0.07757	0.36943	0.00352	0.1255	0.00175	0.785292	2026.7	16.58	2031.3	10.65	2035.861778	24.5	0.2
4.sSMPABC036	9.39459	0.11695	0.44469	0.0045	0.15321	0.0022	0.812892	2371.6	20.09	2377.3	11.42	2382.065326	24.26	0.2
4.sSMPABC084	7.88806	0.11414	0.40956	0.00436	0.1397	0.0023	0.735701	2212.9	19.93	2218.3	13.04	2223.492871	28.23	0.2
4.sSMPABC060	8.22476	0.0786	0.41781	0.00334	0.14278	0.0017	0.836505	2250.5	15.19	2256.1	8.65	2261.195719	20.43	0.2
4.sSMPABC085	7.07722	0.07889	0.3885	0.00351	0.13212	0.00173	0.810507	2115.9	16.29	2121.2	9.92	2126.332752	22.81	0.3
4.sSMPABC095	6.85412	0.08241	0.38213	0.00363	0.13009	0.00182	0.790073	2086.2	16.94	2092.7	10.65	2099.17844	24.36	0.3
4.sSMPABC048	10.23847	0.09513	0.46193	0.00389	0.16074	0.00183	0.90634	2448.1	17.17	2456.6	8.59	2463.459296	19.16	0.3
4.sSMPABC030	6.12916	0.06307	0.36106	0.00319	0.12311	0.00151	0.858597	1987.2	15.11	1994.4	8.98	2001.780537	21.63	0.4
4.sSMPABC051	6.93091	0.07663	0.3839	0.00352	0.13094	0.00169	0.829308	2094.5	16.4	2102.6	9.81	2110.609762	22.45	0.4
4.sSMPABC093	6.49759	0.06231	0.37151	0.00315	0.12683	0.00146	0.884168	2036.5	14.79	2045.6	8.44	2054.490989	20.12	0.4
4.sSMPABC026	1.46403	0.01284	0.15089	0.00117	0.07036	0.00078	0.884118	906	6.55	915.7	5.29	938.8774617	22.6	1.1
4.sSMPABC016	2.86057	0.02438	0.23245	0.00177	0.08925	0.00099	0.893434	1347.3	9.24	1371.6	6.41	1409.53047	20.98	1.8

Sample MPC	Isotopic Ratios						ρ	Age (Ma)						Disc (%)
	$^{207}Pb/^{235}U$	Error 1σ	$^{206}Pb/^{238}U$	Error 1σ	$^{207}Pb/^{206}Pb$	Error 1σ		$^{206}Pb/^{238}U$	Error 1σ	$^{207}Pb/^{235}U$	Error 1σ	$^{207}Pb/^{206}Pb$	Error 1σ	
4.sSMPABC045	4.99369	0.05255	0.32888	0.00268	0.11014	0.00145	0.774365844	1833	12.99	1818.3	8.9	1801.716659	23.72	-0.8
4.sSMPABC036	5.02848	0.05286	0.3296	0.00278	0.11066	0.00143	0.802356105	1836.5	13.49	1824.1	8.9	1810.279632	23.24	-0.7
4.sSMPABC090	1.44496	0.0244	0.15217	0.00151	0.06887	0.0013	0.587643457	913.1	8.47	907.8	10.13	894.8488202	38.52	-0.6
4.sSMPABC040	2.47452	0.04215	0.21806	0.00236	0.08235	0.00157	0.63537392	1271.6	12.48	1264.6	12.32	1253.853176	36.66	-0.6
4.sSMPABC051	4.341	0.03623	0.30388	0.00231	0.10361	0.00113	0.91081739	1710.5	11.4	1701.2	6.89	1689.77164	19.93	-0.5
4.sSMPABC060	2.1964	0.02162	0.20162	0.00153	0.07901	0.00098	0.77092755	1184	8.23	1179.9	6.87	1172.38544	24.35	-0.3
4.sSMPABC069	4.31263	0.04156	0.30188	0.0024	0.10361	0.00125	0.824980268	1700.6	11.87	1695.8	7.94	1689.77164	22.1	-0.3
4.sSMPABC041	6.01802	0.05526	0.36036	0.00291	0.12112	0.00139	0.879425708	1983.9	13.79	1978.5	8	1972.788885	20.38	-0.3
4.sSMPABC050	3.94804	0.03387	0.28702	0.00219	0.09977	0.00111	0.889402411	1626.6	10.98	1623.6	6.95	1619.798792	20.53	-0.2
4.sSMPABC054	5.11227	0.05157	0.33049	0.00281	0.11222	0.00136	0.842877863	1840.8	13.62	1838.1	8.57	1835.676361	21.77	-0.1
4.sSMPABC016	4.68586	0.04904	0.31528	0.0026	0.10782	0.00141	0.78798105	1766.6	12.74	1764.7	8.76	1762.900348	23.61	-0.1
4.sSMPABC038	4.6594	0.07356	0.31426	0.00328	0.10757	0.00195	0.661108913	1761.6	16.1	1760	13.2	1758.656504	32.81	-0.1
4.sSMPABC085	5.04152	0.06453	0.32774	0.00306	0.11156	0.00167	0.729443748	1827.4	14.83	1826.3	10.85	1824.984545	26.85	-0.1
4.sSMPABC017	4.9968	0.04934	0.32616	0.00267	0.11113	0.00137	0.82903599	1819.8	12.96	1818.8	8.35	1817.97702	22.22	-0.1
4.sSMPABC020	11.75694	0.09463	0.49365	0.00376	0.17273	0.00184	0.946311603	2586.5	16.21	2585.2	7.53	2584.272915	17.71	-0.1
4.sSMPABC059	1.72159	0.02436	0.1709	0.0015	0.07307	0.00121	0.620299804	1017.1	8.26	1016.6	9.09	1015.894759	33.16	0.0
4.sSMPABC023	6.46612	0.08618	0.37268	0.00382	0.12586	0.00194	0.769067655	2042	17.95	2041.3	11.72	2040.927618	26.95	0.0
4.sSMPABC086	4.37582	0.0539	0.30339	0.00263	0.1046	0.00153	0.703760958	1708.1	13.01	1707.8	10.18	1707.293156	26.75	0.0
4.sSMPABC043	2.39851	0.02749	0.21256	0.00181	0.08184	0.00112	0.742957254	1242.4	9.63	1242.2	8.21	1241.690386	26.56	0.0
4.sSMPABC068	5.26522	0.06354	0.33513	0.00303	0.11394	0.00164	0.749201492	1863.2	14.61	1863.2	10.3	1863.183217	25.72	0.0
4.sSMPABC024	3.53773	0.03596	0.26899	0.00219	0.0954	0.0012	0.800963971	1535.7	11.11	1535.7	8.05	1535.98409	23.56	0.0
4.sSMPABC067	7.23489	0.08704	0.39367	0.00364	0.13328	0.0019	0.768567673	2139.8	16.82	2140.8	10.73	2141.626455	24.74	0.0
4.sSMPABC018	3.97497	0.04726	0.28736	0.00247	0.10035	0.00144	0.722954185	1628.3	12.34	1629.1	9.64	1630.579446	26.37	0.0
4.sSMPABC029	6.81077	0.06365	0.38188	0.00311	0.12937	0.00151	0.871427541	2085	14.53	2087.1	8.27	2089.425232	20.35	0.1
4.sSMPABC021	11.72837	0.09488	0.4921	0.00368	0.17288	0.00188	0.924394677	2579.8	15.91	2583	7.57	2585.721904	18.07	0.1
4.sSMPABC089	5.56229	0.07379	0.34435	0.00332	0.11715	0.00179	0.726765184	1907.6	15.94	1910.3	11.42	1913.191771	27.16	0.1
4.sSMPABC083	7.28223	0.10586	0.39441	0.00414	0.1339	0.00222	0.72207935	2143.3	19.15	2146.6	12.98	2149.735618	28.68	0.2
4.sSMPABC081	2.43296	0.03302	0.21403	0.00191	0.08244	0.00131	0.657531579	1250.3	10.15	1252.4	9.77	1255.989544	30.61	0.2
4.sSMPABC028	6.64213	0.05728	0.37682	0.00293	0.12786	0.00142	0.901650104	2061.4	13.71	2065	7.61	2068.757574	19.51	0.2
4.sSMPABC063	2.35156	0.05605	0.20943	0.00275	0.08145	0.00211	0.550901872	1225.8	14.66	1228	16.98	1232.323745	49.87	0.2
4.sSMPABC048	2.25533	0.03182	0.2039	0.0019	0.08022	0.0013	0.66045966	1196.3	10.19	1198.5	9.92	1202.401826	31.67	0.2
4.sSMPABC044	4.93411	0.04379	0.32305	0.00247	0.11078	0.00128	0.861511522	1804.6	12.04	1808.1	7.49	1812.248717	20.77	0.2
4.sSMPABC056	3.89083	0.03856	0.28341	0.00231	0.09957	0.00122	0.822435864	1608.5	11.59	1611.8	8.01	1616.063285	22.67	0.2
4.sSMPABC084	4.68786	0.05571	0.31406	0.00272	0.10826	0.00153	0.728782193	1760.6	13.32	1765.1	9.94	1770.34027	25.71	0.3
4.sSMPABC061	7.50447	0.07789	0.39957	0.00346	0.13622	0.00171	0.834298662	2167	15.95	2173.5	9.3	2179.68685	21.68	0.3
4.sSMPABC057	3.87556	0.04541	0.28241	0.00248	0.09953	0.00139	0.749470551	1603.5	12.47	1608.6	9.46	1615.315066	25.86	0.3
4.sSMPABC049	5.02256	0.04617	0.32559	0.00244	0.1119	0.00134	0.815237273	1817	11.89	1823.1	7.78	1830.502065	21.53	0.3
4.sSMPABC030	2.92877	0.03535	0.23935	0.0021	0.08875	0.00126	0.726911789	1383.3	10.95	1389.4	9.14	1398.769737	26.88	0.4
4.sSMPABC039	2.45409	0.03052	0.21447	0.00192	0.083	0.00121	0.71984772	1252.6	10.21	1258.6	8.97	1269.215828	28.02	0.5
4.sSMPABC052	5.84953	0.0518	0.35202	0.00281	0.12053	0.00133	0.901426236	1944.3	13.39	1953.8	7.68	1964.082648	19.59	0.5
4.sSMPABC042	2.47848	0.02809	0.21579	0.00186	0.08331	0.00112	0.760528177	1259.6	9.89	1265.8	8.2	1276.488584	26.08	0.5
4.sSMPABC053	5.89284	0.05714	0.3533	0.00283	0.12098	0.00146	0.826089708	1950.3	13.49	1960.2	8.42	1970.727643	21.37	0.5
4.sSMPABC019	1.69793	0.02174	0.16821	0.00144	0.07322	0.0011	0.668607006	1002.3	7.94	1007.8	8.18	1020.048071	30.23	0.5
4.sSMPABC025	3.53764	0.05132	0.26717	0.00271	0.09608	0.00159	0.699211542	1526.4	13.8	1535.7	11.48	1549.33701	30.74	0.6
4.sSMPABC022	2.15385	0.02381	0.19694	0.00167	0.07937	0.00105	0.767076356	1158.9	8.99	1166.3	7.67	1181.377446	25.84	0.6
4.sSMPABC080	2.50359	0.03718	0.21678	0.00205	0.08376	0.00143	0.636778618	1264.9	10.85	1273.1	10.77	1286.984553	33.02	0.6
4.sSMPABC065	2.29381	0.02257	0.20506	0.00166	0.08114	0.00098	0.822721824	1202.4	8.87	1210.4	6.96	1224.837362	23.46	0.7
4.sSMPABC037	2.51988	0.03836	0.2174	0.00216	0.08407	0.00145	0.652672738	1268.1	11.44	1277.8	11.06	1294.173349	33.28	0.8
4.sSMPABC027	1.42262	0.02109	0.14811	0.00133	0.06967	0.00119	0.605730705	890.4	7.49	898.5	8.84	918.6429034	34.73	0.9
4.sSMPABC066	2.12804	0.02402	0.19398	0.00162	0.07957	0.00107	0.739886057	1142.9	8.75	1157.9	7.8	1186.35034	26.39	1.3

Sample TR-01	Isotopic Ratios				ρ	Age	
	$^{207}Pb/^{235}U$	Error 1σ	$^{206}Pb/^{238}U$	Error 1σ		$^{207}Pb/^{206}Pb$	Error 1σ
05150612d	6.0931	0.1761	0.36160	0.00973	0.93	1989	49
06150612d	1.6243	0.0511	0.16392	0.00443	0.86	982	62
07150612d	5.3019	0.1585	0.33563	0.00905	0.90	1873	52
08150612d	6.7918	0.1887	0.38078	0.01015	0.96	2089	46
09150612d	18.1788	0.5453	0.58867	0.01615	0.91	3009	46
10150612d	6.7856	0.1933	0.37708	0.01008	0.94	2105	48
11150612d	12.0949	0.3302	0.49544	0.01313	0.97	2625	43
12150612d	15.3974	0.4267	0.54799	0.01458	0.96	2857	43
15150612d	6.7419	0.1850	0.37708	0.00998	0.96	2093	46
16150612d	6.7782	0.1869	0.37679	0.00995	0.96	2104	46
17150612d	7.0634	0.1986	0.38745	0.01028	0.94	2127	47
18150612d	15.2765	0.4582	0.54918	0.01493	0.91	2840	47
19150612d	6.0697	0.1729	0.35032	0.00930	0.93	2038	48
20150612d	15.2359	0.4258	0.54785	0.01453	0.95	2840	44
21150612d	6.7310	0.1967	0.37778	0.01005	0.91	2087	50
22150612d	4.1813	0.1462	0.29513	0.00808	0.78	1674	64
25150612d	6.7572	0.1881	0.37939	0.00998	0.94	2086	47
26150612d	6.0270	0.1716	0.35884	0.00945	0.92	1983	49
27150612d	6.6183	0.1844	0.37623	0.00988	0.94	2065	47
28150612d	1.4384	0.0470	0.14940	0.00398	0.81	923	66
29150612d	6.9014	0.2009	0.38520	0.01018	0.91	2097	50
30150612d	1.3997	0.0522	0.14707	0.00398	0.73	899	76
31150612d	6.3348	0.1811	0.36569	0.00960	0.92	2037	49
32150612d	6.5075	0.1802	0.37070	0.00968	0.94	2061	47
35150612d	15.5991	0.4393	0.55480	0.01450	0.93	2858	45
36150612d	6.5876	0.1839	0.37370	0.00973	0.93	2068	48
37150612d	6.5552	0.1847	0.37300	0.00970	0.92	2063	48
38150612d	6.6774	0.1920	0.37724	0.00985	0.91	2076	50
39150612d	5.8703	0.1682	0.34927	0.00910	0.91	1984	50
40150612d	6.0410	0.1799	0.35890	0.00943	0.88	1986	52
41150612d	7.5243	0.2280	0.39720	0.01048	0.87	2194	52
42150612d	6.6531	0.1869	0.37600	0.00973	0.92	2075	48
05290612a	6.4680	0.1782	0.3678	0.0098	0.96	2064	46
06290612a	6.4054	0.1768	0.3680	0.0098	0.96	2046	46
07290612a	6.6788	0.1845	0.3763	0.0100	0.96	2081	46
08290612a	12.0765	0.3434	0.4973	0.0133	0.94	2617	45
09290612a	6.3778	0.1771	0.3685	0.0098	0.96	2036	47
10290612a	6.2154	0.1719	0.3646	0.0097	0.96	2009	47
11290612a	6.7893	0.1952	0.3713	0.0099	0.93	2133	48
12290612a	12.1521	0.3399	0.4935	0.0131	0.95	2640	44
15290612a	4.8003	0.1377	0.3142	0.0083	0.92	1812	50
16290612a	4.0539	0.1169	0.2885	0.0077	0.92	1659	51
17290612a	9.9248	0.2751	0.4462	0.0118	0.95	2469	45

18290612a	7.2583	0.2112	0.3878	0.0103	0.92	2173	49
19290612a	6.5393	0.1879	0.3715	0.0099	0.92	2066	49
20290612a	7.0400	0.2265	0.3870	0.0105	0.85	2124	55
21290612a	6.3736	0.1774	0.3623	0.0095	0.94	2065	47
22290612a	6.6402	0.1818	0.3756	0.0099	0.96	2073	46
25290612a	6.5621	0.1799	0.3737	0.0098	0.95	2061	47
26290612a	6.7185	0.1920	0.3768	0.0099	0.92	2088	49
27290612a	7.1591	0.2045	0.3901	0.0103	0.92	2139	48
28290612a	6.7450	0.1898	0.3780	0.0099	0.93	2090	48
29290612a	6.8326	0.1862	0.3834	0.0100	0.96	2088	46
30290612a	7.4019	0.2041	0.3986	0.0104	0.95	2160	47
31290612a	6.6219	0.1889	0.3749	0.0099	0.92	2072	49
32290612a	12.2059	0.3340	0.4893	0.0128	0.95	2661	44
35290612a	7.0596	0.2092	0.3871	0.0102	0.89	2128	51
36290612a	7.0792	0.2087	0.3887	0.0103	0.89	2126	51
37290612a	6.4665	0.1856	0.3693	0.0097	0.91	2056	50
38290612a	7.3610	0.2219	0.3917	0.0104	0.88	2180	52
39290612a	15.6555	0.4622	0.5526	0.0147	0.90	2870	47
40290612a	6.6026	0.1846	0.3755	0.0098	0.93	2064	48
41290612a	20.4444	0.5561	0.6193	0.0160	0.95	3116	42
42290612a	15.5590	0.4276	0.5533	0.0144	0.94	2858	44
45290612a	6.3582	0.1748	0.3658	0.0095	0.94	2044	48
46290612a	6.4564	0.1772	0.3615	0.0093	0.94	2091	47
47290612a	6.4683	0.1767	0.3722	0.0096	0.94	2043	47
48290612a	6.5865	0.1800	0.3748	0.0097	0.94	2063	47
49290612a	6.5466	0.1794	0.3676	0.0095	0.94	2087	47
50290612a	20.1049	0.5512	0.6131	0.0158	0.94	3105	43
51290612a	6.5843	0.1842	0.3736	0.0096	0.92	2068	49
52290612a	21.4845	0.5856	0.6261	0.0161	0.94	3177	42
55290612a	7.2689	0.2159	0.3906	0.0102	0.88	2163	51
56290612a	7.2863	0.2048	0.3913	0.0101	0.92	2164	48
57290612a	7.0225	0.1940	0.3875	0.0099	0.93	2117	48
58290612a	6.5469	0.1821	0.3691	0.0095	0.92	2079	48
59290612a	6.2968	0.1746	0.3640	0.0093	0.92	2035	49
60290612a	6.6453	0.1842	0.3756	0.0096	0.92	2075	48
61290612a	6.4308	0.1806	0.3592	0.0092	0.91	2096	49
62290612a	7.1683	0.1984	0.3720	0.0095	0.92	2224	48
65290612a	6.7640	0.1918	0.3791	0.0097	0.90	2090	50
66290612a	12.3840	0.3542	0.5025	0.0129	0.90	2641	47
67290612a	6.6497	0.1849	0.3785	0.0096	0.91	2063	49
68290612a	6.8790	0.1947	0.3755	0.0096	0.90	2136	49
69290612a	6.3749	0.1800	0.3668	0.0094	0.90	2043	50
70290612a	6.6741	0.1858	0.3748	0.0095	0.91	2086	49
71290612a	6.4276	0.1796	0.3693	0.0094	0.91	2046	49
72290612a	9.7950	0.2731	0.4516	0.0115	0.91	2427	47
75290612a	6.2695	0.1764	0.3627	0.0092	0.90	2034	50
76290612a	6.4282	0.1817	0.3672	0.0093	0.90	2056	50
77290612a	6.5922	0.1872	0.3733	0.0095	0.89	2071	50

Appendix c - Analytical techniques in the Clermont Ferrand- France

In the Clermont Ferrand the analyses involved the ablation of minerals with a Resonetics Resolution M-50 powered by an ultra-short-pulse (<4ns) ATL Atlex Excimer laser system operating at a wavelength of 193 nm (detailed description in Müller et al., 2009). Spot diameters of 20 μm associated to repetition rates of 3 Hz and laser energy of 4 mJ producing a fluence of 9.5 J/cm2 were used for zircon dating. The ablated material was carried into helium and then mixed with nitrogen and argon before injection into the plasma source of an Agilent 7500 cs ICP-MS equipped with a dual pumping system to enhance sensitivity. The alignment of the instrument and mass calibration were performed before every analytical session using the NIST SRM 612 reference glass, by inspecting the signal of 238U and by minimising the ThO+/Th+ ratio (<< 1%). The mean sensitivity on 238U using a spot size of 44 □m is about 20,000 cps/ppm. The analytical method for isotope dating of zircon with laser ablation ICPMS is basically similar to that developed for zircon and monazite and reported in Tiepolo (2003) and Paquette and Tiepolo (2007). The signal of ^{204}(Pb+Hg), ^{206}Pb, ^{207}Pb, ^{208}Pb, ^{232}Th and ^{238}U masses are acquired. The occurrence of common Pb in the sample can be monitored by the evolution of the 204(Pb+Hg) signal intensity, but no common Pb correction was applied owing to the large isobaric interference from Hg. The ^{235}U signal is calculated from 238U on the basis of the ratio ^{238}U/^{235}U= 137.88. Single analyses consisted of 30 seconds of background integration with laser off followed by 1 minute integration with the laser firing and a 30 seconds delay to wash out the previous sample and prepare the next analysis.

Data are corrected for U-Pb fractionation occurring during laser sampling and for instrumental mass discrimination (mass bias) by standard bracketing with repeated measurements of GJ-1 zircon standard (Jackson et al., 2004). At the beginning and at the end of every run, repeated analyses of 91500 zircon standard (Wiedenbeck et al., 1995), treated as unknowns, independently control the reproducibility and accuracy of the corrections. Data reduction was carried out with the software package GLITTER® from Macquarie Research Ltd (van Achterbergh et al., 2001; Jackson et al., 2004). For each analysis, the time resolved signal of single isotopes and isotope ratios was monitored and carefully inspected to verify the presence of perturbations related to inclusions, fractures, mixing of different age domains or common Pb. Calculated ratios were exported and Concordia ages and diagrams were generated using Isoplot/Ex v. 2.49 software package by Ludwig (2001). The concentrations in U-Th-Pb were calibrated relative to the certified contents of GJ-1 zircon standard (Jackson et al., 2004).

CAPÍTULO 3
ARCABOUÇO ESTRUTURAL

Nesse capítulo serão apresentados os dados estruturais da porção sul do Cinturão de Dobramentos e Cavalgamentos, um importante componente da zona de deformação do Aulacógeno do Paramirim, região intracontinental do Orógeno Araçuaí.

1. Introdução

O Aulacógeno do Paramirim foi parcialmente invertido no Ediacarano durante a amalgamação de Gondwana Ocidental, no domínio intracontinental do Orógeno Araçuaí-Oeste Congo (Fig. 1). Circundado pelo Cráton São Francisco-Congo, esse orógeno representa uma incisão confinada com concavidade voltada para sul, cujos componentes magmáticos pré a pós-colisionais datam de ca. 650 a 480 Ma (Pedrosa-Soares et al., 2011). As deformações endodérmicas nesse setor foram responsáveis pela justaposição de rochas arqueanas e paleproterozoicas sobre unidade tonianas do Grupo Santo Onofre.

2. Contexto geológico

O Corredor de deformações do Paramirim consiste em uma mega feição tectônica e representa a zona de máxima inversão neoproterozoica do Aulacógeno do Paramirim, que se desenvolveu entre 1.75 e 0.67 Ga (Pedrosa Soares & Alkmim, 2011). Essa mega feição possui orientação NNW-SSE e suas extremidades são limitadas pelas faixas orogênicas Rio Preto a norte e Araçuaí a sul, o que lhe confere uma complexidade estrutural (Cruz *et al.* 2012).

O Embasamento do Corredor do Paramirim compreende as rochas da porção meridional da Placa Gavião, sendo constituído, principalmente, por ortognaisses tonalíticos-granodioríticos com enclaves anfibolíticos, às vezes migmatizados, além de sequências metavulcanossedimentares e granitoides riacianos – orosirianos (Arcanjo *et al.* 2000, Cruz *et al.* 2009). Localmente, podem ser encontrados ortognaisses charnockíticos (Arcanjo *et al.* 2000). Incluso nesse embasameto, o magmatismo anorogênico, alcalino (Machado 2008), é marcado pelos metagranitoides da Suíte Intrusiva Lagoa Real (Arcanjo *et al.* 2005). Essas rochas foram cristalizadas em torno de 1750 Ma (Turpin *et al.* 1988; Cordani *et al.* 1992;

Pimentel *et al.* 1994; Cruz *et al.* 2007; Lobato *et al.* 2015), bem como deformadas e gnaissificadas em zonas de cisalhamento no Ediacarano (Cruz & Alkmim, 2006).

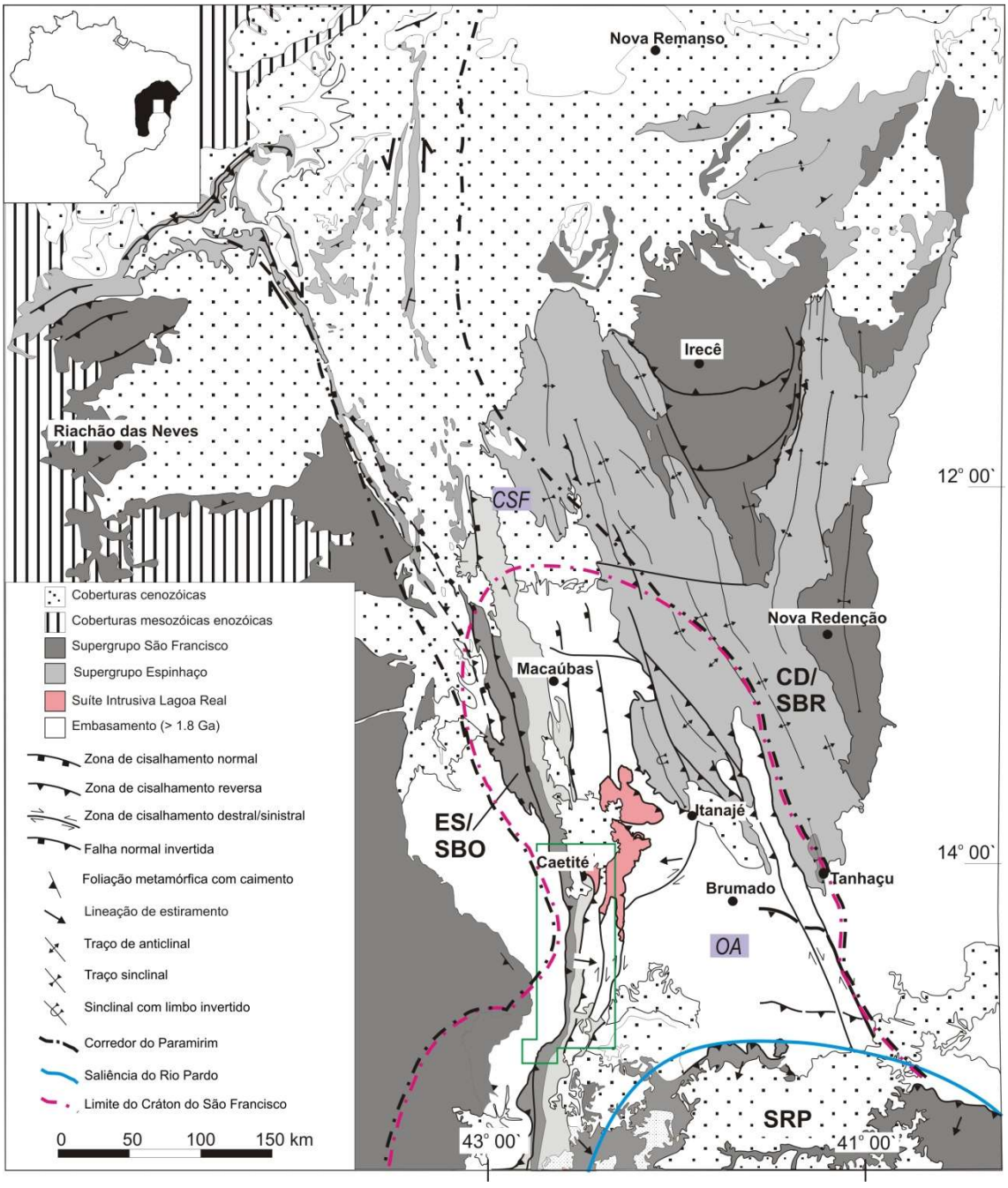

Fig. 18. Mapa Geológico simplificado do Aulacógeno do Paramirim, enfatizando as principais unidades geológicas e estruturas tectônicas de idade brasiliana. ES- Cinturão de Dobramentos e Cavalgamentos Serra do Espinhaço Setentrional, CD- Cinturão de Dobramentos e Cavalgamentos da Chapada Diamantina, SRP- Saliência do Rio Pardo, SBO- Bacia Ocidental, SBR- Bacia Oriental, CSF – Cráton do São Francisco, OA- Orógeno Araçuaí. A área de trabalho está indicada pelo polígono verde. Fonte: Cruz (2004).

Como representantes das unidades sedimentares que preencheram as bacias precursoras as deformações do neoproterozoicas tem-se as unidades do Supergrupo Espinhaço e São Francisco. Elas afloram nos cinturões Serra do Espinhaço Setentrional, à oeste do Aulacógeno do Paramirim e o Chapada Diamantina à leste. O Supergrupo Espinhaço compreende uma sucessão de rochas siliciclásticas (metarenitos, metapelitos e metaconglomerados) com rochas metavulcânicas ácidas, alcalinas e anorogênicas, subordinadas, que afloram nos cinturões de dobramentos e cavalgamentos da Serra do Espinhaço Setentrional e da Chapada Diamantina, com espessura de até 9300 e 5000 metros, respectivamente (Guimarães *et al.* 2012). Gabros/diabásios e dioritos cinza-escuro a esverdeados (Arcanjo *et al.* 2005; Brito 2008; Pereira-Varjão 2011; Damasceno 2013) intrudem as unidades dos Supergrupos Espinhaço formando soleiras e diques. Predominam gabros/diabásios e dioritos cinza-escuro a esverdeados (Arcanjo *et al.* 2005; Brito 2008; Pereira-Varjão 2011; Damasceno 2013).

O Supergrupo São Francisco compreende o Grupo Santo Onofre, um dos objetos desse estudo, no Cinturão de Dobramentos e Cavalgamentos Serra do Espinhaço Setentrional. Da base para o topo, segundo Guimarães *et al.* (2012), o Grupo Santo Onofre, com 2040 metros de espessura, compreende as formações Fazendinha, Serra da Vereda, Serra da Garapa e Boqueirão, separadas por contatos gradacionais muito bem expostos a norte de Caetité. A norte da cidade de Caetité, o Grupo Santo Onofre estrutura duas sinclinais regionais. A sul dessa cidade, o contato entre as unidades desse grupo é por zonas de cisalhamento transpressionais. Genericamente, é constituído por metarenitos feldspáticos, metarcóseos líticos e metaquartzarenitos, estratificados e maciços, com metaconglomerados oligomíticos matriz-sustentados (Guimarães *et al.* 2008).

O Corredor do Paramirim, formado no Ediacarano (Cruz & Alkmim, 2006) é resultado do desenvolvimento de uma tectônica endodérmica no setor intracontinental do Orógeno Araçuaí-Oeste Congo (Cruz & Alkmim 2006, Cruz *et al.* 2015; Borges *et al.* 2015). Nesse contexto, três famílias de estruturas foram encontradas envolvendo tanto o embasamento quanto as unidades de cobertura estateriana-toniana (Cruz & Alkmim, 2006; Cruz *et al.* 2015): (i) a mais antiga (Fase D_a) compreende zonas de cisalhamento dúcteis e dobras com orientação geral E-W e vergência para N relacionadas com a Saliência do Rio Pardo. Este conjunto de elementos estruturais registra a propagação do *front* de deformação do Orógeno Araçuaí – Oeste Congo para o norte; (ii) o segundo e dominante conjunto de estruturas (Fase D_p) é composto de uma grande variedade de elementos tectônicos, incluindo zonas de cisalhamento reversas, de empurrão e em associação com dobras e várias categorias de estruturas de grande

escala. Essas estruturas nuclearam em resposta a um encurtamento orientado segundo WSW-ENE e foram responsáveis pela gnaissificação das rochas da Suíte Intrusiva Lagoa Real, bem como pelo cavalgamento das unidades do embasamento do aulacógeno do Paramirim sobre as suas unidades de cobertura; (iii) as estruturas mais jovens são zonas de cisalhamento normais que reativam as estruturas contracionais pré-existentes e formam um conjunto de elementos tectônicos (D_e) distensivos relacionados com o colapso do Orógeno Araçuaí-Oeste Congo.

3. Resultados

3.1 Arcabouço estrutural

Na área de estudo foram identificados três domínios estruturais associados com o Cinturão de Dobramentos e Cavalgamentos Serra do Espinhaço Setentrional, denominados de Jacaraci *Fold Thrust Belt*, *Nappe* de Caetité e Domínio Transpressional (Fig. 19). A conexão entre Jacaraci Fold Thrust Belt e o Domínio Transpressional se faz por uma zona de cisalhamento transcorrente sinistral (Fig. 20).

3.1.1. Jacaraci Fold Thrust Belt

Nesse compartimento predomina a formação Algodão (Figs. 20, 21), com estratificações plano paralela e cruzada de médio a grande porte. Os planos do acamamento primários (S_0) estão representados na Figura 22A e nela pode-se verificar uma forte dispersão dessa estrutura. Na base desse cinturão, especialmente no contato das rochas do Supergrupo Espinhaço com o embasamento do Aulacógeno, são encontradas as estruturas deformacionais mais antigas da área, que são a foliação S_1 (Fig. 23A) a lineação de estiramento (Lx_1). Ambas as estruturas também apresentam intensa dispersão nas Figuras 22B, C. Embora dispesa, a lineação de estiramento ocupa, principalmente, os quadrantes SW e SE. Indicadores de movimento, tais como estrutura S/C, sugerem topo estrutural, em geral, para NW. Na medida em que se afasta da base do cinturão há uma diminuição gradativa da deformação e o acamadamento primário (S_0) volta a predominar. Neste caso, falhas e zonas de cisalhamento reversas e de empurrão, intra e interestratais, são observadas com menor frequência.

A foliação $S_0//S_1$ do Jacaraci Fold Thrust Belt encontra-se dobrada, formando estruturas abertas, em geral simétricas, harmônicas, com orientação geral ENE-WSW (Fig. 21). Um segundo conjunto de dobras, abertas a suaves e harmônicas, com orientação, em geral, N-S, é observado (Figs. 21, 22D).

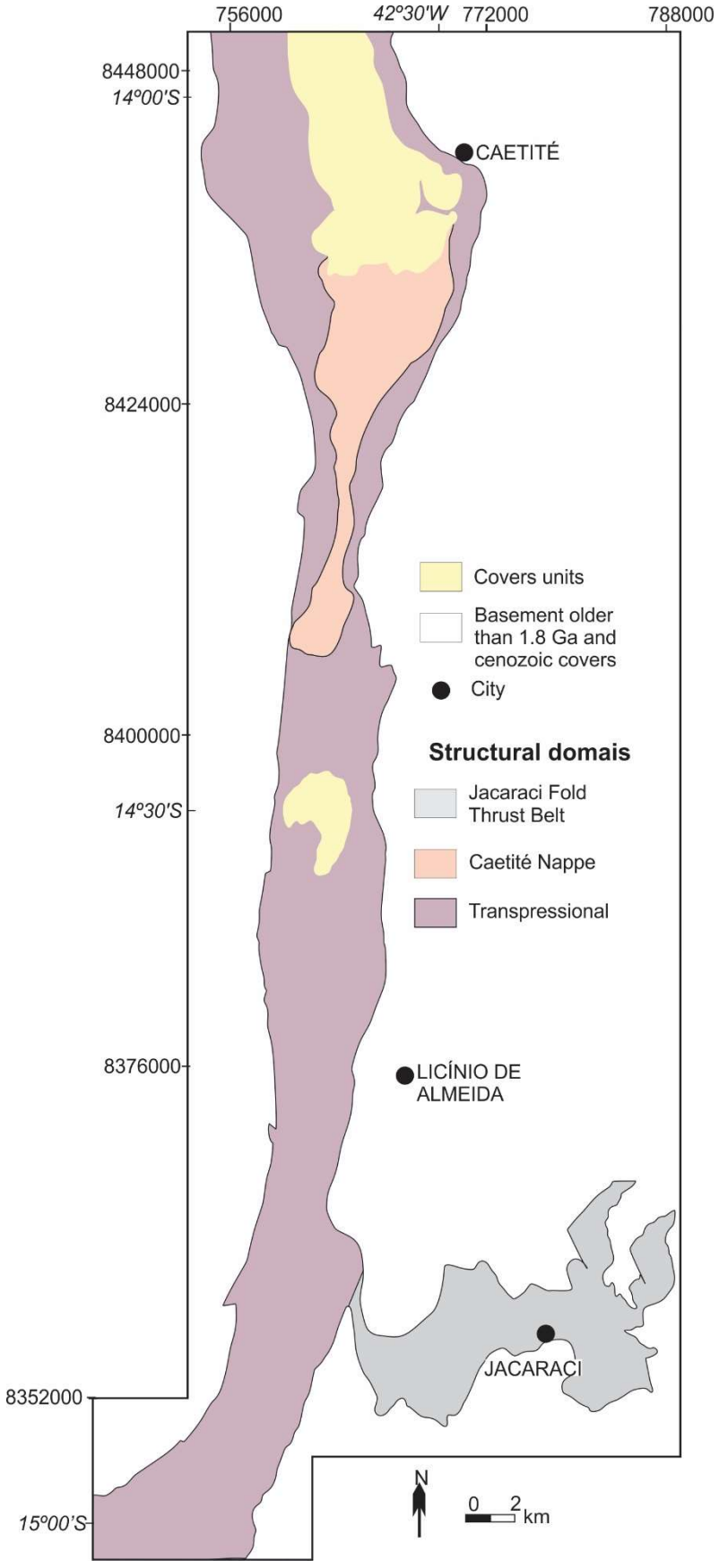

Fig. 19. Mapa dos domínios estruturais no Cinturão de Dobramentos e Cavalgamentos Serra do Espinhaço Setentrional.

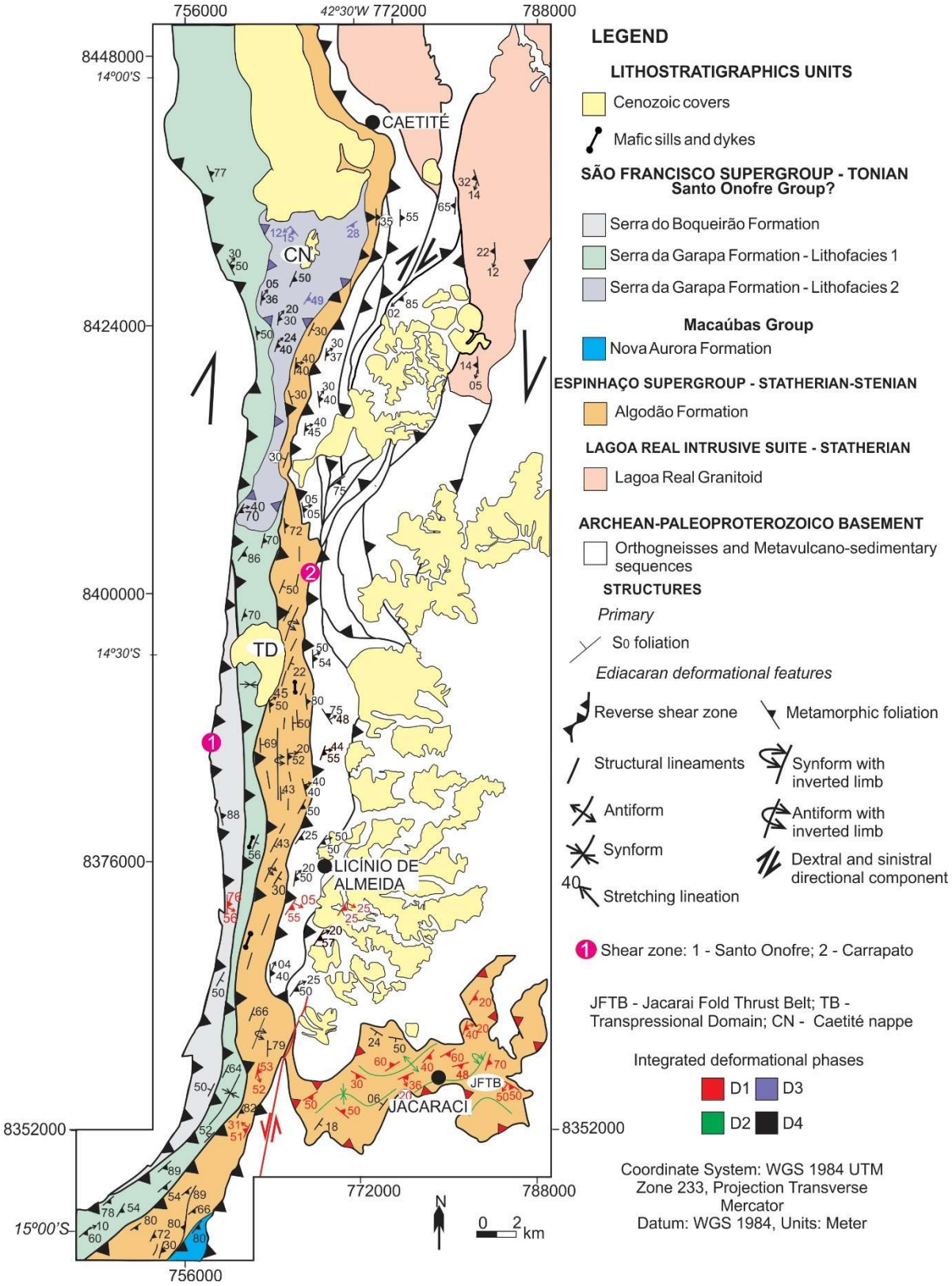

Fig. 5. Mapa geológico da área de estudo.

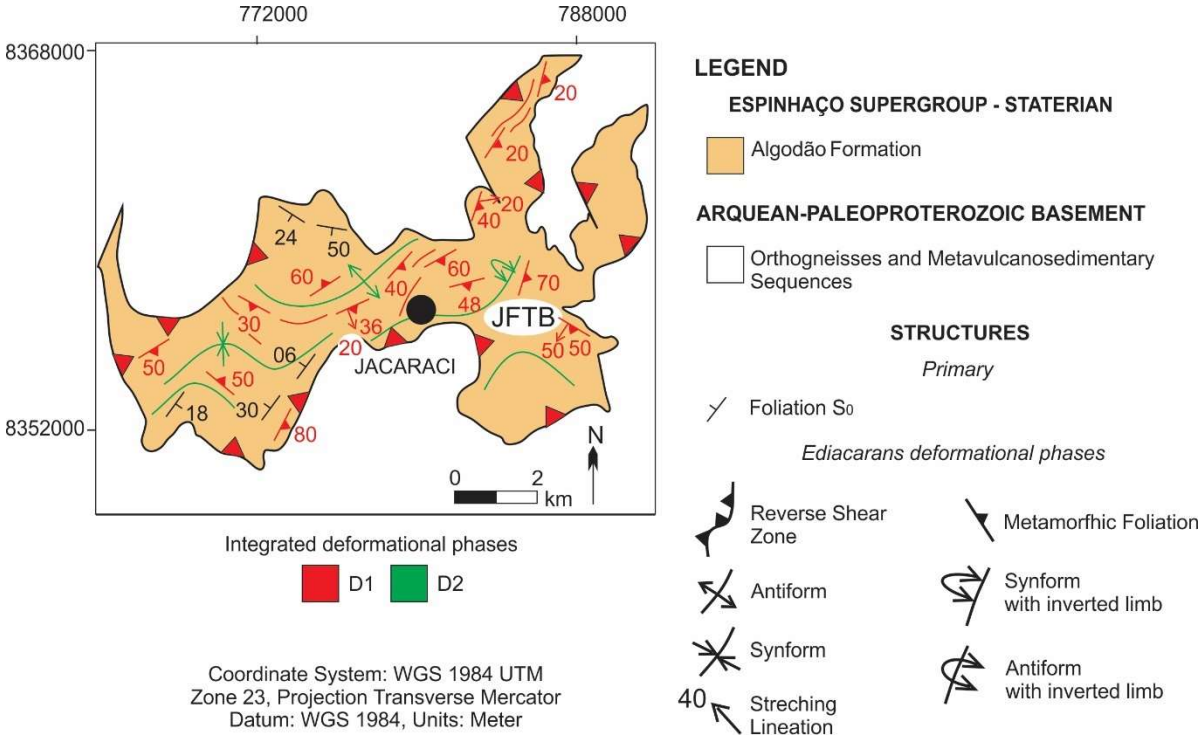

Fig. 21. Mapa Geológico do Jacaraci Fold Thrust Belt (JFTB). A localização da Figura na área de estudo encontra-se apresentada na Figura 5.

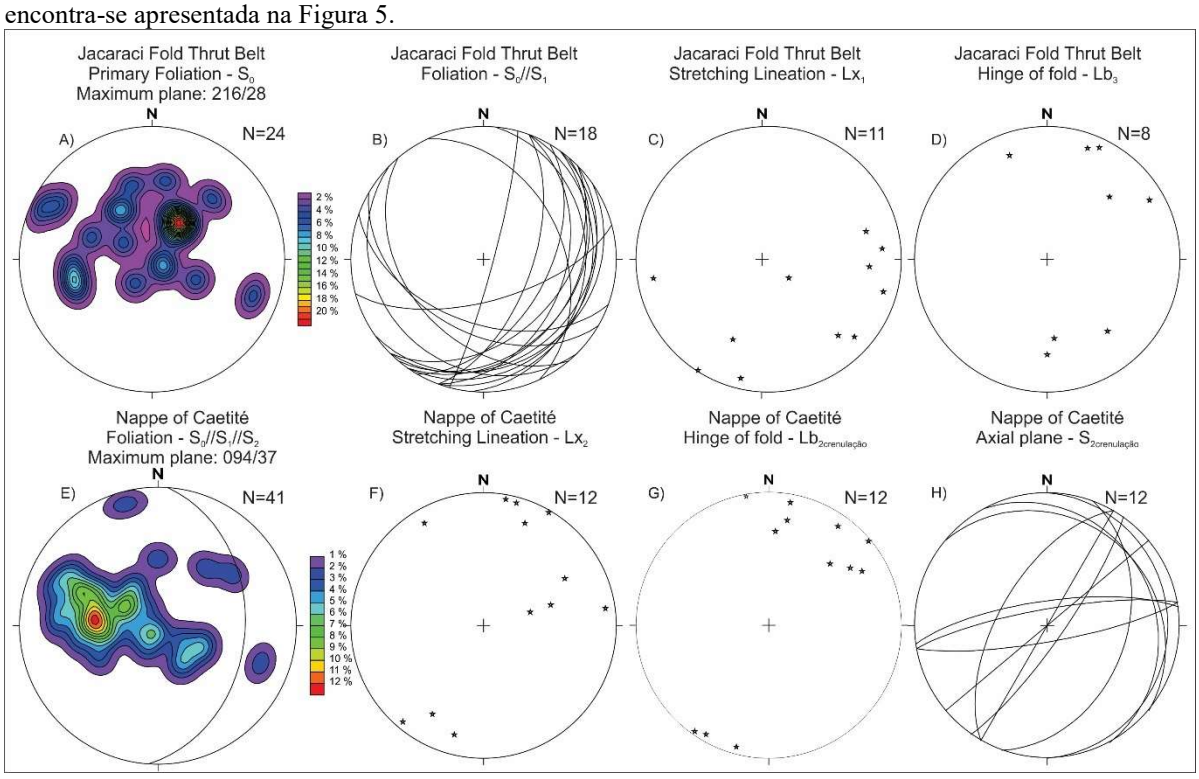

Fig. 22. Diagramas estereográficos das estruturas dos domínios Jacaraci Fold Thrust Belt e *Nappe* de Caetité. Hemisfério Inferior, diagrama de igual área. Valores calculados para 1% da área do círculo. N= número de medidas.

Fig. 23. Aspecto geral das estruturas deformacionais no Jacaraci Fold Thrust Belt (A) e da *Nappe* de Caetité (B-F). A) foliação $S_0//S_1$ na base (23L, 774833/8357443); B) dobras isoclinais intrafoliais (23L, 767211/8432119); C) lineação de estiramento (Lx_2) (23L, 765694/8432518); D) dobras de crenulação (23L, 767211/8432119); E) Dobras regionais com orientação geral NW-SE (23L, 763339/8427068; F) zona de cisalhamento transpressional destral que estrutura o contato oeste da Formação Serra da Garapa com a Formação Boqueirão (23L, 762790/8427234).

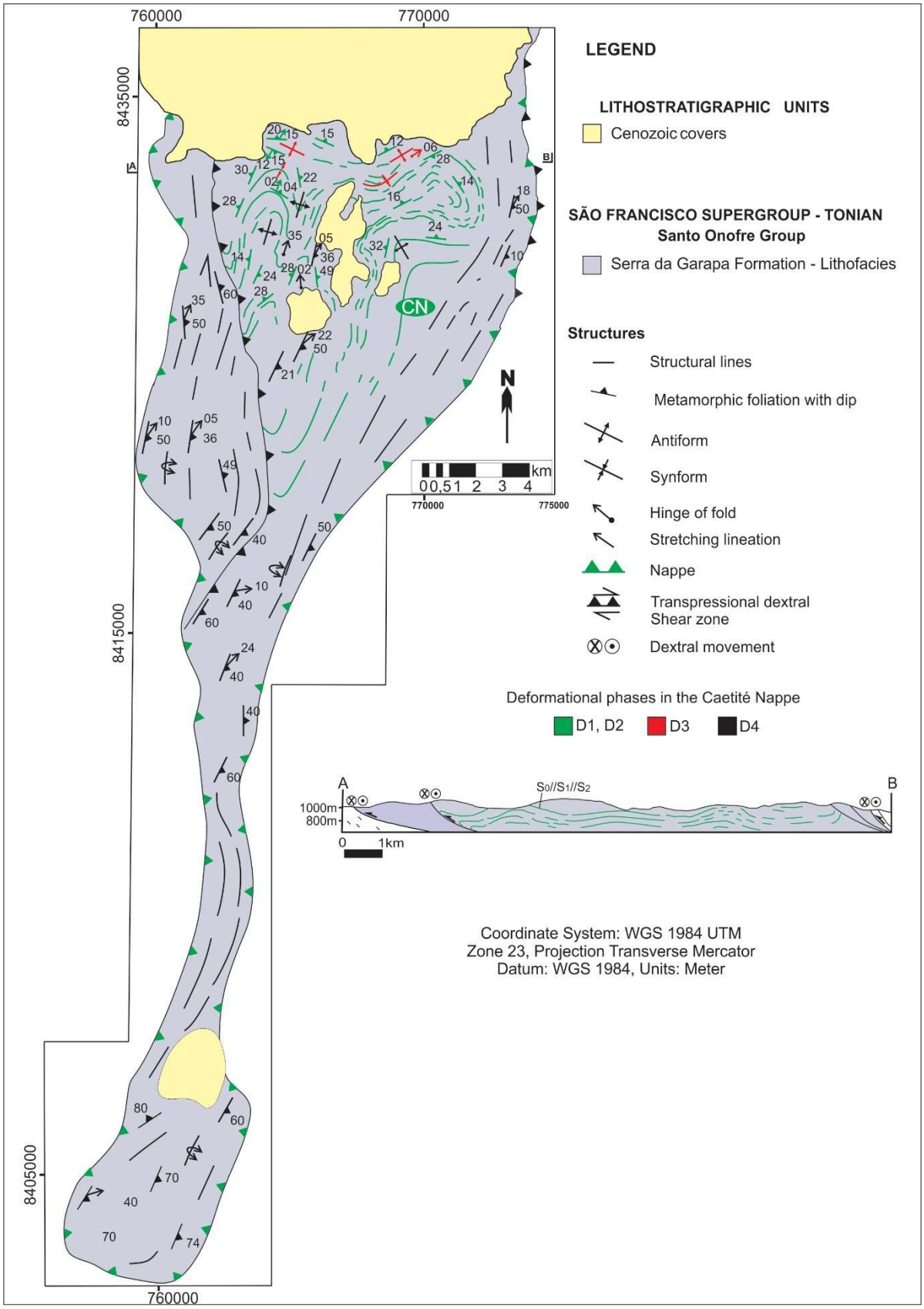

Fig. 24. Mapa geológico (A) e seção geológica (B) da *Nappe* de Caetité (NC). A localização da Figura encontra-se na Figura 5.

3.1.2. Nappe de Caetité

Essa estrutura foi cartografada a sudoeste da cidade de Caetité (Figs. 19, 20, 24), sendo representada rochas da associação de litofácies 2 da Formação Serra da Garapa. Uma foliação $S_0//S_1$ é observada em dobras isoclinais intrafoliais sem raiz (Fig. 23B), sendo transposta por uma foliação $S_0//S_1//S_2$ (Fig. 23B). Essa foliação compreende um bandamento composicional e uma xistosidade. O bandamento composicional apresenta alternância de xistos aluminosos (Figs. 8D, E; 9A, B), com com proporções variáveis de quartzo, moscovita, biotita, granada, estaurolita, clorita, pirita, hematita e grafita, e quartzitos (Fig. 8E). Por sua vez, a xistosiade é marcada pela orientação de filossilicatos (Fig. 9A). A orientação de $S_0//S_1//S_2$ apresenta forte dispersão (Fig. 15E). Internamente à essa estrutura, além de dobras isoclinais intrafoliais sem raiz, também são encontrados *boudins* simétricos de quartzitos. Associada com a foliação $S_0//S_1//S_2$ ocorrem as microestruturas: (i) granoblástica, por vezes poligonal, porfiroclástica e núcleo-manto, todas associadas com quartzo.

Novos grãos poligonais são observados contornando porfiroclastos de quartzo: (i) porfiroblástica, poiquiloblástica, peneira, helicítica e sombra de pressão, associadas com granada e estaurolita; (ii) lepidoblástica, pela orientação preferencial de biotita e moscovita; (iii) decussada, pelo arranjo radial de grãos de estaurolita; e (iv) nematoblástica, associada aos grãos de quartzo alongados. O quartzo apresenta extinção fraca a moderada. Na maioria das rochas o contato quartzo-quartzo é suavemente curvo, mas podem ser interlobados.

Uma lineação de estiramento (Lx_2) (Fig. 23C) é observada, sendo marcada pela orientação preferencial de quartzo. Essa estrutura está paralelizada com uma lineação mineral por orientação de moscovita e biotita. A orientação geral dessas estruturas é segundo NE (Fig. 22F). Ambas lineações estão paralelizadas com charneiras de dobras de crenulação (L_{b2}) (Fig. 22G e 23D). A foliação plano axial das dobras de crenulação possui forte dispersão no diagrama da Figura 22H.

Uma estrutura de interferência em laço é interpretada para o setor norte da nappe (Fig. 24), sugerindo duas fases de dobramentos na Nappe de Caetité. Associadas com a primeira fase (F_3) encontram-se dobras abertas a suave e harmônicas (Ramsay and Huber, 1987). As estruturas da segunda fase de dobramento são classificadas como normal horizontal (*sensu* Fleuty, 1964), abertas e desarmônicas (Ramsay and Huber, 1987). Essas estruturas são truncadas por zonas de cisalhamento transpressionais destrais (Fig. 23F) que estruturam os contatos da Formação Serra da Garapa com a Formação Algodão e desta formação com o embasamento do Aulacógeno do Paramirim.

3.1.3. Domínio Transpressional

Neste domínio (Fig.19) afloram unidades da Formação Algodão, do Grupo Santo Onofre (Formações Serra da Garapa e Boqueirão) e do Grupo Macaúbas (Formação Nova Aurora) (Fig. 20), além das rochas do embasamento do Aulacógeno do Paramirim e da Suíte Intrusiva Lagoa Real. Como já mencionado, estratificações primárias plano-paralelas e cruzadas são observadas em metarenitos, especialmente em afloramentos mais distantes das zonas de cisalhamento que estruturam os contatos dessas unidades. A distribuição dessas zonas de cisalhamento no diagrama da Figura 25A mostra máximo em 097º/50º. Mergulhos para WNW também são observados. Predominantemente a sul do paralelo 14º30' (Fig. 20), pode ser observada uma xistosidade $S_0//S_1$, que se posiciona paralelamente ao bandamento composicional. As microestruturas associadas com essa foliação são: (i) granoblástica, predominantemente poligonal, além de porfiroclástica, núcleo-manto, milonítica, sombra de pressão, *ribbons,* calda de grão tipo sigma, todas relacionadas com grãos de quartzo; e (ii) lepidoblástica, pela orientação preferencial de moscovita. Essa estrutura, em geral, orienta-se segundo NS a NE-SW, com mergulhos entre 30º e 78º para E (Fig. 25B).

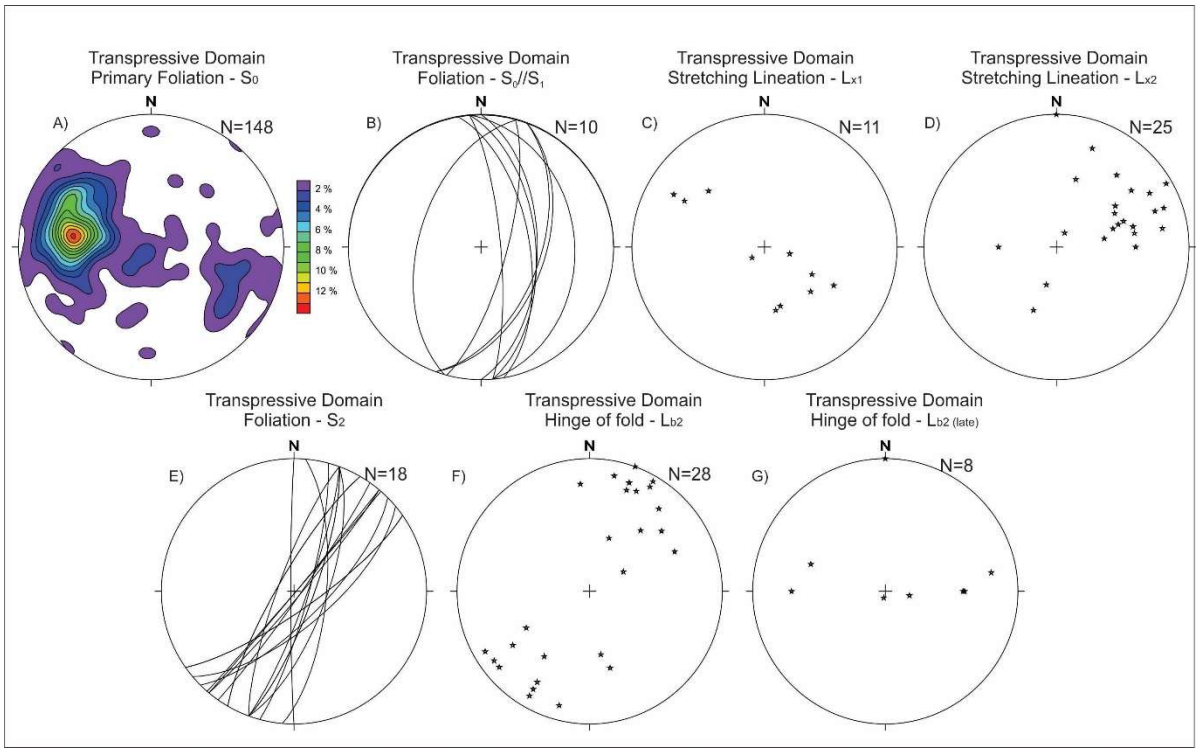

Fig. 25. Diagramas estereográficos das estruturas do domínio transpressional. Hemisfério Inferior, diagrama de igual área. Valores calculados para 1% da área do círculo. N= número de medidas.

A lineação de estiramento (L_{x1}) é marcada pela orientação preferencial de quartzo, bem como de clastos em metaconglomerados, e ocupa os quadrantes NW e SE (Fig. 25C).

Também neste caso, uma lineação mineral posiciona-se paralelamente a L_{x1}, sendo revelada pela orientação de filossilicatos. *Duplexes* e leques imbricados compressionais e frontais são encontrados no contato ocidental entre as rochas da Formação Boqueirão (Grupo Santo Onofre) e as rochas do embasamento do Aulacógeno do Paramirim, ou seja, na Zona de cisalhamento Santo Onofre (Figs. 20, 26A).

O acamamento primário S_0 e a foliação metamórfica S_1 encontram-se dobrados (Fig. 26B-D). Predominam dobras com envoltórias assimétricas, desarmônicas, acilíndricas, abertas e fechadas (*sensu* Ramsay and Huber, 1987), desde normal horizontal, predominante, a inclinadas com caimento e reviradas (*sensu* Fleuty, 1964). Neste último caso, a vergência geral é para oeste e essas estruturas se localizam nas proximidades de zonas de cisalhamento que limitam as unidades do Grupo Santo Onofre (Fig. 20). Dobras parasíticas em S, Z, M ou W são encontradas e, localmente, dobras *chevron* são observadas. Especialmente nos filitos e metapelitos, as dobras desenvolvem foliação plano axial (S_2), espaçada e descontínua (*sensu* Passchier and Trouw, 2005). Em geral, essa foliação possui trend NE-SW (Fig. 25E).

Zonas de cisalhamento transpressionais, reversa-destrais (Fig. 26E) truncam as estruturas anteriores e predominam na área de estudo. Essas estruturas possuem orientação geral NNE-SSW com inflexão para NS e estão principalmente localizadas: (i) nos contatos entre as unidades do Grupo Santo Onofre com a Formação Algodão; e (ii) no contato das rochas da Formação Algodão com o embasamento do Aulacógeno do Paramirim, neste caso, através da Zona de cisalhamento Carrapato (Fig. 20). Leques imbricados e duplexes compressionais frontais são encontrados neste contexto, sendo observados no contato entre rochas da Formação Algodão com o embasamento do Aulacógeno do Paramirim, na zona de cisalhamento Carrapato. A lineação de estiramento (Lx_2) presente nessas estruturas é marcada pela orientação preferencial de quartzo, segundo preferencialmente a direção NE-SW. Uma estrutura em flor positiva associada com zona de cisalhamento transcorrente destral orientada segundo NNE-SSW foi interpretada a E-SE da cidade de Caetité e envolve as unidades do embasamento do Aulacógeno, da Suíte Intrusiva Lagoa Real, da Formação Algodão e do Grupo Santo Onofre (Figs. 5 e 6A). Os indicadores cinemáticos são estruturas S/C (Fig. 26F) e dobras de arrasto.

Relacionada com essas zonas de cisalhamento, um segundo conjunto de dobras, menos penetrativo, assimétrico em Z com charneira de médio a alto ângulo de caimento (Fig.25G), rotaciona as dobras F_2. Essa assimetria pode ser observada em mapa (Fig. 5).

Fig. 26. Aspecto geral das estruturas deformacionais do domínio transpressional. A) *duplex* no contato da Formação Boqueirão com o embasamento do Aulacógeno do Paramirim (23L, 758665/8370897); B) dobras nas formações Algodão (23L, 761245/8368125); C e D) dobras na litofácies 1 da Serra da Garapa (23L, 760032/8369363); E) zona de cisalhamento no contato entre as formações Boqueirão e Serra da Garapa (23L, 759258/8368589); F) detalhe do indicador de movimento (estrutura S/C) de zona de cisalhamento da Figura E.

3.2. Evolução deformacional

O arcabouço estrutural da área estudada é complexo e cada domínio estrutural individualizado neste trabalho apresenta uma história deformacional distinta. Considerando que: (i) o Jacaraci Fold Thrust Bel possui estuturas deformacionais cujos indicadores

cinemáticos sugerem transporte de massa genericamente para NW; (ii) a similaridade do arcabouço estrutural e da vergência desse cinturão com o que foi definido para setor ocidental da Saliência do Rio Pardo por Cruz and Alkmim (2006); (iii) que as estruturas mais antigas verificadas no Domínio Transpressional apresentam geometria e vergência semelhantes às encontradas no Jacaraci Fold Thrust Bel, definida neste trabalho, e na Saliência do Rio Pardo; (iv) que as estruturas da Saliência do Rio Pardo são as estruturas mais antigas relacionadas com a inversão do Aulacógeno do Paramirim e que regionalmente são truncadas por um sistema transpressional destral relacionado com a fase de inversão frontal do Aulacógeno do Paramirim (Cruz and Alkmim 2006), cujas estruturas apresentam similaridades geométicas e cinemática, bem como continuidade física com o domínio transpressional definido neste trabalho; (v) que as estruturas da Nappe de Caetité, e suas feições de interferências, associam-se com o sistema transpressional regional tardio à inversão do Aulacógeno do Paramirim (Fase Dp de Cruz and Alkmim 2006), que trunca as estruturas da Saliência do Rio Pardo, um total de seis fases deformacionais (D_1, D_2, D_3, D_4, D_5 e D_6) foram interpretadas para a área de estudo. As correlações entre os três domínios estruturais definidos neste trabalhos estão apresentadas na Tabela 3. Essas deformações, predominantemente compressionais, foram desenvolvidas sob campo de tensão regional máximo orientado segundo WSW-ENE, que inverteu e/ou reativou as estruturas distensionais relacionadas com a longa evolução do Aulacógeno do Paramirim e das bacias precursoras do Orógeno Araçuaí-Oeste Congo (Fig. 24A).

Tabela 3

Integração de estruturas e fases deformacionais regionais interpretadas para a área de estudo. Ver texto para discussão e integração.

Fase Deformacional Integrada / Domínio Estrutural	**Jacaraci Fold Thrust Belt**	**Caetité Nappe**	**Transpressional**
D_1	Xistosidade e bandamento composicional metamórfico ($S_0//S_1$), lineação de estiramento mineral (L_{x1}); zonas de cisalhamento	-----	Foliação $S_0//S_1$ NE-SW, lineação de estiramento (L_{x1}) com cimento geral para SE; duplex compressional
D_2	Dobras (F_2)	-----	
D_3	-----	Xistosidade e bandamento metamórfico $S_0//S_1$.	

		Zonas de cisalhamento transpressionais e flor positiva são nucleadas	-----
D_4	-----	Xistosidade e bandamento metamórfico (S_0//S_1//S_2), lineação de estiramento (L_{x2}), dobras isoclinais intrafoliais e *boudins*	-----
D_5	----	Dobras (F_3) com orientação geral NE-SW e NW-SE	
D_6	Dobras (F_3)	Dobras (F_4) com trend geral NW-SE, feição de interferência em laço. Zonas de cisalhamento transpressionais destrais e flor positiva continuam ativas e atingem o ápice.	Zonas de cisalhamento reversas a transpressionais destrais, foliação milonítica (S_0//S_1//S_2) , lineação de estiramento mineral (L_{x2}), dobra (F_2), foliação plano axial (S_2). Ampliação do sistema transpressional e desenvolvimento de estruturas *pop-up de* Borges et al. (2015). Tardiamente: dobras com assimetria em Z e charneira de alto ângulo

A primeira fase de deformação compressional (D_1) (Fig. 24B) interpretada foi responsável pela formação do Jacaraci Fold Thrust Belt e pelas estruturas mais antigas descritas no Domínio Transpressional. Esta fase é correlacionável com a geração D_a de Cruz e Alkmim (2006) e está associada com o desenvolvimento da Saliência do Rio Pardo, um dos compartimentos do Orógeno Araçuaí-Oeste Congo (Alkmim et al., 2007). O desenvolvimento dessas estruturas e de sua evoução deformacional está associada com o modelo "*Nutcracker*" proposto por Alkmim et al. (2006), em que a rotação antihorária da Placa São Francisco-Congo promoveu a fuga de massa para norte. Na Saliência do Rio Pardo o transporte tectônico varia de SE para NW em sua região ocidental, de N para S em sua região central e de SW para NE em sua região oriental (Cruz and Alkmim, 2006). As estruturas deformacionais D_1 deste trabalho estão posicionadas no setor ocidental dessa saliência e refletem topo estrutural para NW.

A apesar de serem interpretadas como relacionadas a um fold thrust belt, considerando a geometria das estruturas presentes na região de Jacaraci, uma hipótese que ainda deverá ser testada é que esse cinturão na verdade represente uma *klippe* associada com uma estrutura em nappe com movimento dirigido para NW, que foi amalgamada ao Domínio Transpressional através de uma zona de cisalhamento sinistral (Fig.5).

A segunda fase de deformação (D_2) (Fig. 24 C) foi responsável pelo desenvolvimento progressivo de dobras (F_2) observadas no Jacaraci Fold Thrust Belt. As terceira, quarta e quinta fases deformacionais (D_3, D_4 e D_5) (Fig. 24D) estão relacionadas com a evolução da *Nappe* de Caetité. A terceira fase (D_3) foi responsável pela justaposição de xistos aluminosos e quartzitos da Formação Serra da Garapa (Associação de litofacies 2) sobre filitos grafitosos e quartzitos da associação de litofácies 1 dessa formação. Nesta fase houve a nucleação da foliação $S_0//S_1$ descrita na nappe, que foi observada em dobras isoclinais intrafoliais à foliação $S_0//S_1//S_2$. O contraste metamórfico entre as duas litofácies da Formação Serra da Garapa sugere que uma estrutura de alto ângulo foi responsável por justapor essas unidades. Essa justaposição se deu através de uma zona de cisalhamento frontal e de baixo ângulo, que esteve conectada a um sistema de flor positiva. A nucleação desse sistema, por sua vez, está relacionada com a evolução progressiva do sistema transpressional destral descrito por Cruz and Alkmim (2006) e Borges et al. (2015) durante e inversão frontal do Aulacógeno do Paramirim. Esse sistema transpressional reativa e inverte as estruturas distensionais do Aulacógeno do Paramirim (Fig. 6A) levando à justaposição de rochas de grau metamórfico mais alto, de fácies anfibolito (Bitencourt, 2014) da associação de litofácies 2 da Formação Serra da Garapa sobre rochas da associação de litofácies 1 dessa formação, de fácies xisto verde. Considerando o aumento do grau metamórfico local em direção a leste (Cruz et al., 2015) e o modelo proposto por Cruz and Alkmim (2006) e Borges et al. (2015), a vergência interpretada para essa fase é para SW (Fig. 6A).

Na quarta fase de deformação (D_4) houve o desenvolvimento da foliação localmente hierarquizada na nappe como $S_0//S_1//S_2$, bem como de lineação de estiramento (L_{x2}), dobras isoclinais intrafoliais e *boudins*. Essas estruturas foram dobradas em uma quinta fase deformacional (D_5).

A sexta e última fase deformacional (D_6) (Fig. 24E) foi observada em todos os três compartimentos individualizados, tendo sido responsável pelo desenvolvimento de: (i) zonas de cisalhamento reversas a transpressionais destrais que estruturam os contatos entre as unidades do Grupo Santo Onfre com a Formação Algodão, assim como dessas unidades com o embasamento do Aulacógeno do Paramirim, nesse caso invertendo e reativando as zonas de cisalhamento Santo Onofre e Carrapato, a oeste e leste, respectivamente (Fig. 5); (ii) dobras regionais com *trend* geral NS, vergência geral nula a WSW observadas no Jacaraci Fold Thrust Belt, no Domínio Transpressional e na Nappe de Caetité; (iii) estrutura de interferência em laço (*Type III, sensu* Ramsay and Huber, 1997) na *Nappe* de Caetité; e (iv) tardiamente,

houve o desenvolvimento de dobra assimétricas em Z com charneira de alto ângulo, que refletem a componente destral da transpressão regional. A fase deformacional D_6 é correlacionável com a fase D_p de Cruz and Alkmim (2006) e com as fases D_n e D_{n+1} de Borges et al. (2015), que levou também ao desenvolvimento de estruturas pop-up com embasamento envolvido.

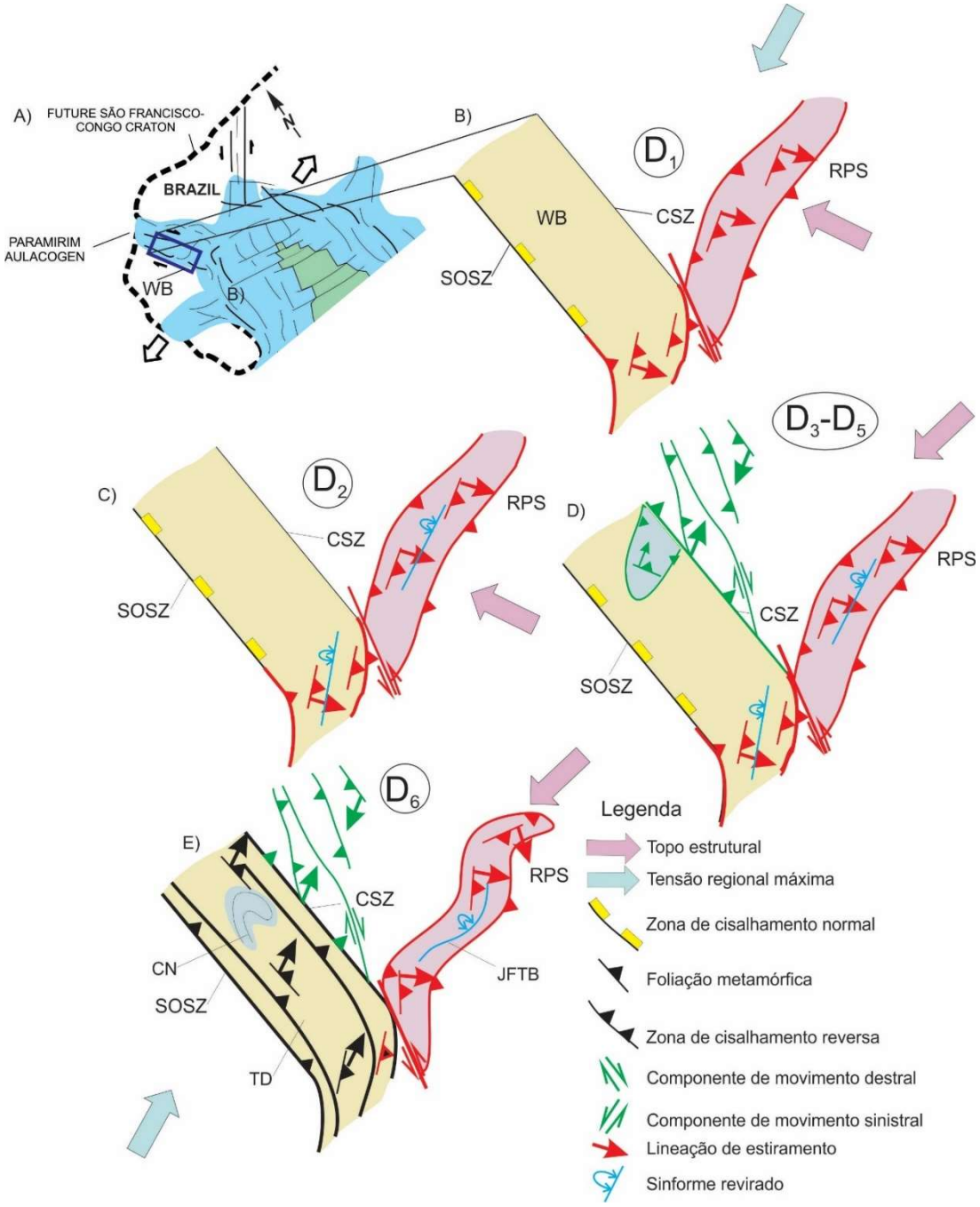

Fig. 27. A) Contexto tectônico da Bacia Ocidental (WB) no Paramirim Aulacogen. B-E) Proposta de modelo deformacional esquemático para a inversão do Paramirim Aulacogen no setor sul da Bacia Ocidental (WB). A tensão regional máxima se mantém em todas as fases. D- Fase deformacional; Shear Zones: SOSZ –Santo Onofre, CSZ- Carrapato; RPS – Rio Pardo Salient. Modelo adimensional.

4. Conclusão

Três domínios estruturais foram identificados na área de estudo*:* Jacarac*i Fold Thrust Belt, Nappe* de Caetité e Domínio Transpressional. A evolução deformacional desses domínios é complexa, compreendendo seis fases deformacionais compressionais e progressivas. Essas fases estão relacionadas com um campo de tensão com orientação geral WSW-ENE e associado com a estruturação do Orógeno Araçuaí-Oeste Congo. A primeira fase (D_1), encontrada no Jacarac*i Fold Thrust Belt* e no Transpressional Domain, está relacionada com a evolução da Saliência do Rio Pardo. Um sistema transpressional destral foi responsável pela nucleação de uma estrutura em flor positiv*a,* pela *Nap*pe de Caetité, pelas deformações nos domínios transpressional e no Jacarac*i Fold Thrust Belt,* bem como por estruturas de maior escala. Regionalmente, esse sistema relaciona-se com a inversão frontal do Aulacógeno do Paramirim. Na *Nap*pe de Caetité houve a justaposição de litofácies de mais alta temperatura sobre litofácies de mais baixa temperatura, ambas da Formação Serra da Garapa.

Referências

Arcanjo J. B., Marques-Martins A. A., Loureiro H. S. C., Varela P. H. L. 2005. Projeto Vale do Paramirim, Bahia: geologia e recursos minerais. Série arquivos abertos, 22. Salvador, CBPM, 82p.

Arcanjo J. B., Marques-Martins A. A., Loureiro H. S. C., Varela P. H. L. 2000. Projeto vale do Paramirim, escala 1:100.000. Programa de Levantamentos Geológicos Básicos do Brasil, CD-ROOM.

Brito D.C. 2008. Geologia, petrografia e litogeoquímica dos diques máficos que ocorrem na porção sudoeste da Chapada Diamantina, Bahia, Brasil. M. Sc. Thesis, Instituto de Geociências, Universidade Federal da Bahia, Salvador, 77p.

Cruz S.C.P. & Alkmim F.F. 2006. The tectonic interaction between the Paramirim Aulacogen and the Araçuaí Belt, São Francisco Craton region, Easter Brazil. Anais da Academia Brasileira de Ciências 1, 151-173.

Cruz S.C.P., Alkmim F.F., Leite C.M.M., Evangelista H.J. Cunha J.C., Matos E.C., Noce C.M., Marinho M.M. 2007. Geologia e arcabouço estrutural do Complexo Lagoa Real, Vale do Paramirim, Centro-Oeste da Bahia. Revista Brasileira de geociências **37** (4, suplemento), 28-146.

Cruz S. C. P. Barbosa J. S. F., Alves J. E., Damasceno G. C., Machado G. S., Borges J. O., Gomes A. M., Mesquita, L., Pimentel I., Leal A. B. M., Palmeiras D. 2009. Folha Caetité, 1:100.000: Mapeamento geológico e cadastramento de ocorrências minerais. Convênio UFBA-FAPEX-CPRM, 180p.

Cruz S.C.P., Alkmim F.F., Pedreira A., Teixeira L., Pedrosa-Soares A.C., Gomes L.C.C., Souza J.S., Leal A.B.M., 2012. O Orógeno Araçuaí. In: Barbosa J.S.F., Mascarenhas J.F.; Corrêa-Gomes L.C.; Domingues J.M.L. (eds.), Geologia da Bahia, Pesquisa e Atualização de dados, v. 2. Salvador, CBPM, p. 131-178.

Cruz S.C.P., Alkmim F.F., Barbosa J.S.F., Dussin I., Gomes L.C.C. 2015. Tectonic inversion of compressional structures in the Southern portion of the Paramirim Corridor, Bahia, Brazil. Brazilian Journal of Geology **45**: 541-567.

Damasceno G.C. 2013. Geologia, Petrografia e Geoquímica dos diques máficos da Folha Caetité (SD.23-Z-B-III). M. Sc. Thesis. Instituto de Geociências. Universidade Federal da Bahia, Salvador, 145p.

Guimarães J.T., Santos R.A., Melo R.C. 2008. Geologia da Chapada Diamantina (Projeto Ibitiara-Rio de Contas). CBPM Série arquivos abertos, 31. Salvador, CBPM, 68 p.

Guimarães J.T., Alkmim F.F., Cruz S.C.P. 2012. Supergrupo Espinhaço e São Francisco. In: Barbosa, J.S.F. (eds.) Geologia Da Bahia, Pesquisa e Atualização de dados, v. 2. Salvador, CBPM, p. 33–85.

Lobato L.M., Pimentel M., Cruz S.C.P., Machado N., Noce C.M., Alkmim F.F. 2015. U-Pb Geochronology of the Lagoa Real Uranium District, Brazil: Implications for the age of the uranium mineralization. Journal of South American Earth Sciences **58**: 129-140.

Machado, G. S. 2008. Geologia da porção sul do complexo Lagoa Real, Caetité, Bahia. Undergraduate, Instituto de Geociências, Universidade Federal da Bahia, Salvador, 90p.

Pedrosa-Soares A.C. & Alkmim F.F., 2011. How many rifting events preceded the development of the Araçuaí-West Congo orogen? Geonomos **12**: 244-251.

Pereira-Varjão L.M., 2011. Geologia, Petrografia e Litogeoquímica dos Diques Máficos da Porção Sudeste do Bloco Gavião, Bahia, Brasil. M. Sc. Thesis, Instituto de Geociências, Universidade Federal da Bahia, Salvador, 114 p.

Pimentel M. M., Machado N., Lobato L. M. 1994. Geocronologia U/Pb de rochas graníticas e gnáissicas da região de Lagoa Real, Bahia, e implicações para a idade da mineralização

de urânio. *In*: 38º Congresso Brasileiro de Geologia, Boletim de Resumos Expandidos, p. 389-390.

Turpin L., Maruèjol, P., Cuney M. 1988. U-Pb, Rb-Sr and Sm-Nd chronology of granitic basement, hydrotermal albitites and uranium mineralization, Lagoa Real, South Bahia, Brazil. Contribution Mineralogy Petrolology, **98:** 139-147.

APÊNDICE A – JUSTIFICATIVA DA PARTICIPAÇÃO DOS CO-AUTORES

Simone Cerqueira Pereira Cruz: orientadora do trabalho. Possui diversos trabalhos publicados acerca do Aulácogeno do Paramirim, Corredor do Paramirim e assuntos correlacionados. Ampla experiência de mapeamento geológico na área de estudo.

Vanderlucia dos Anjos Cruz: Auxilou na revisão do manuscrito e na produção das figuras.

Antônio Carlos Pedrosa Soares: Auxliou na revisão do manuscrito.

Ana Ramalho Alkmim: Orientou as análises geocronológicas e auxiliou no tratamento desses dados.

APÊNDICE B – TABELA DE PONTOS

Meridiano – 23 L				
SIGLA	**NUMERO**	**LONGITUDE**	**LATITUDE**	**UNIDADE**
ATE	21	768934	8444101	Formação Algodão/ Supergrupo Espinhaço
ATE	88	767235	8421923	Formação Algodão/ Supergrupo Espinhaço
ATE	89	766004	8421456	Formação Algodão/ Supergrupo Espinhaço
ATE	117	766353	8419983	Formação Algodão/ Supergrupo Espinhaço
ATE	118	765397	8417411	Formação Algodão/ Supergrupo Espinhaço
CNB	1	767211	8432119	Formação Serra da Garapa/ Grupo Santo Onofre
CNB	2	765694	8432518	Formação Serra da Garapa/ Grupo Santo Onofre
CNB	3	765694	8432518	Formação Serra da Garapa/ Grupo Santo Onofre
CNB	4	783100	8435200	Suíte Intrusiva Lagoa Real
CNB	5	763960	8433032	Formação Serra da Garapa/ Grupo Santo Onofre
CNB	6	763953	8430904	Formação Serra da Garapa/ Grupo Santo Onofre
CNB	7	763006	8427564	Formação Serra da Garapa/ Grupo Santo Onofre
CNB	8	762790	8427234	Formação Serra da Garapa/ Grupo Santo Onofre
CNB	9	762000	8428300	Formação Serra da Garapa/ Grupo Santo Onofre
CNB	10	760547	8425666	Complexo Santa Isabel
CNB	11	760005	8425894	Complexo Santa Isabel
CNB	12	760250	8424380	Complexo Santa Isabel
CNB	13	759582	8425780	Complexo Santa Isabel
CNB	14	759833	8424684	Complexo Santa Isabel
CNB	15	759988	8424228	Complexo Santa Isabel
CNB	16	764308	8430498	Formação Serra da Garapa/ Grupo Santo Onofre
CNB	17	764350	8435356	Formação Serra da Garapa/ Grupo Santo Onofre
CNB	18	763339	8427068	Formação Serra da Garapa/ Grupo Santo Onofre
CNB	19	763701	8426688	Formação Serra da Garapa/ Grupo Santo Onofre
CNB	20	764518	8425428	Formação Serra da Garapa/ Grupo Santo Onofre
CNB	21	764192	8424436	Formação Serra da Garapa/ Grupo Santo Onofre
CNB	22	760794	8425526	Complexo Santa Isabel

CNB	23	761529	8426026	Formação Serra da Garapa/ Grupo Santo Onofre
CNB	24	764488	8433996	Formação Serra da Garapa/ Grupo Santo Onofre
CNB	25	761408	8367942	Formação Serra da Garapa/ Grupo Santo Onofre
CNB	26	763660	8426643	Formação Serra da Garapa/ Grupo Santo Onofre
CNB	27	762749	8427221	Formação Serra da Garapa/ Grupo Santo Onofre
CNB	28	763775	8429910	Formação Serra da Garapa/ Grupo Santo Onofre
CNB	29	767244	8422360	Formação Algodão/ Supergrupo Espinhaço
CNB	30	767052	8421403	Formação Algodão/ Supergrupo Espinhaço
CNB	31	767028	8420907	Formação Algodão/ Supergrupo Espinhaço
CNB	32	766333	8420089	Formação Algodão/ Supergrupo Espinhaço
CNB	33	765880	8418987	Formação Algodão/ Supergrupo Espinhaço
CNB	34	765200	8418826	Formação Serra da Garapa/ Grupo Santo Onofre
CNB	35	765343	8417258	Formação Algodão/ Supergrupo Espinhaço
CNB	36	765343	8412357	Formação Algodão/ Supergrupo Espinhaço
CNB	37	763492	8410150	Formação Algodão/ Supergrupo Espinhaço
CNB	38	763518	8409690	Formação Serra da Garapa/ Grupo Santo Onofre
CNB	39	764388	8410254	Formação Serra da Garapa/ Grupo Santo Onofre
CNB	40	758664	8370889	Complexo Santa Isabel
CNB	41	758749	8370741	Formação Boqueirão/ Grupo Santo Onofre
CNB	42	758854	8370575	Formação Boqueirão/ Grupo Santo Onofre
CNB	43	758922	8370524	Formação Boqueirão/ Grupo Santo Onofre
CNB	44	759125	8370167	Formação Boqueirão/ Grupo Santo Onofre
CNB	45	759117	8369701	Formação Boqueirão/ Grupo Santo Onofre
CNB	46	759171	8369359	Formação Boqueirão/ Grupo Santo Onofre
CNB	47	759254	8369168	Formação Boqueirão/ Grupo Santo Onofre
CNB	48	759258	8368589	Formação Boqueirão/ Grupo Santo Onofre
CNB	49	759507	8368497	Formação Serra da Garapa/ Grupo Santo Onofre

CNB	50	759633	8368566	Formação Serra da Garapa/ Grupo Santo Onofre
CNB	51	759700	8368651	Formação Serra da Garapa/ Grupo Santo Onofre
CNB	52	759851	8369038	Formação Serra da Garapa/ Grupo Santo Onofre
CNB	53	759851	8369038	Formação Serra da Garapa/ Grupo Santo Onofre
CNB	54	760032	8369353	Formação Serra da Garapa/ Grupo Santo Onofre
CNB	55	760105	8369198	Formação Serra da Garapa/ Grupo Santo Onofre
CNB	56	760087	8368997	Formação Algodão/ Supergrupo Espinhaço
CNB	57	760132	8368873	Formação Algodão/ Supergrupo Espinhaço
CNB	58	760441	8368712	Formação Algodão/ Supergrupo Espinhaço
CNB	59	760510	8368652	Formação Algodão/ Supergrupo Espinhaço
CNB	60	760598	8368575	Formação Algodão/ Supergrupo Espinhaço
CNB	61	760701	8368496	Formação Algodão/ Supergrupo Espinhaço
CNB	62	761091	8368162	Formação Algodão/ Supergrupo Espinhaço
CNB	63	761245	8368125	Formação Algodão/ Supergrupo Espinhaço
CNB	64	761416	8368232	Formação Algodão/ Supergrupo Espinhaço
CNB	65	764086	8405886	Formação Serra da Garapa/ Grupo Santo Onofre
CNB	66	764389	8406043	Formação Serra da Garapa/ Grupo Santo Onofre
CNB	67	764646	8405758	Formação Algodão/ Supergrupo Espinhaço
CNB	68	763339	8405950	Formação Serra da Garapa/ Grupo Santo Onofre
CNB	69	760535	8407779	Complexo Santa Isabel
CNB	70	761059	8407773	Formação Serra da Garapa/ Grupo Santo Onofre
CNB	71	763723	8405169	Formação Serra da Garapa/ Grupo Santo Onofre
CNB	72	763891	8404627	Formação Serra da Garapa/ Grupo Santo Onofre
CNB	73	764218	8403465	Formação Algodão/ Supergrupo Espinhaço
CNB	74	761262	8401570	Formação Serra da Garapa/ Grupo Santo Onofre
CNB	75	761108	8400804	Formação Serra da Garapa/ Grupo Santo Onofre
CNB	76	765626	8400765	Formação Algodão/ Supergrupo Espinhaço

CNB	77	766125	8400873	Formação Algodão/ Supergrupo Espinhaço
CNB	78	767444	8400481	SMVS Caetité Licínio de Almeida
CNB	79	766823	8421008	Formação Algodão/ Supergrupo Espinhaço
CNB	80	766505	8421326	Formação Algodão/ Supergrupo Espinhaço
CNB	81	766331	8421298	Formação Algodão/ Supergrupo Espinhaço
CNB	82	765995	8421369	Formação Algodão/ Supergrupo Espinhaço
CNB	83	765582	8421585	Formação Serra da Garapa/ Grupo Santo Onofre
CNB	84	765086	8421836	Formação Serra da Garapa/ Grupo Santo Onofre
CNB	85	764714	8422644	Formação Serra da Garapa/ Grupo Santo Onofre
CNB	86	764817	8423667	Formação Serra da Garapa/ Grupo Santo Onofre
CNB	87	763837	8422474	Formação Serra da Garapa/ Grupo Santo Onofre
CNB	88	762341	8421851	Complexo Santa Isabel
CNB	89	767059	8422070	Formação Algodão/ Supergrupo Espinhaço
CNB	90	766151	8397488	Formação Algodão/ Supergrupo Espinhaço
CNB	91	766410	8396265	Formação Algodão/ Supergrupo Espinhaço
CNB	92	766430	8395682	Formação Algodão/ Supergrupo Espinhaço
CNB	93	766534	8395215	SMVS Caetité Licínio de Almeida
CNB	94	766548	8393692	Formação Algodão/ Supergrupo Espinhaço
CNB	95	766594	8393329	Formação Algodão/ Supergrupo Espinhaço
CNB	96	766603	8391581	Formação Algodão/ Supergrupo Espinhaço
CNB	97	766078	8391742	Formação Algodão/ Supergrupo Espinhaço
CNB	98	765804	8391650	Formação Algodão/ Supergrupo Espinhaço
CNB	99	765735	8391204	Formação Algodão/ Supergrupo Espinhaço
CNB	100	765308	8390972	Formação Algodão/ Supergrupo Espinhaço
CNB	101	766978	8389232	Formação Algodão/ Supergrupo Espinhaço
CNB	102	766719	8387507	Formação Algodão/ Supergrupo Espinhaço
CNB	103	766647	8387171	Formação Algodão/ Supergrupo Espinhaço

CNB	104	765810	8385969	Formação Algodão/ Supergrupo Espinhaço
CNB	105	765206	8385442	Formação Algodão/ Supergrupo Espinhaço
CNB	106	765079	8385680	Formação Algodão/ Supergrupo Espinhaço
CNB	107	765026	8385868	Formação Algodão/ Supergrupo Espinhaço
CNB	108	764949	8386383	Formação Algodão/ Supergrupo Espinhaço
CNB	109	764220	8386772	Formação Algodão/ Supergrupo Espinhaço
CNB	110	763131	8386663	Formação Algodão/ Supergrupo Espinhaço
CNB	111	769405	8394496	PONTO CONTROLE
CNB	112	766544	8381291	Formação Algodão/ Supergrupo Espinhaço
CNB	113	766465	8382553	Formação Algodão/ Supergrupo Espinhaço
CNB	114	766195	8382234	Formação Algodão/ Supergrupo Espinhaço
CNB	115	764715	8376262	Formação Algodão/ Supergrupo Espinhaço
CNB	116	764239	8377171	Formação Algodão/ Supergrupo Espinhaço
CNB	117	764134	8377467	Formação Algodão/ Supergrupo Espinhaço
CNB	118	763488	8377516	Formação Algodão/ Supergrupo Espinhaço
CNB	119	763126	8377304	Formação Algodão/ Supergrupo Espinhaço
CNB	120	763745	8388817	Formação Algodão/ Supergrupo Espinhaço
CNB	121	765148	8385532	Formação Algodão/ Supergrupo Espinhaço
CNB	122	765414	8385636	Formação Algodão/ Supergrupo Espinhaço
CNB	123	761743	8367209	Formação Algodão/ Supergrupo Espinhaço
CNB	124	761043	8367414	Formação Algodão/ Supergrupo Espinhaço
CNB	125	761944	8366916	Formação Algodão/ Supergrupo Espinhaço
CNB	126	761415	8364676	Formação Algodão/ Supergrupo Espinhaço
CNB	127	760815	8363277	Formação Algodão/ Supergrupo Espinhaço
CNB	128	760891	8358203	Formação Algodão/ Supergrupo Espinhaço
CNB	129	760323	8358203	Formação Algodão/ Supergrupo Espinhaço
CNB	130	760360	8355545	Formação Algodão/ Supergrupo Espinhaço

CNB	131	760695	8359450	Formação Algodão/ Supergrupo Espinhaço
CNB	132	761013	8364088	Formação Algodão/ Supergrupo Espinhaço
CNB	133	775432	8356920	Supergrupo Espinhaço Indiviso
CNB	134	774665	8357138	Supergrupo Espinhaço Indiviso
CNB	135	770850	8353319	Supergrupo Espinhaço Indiviso
CNB	136	768925	8354167	Supergrupo Espinhaço Indiviso
CNB	138	768252	8354435	Supergrupo Espinhaço Indiviso
CNB	139	769158	8358152	Supergrupo Espinhaço Indiviso
CNB	140	763008	8390075	PONTO DE CONTROLE
CNB	141	762098	8390651	Formação Algodão/ Supergrupo Espinhaço
CNB	142	760195	8397627	Formação Serra da Garapa/ Grupo Santo Onofre
CNB	143	772969	8353603	Supergrupo Espinhaço Indiviso
CNB	144	772496	8352758	Supergrupo Espinhaço Indiviso
CNB	145	772270	8352300	Supergrupo Espinhaço Indiviso
CNB	146	771922	8353107	Supergrupo Espinhaço Indiviso
CNB	147	770462	8354042	Supergrupo Espinhaço Indiviso
CNB	149	768819	8354176	Supergrupo Espinhaço Indiviso
CNB	150	768346	8354338	Supergrupo Espinhaço Indiviso
CNB	151	770073	8354687	Supergrupo Espinhaço Indiviso
CNB	152	770481	8354520	Supergrupo Espinhaço Indiviso
CNB	153	769888	8356914	Supergrupo Espinhaço Indiviso
CNB	154	769360	8357885	Supergrupo Espinhaço Indiviso
CNB	155	776919	8357188	Supergrupo Espinhaço Indiviso
CNB	156	777478	8357442	Supergrupo Espinhaço Indiviso
CNB	157	778114	8358092	Supergrupo Espinhaço Indiviso
CNB	158	779040	8360698	Supergrupo Espinhaço Indiviso
CNB	158	778939	8361243	Supergrupo Espinhaço Indiviso

CNB	159	777842	8362522	Supergrupo Espinhaço Indiviso
CNB	160	777506	8358011	Supergrupo Espinhaço Indiviso
CNB	161	772290	8351844	Supergrupo Espinhaço Indiviso
CNB	162	771479	8350528	Supergrupo Espinhaço Indiviso
CNB	163	771068	8349486	Supergrupo Espinhaço Indiviso
CNB	164	759320	8368211	Formação Boqueirão/ Grupo Santo Onofre
CNB	165	748068	8346306	Formação Boqueirão/ Grupo Santo Onofre
CNB	166	748621	8345680	Formação Serra da Garapa/ Grupo Santo Onofre
CNB	167	748821	8344869	Formação Serra da Garapa/ Grupo Santo Onofre
CNB	168	748882	8344481	Formação Serra da Garapa/ Grupo Santo Onofre
CNB	169	748972	8344316	Formação Serra da Garapa/ Grupo Santo Onofre
CNB	170	749789	8343040	Formação Serra da Garapa/ Grupo Santo Onofre
CNB	171	750578	8342466	Formação Algodão/ Supergrupo Espinhaço
CNB	172	751491	8343099	Formação Algodão/ Supergrupo Espinhaço
CNB	173	752430	8342702	Formação Algodão/ Supergrupo Espinhaço
CNB	174	753551	8341133	Formação Algodão/ Supergrupo Espinhaço
CNB	175	754080	8342382	Formação Algodão/ Supergrupo Espinhaço
CNB	176	755100	8343090	Formação Algodão/ Supergrupo Espinhaço
CNB	177	756435	8343812	Formação Algodão/ Supergrupo Espinhaço
CNB	178	756819	8344154	Formação Algodão/ Supergrupo Espinhaço
CNB	179	781325	8365486	Supergrupo Espinhaço Indiviso
CNB	180	781491	8366231	Supergrupo Espinhaço Indiviso
CNB	181	781154	8365399	Supergrupo Espinhaço Indiviso
CNB	182	779692	8563310	Supergrupo Espinhaço Indiviso
CNB	182	774833	8357443	Supergrupo Espinhaço Indiviso
CNB	183	774617	8357522	Supergrupo Espinhaço Indiviso
CNB	184	774217	8357807	Supergrupo Espinhaço Indiviso

CNB	185	774195	8357728	Supergrupo Espinhaço Indiviso
CNB	133.1	775432	8356920	Supergrupo Espinhaço Indiviso
CNB	135.1	770850	8353319	Supergrupo Espinhaço Indiviso
CNB	141.1	762098	8390651	Formação Serra da Garapa/ Grupo Santo Onofre
CNB	155.1	776919	8357188	Supergrupo Espinhaço Indiviso
CNB	157.1	778114	8358092	Supergrupo Espinhaço Indiviso
E	07	765775	8432732	Formação Serra da Garapa/ Grupo Santo Onofre
E	08	775082	8435782	SMVS Caetité – Licínio de Almeida
E	06	7746767	8434794	Suíte Intrusiva Lagoa Real
E	13	783600	8435166	Suíte Intrusiva Lagoa Real
E	15	783249	8435840	Suíte Intrusiva Lagoa Real
E	36	781459	8432772	Suíte Intrusiva Lagoa Real
GNC	14	760.858	8.400.880	Formação Serra da Garapa/ Grupo Santo Onofre
GNE	16	757460	8442774	Formação Serra da Garapa/ Grupo Santo Onofre
GNE	20	759404	8439699	Formação Serra da Garapa/ Grupo Santo Onofre
I	9	766512	8386324	Formação Algodão/ Supergrupo Espinhaço
I	I0	766670	8387248	Formação Algodão/ Supergrupo Espinhaço
I	13	765749	8391954	Formação Algodão/ Supergrupo Espinhaço
I	I0	765963	8393880	Formação Algodão/ Supergrupo Espinhaço
K	40	761590	8361835	Formação Algodão/ Supergrupo Espinhaço
K	41	760134	8368071	Formação Algodão/ Supergrupo Espinhaço
K	45	760152	8364525	Formação Algodão/ Supergrupo Espinhaço
K	46	760423	8364464	Formação Algodão/ Supergrupo Espinhaço
K	48	759785	8364676	Formação Serra da Garapa/ Grupo Santo Onofre
K	49	758866	8365058	Formação Serra da Garapa/ Grupo Santo Onofre
MP	A	767211	8432119	Formação Serra da Garapa/ Grupo Santo Onofre
MP	C	766621	8432139	Formação Serra da Garapa/ Grupo Santo Onofre
N	2	766342	8388690	Formação Algodão/ Supergrupo Espinhaço

N	3	766342	8388690	Formação Algodão/ Supergrupo Espinhaço
N	27	769292	8390426	SMVS Caetité Licínio de Almeida
N	28	766709	8387517	Formação Algodão/ Supergrupo Espinhaço
N	31	770242	8394740	SMVS Caetité Licínio de Almeida
O	36	764827	8376414	Formação Algodão/ Supergrupo Espinhaço
O	37	764732	8376289	Formação Algodão/ Supergrupo Espinhaço
O	38	764820	8376582	Formação Algodão/ Supergrupo Espinhaço
O	40	764208	8377380	Formação Algodão/ Supergrupo Espinhaço
O	55	764609	8382074	Formação Algodão/ Supergrupo Espinhaço
O	56	765026	8382574	Formação Algodão/ Supergrupo Espinhaço
S	3	764231	8403641	Formação Algodão/ Supergrupo Espinhaço
S	27	764248		Formação Algodão/ Supergrupo Espinhaço
S	29	761632	8367905	Formação Serra da Garapa/ Grupo Santo Onofre
S	40	765237	8390490	Formação Algodão/ Supergrupo Espinhaço
S	41	765132	8390434	Formação Algodão/ Supergrupo Espinhaço
S	44	764076	8390592	Formação Algodão/ Supergrupo Espinhaço
S	45	763805	8390649	Formação Serra da Garapa/ Grupo Santo Onofre
S	46	764852	8389734	Formação Algodão/ Supergrupo Espinhaço
S	46 A	764917	8389709	Formação Algodão/ Supergrupo Espinhaço
S	54	765509	8397180	Formação Algodão/ Supergrupo Espinhaço
S	55	765789	8385969	Formação Algodão/ Supergrupo Espinhaço
S	56	765037	8385735	Formação Algodão/ Supergrupo Espinhaço
S	60	763164	8386697	Formação Algodão/ Supergrupo Espinhaço
S	61	761994	8386086	Formação Serra da Garapa/ Grupo Santo Onofre
S	69	760633	8391809	Formação Serra da Garapa/ Grupo Santo Onofre
S	75	761635	8392656	Formação Serra da Garapa/ Grupo Santo Onofre
SCP	Salto	769059	8444083	Formação Algodão/ Supergrupo Espinhaço

TQ	2	753884	8347653	Formação Algodão/ Supergrupo Espinhaço
TQ	3	754281	8347389	Formação Algodão/ Supergrupo Espinhaço
TQ	5	755629	8346184	Formação Algodão/ Supergrupo Espinhaço
TQ	6	755793	8344106	Formação Algodão/ Supergrupo Espinhaço
TQ	9	761358	8351768	Formação Algodão/ Supergrupo Espinhaço
TQ	10	761320	8351784	Formação Algodão/ Supergrupo Espinhaço
TQ	12	761234	8352374	Formação Algodão/ Supergrupo Espinhaço
TQ	13	759296	8368538	Formação Serra da Garapa/ Grupo Santo Onofre
TQ	14	761131	8352396	Formação Algodão/ Supergrupo Espinhaço
TQ	16	760811	8352962	Formação Algodão/ Supergrupo Espinhaço
TQ	17	760988	8355070	Formação Serra da Garapa/ Grupo Santo Onofre
TQ	18	759924	8355334	Formação Serra da Garapa/ Grupo Santo Onofre
TQ	19	759614	8355387	Formação Serra da Garapa/ Grupo Santo Onofre
TQ	20	758666	8356114	Formação Serra da Garapa/ Grupo Santo Onofre
TR	1	758749	8370741	Formação Boqueirão/ Grupo Santo Onofre
TR	7	760422	8368726	Formação Serra da Garapa/ Grupo Santo Onofre
TR	12	759100	8369520	Formação Serra da Garapa/ Grupo Santo Onofre
TR	14	758748	8370740	Formação Serra da Garapa/ Grupo Santo Onofre
TR	20	758854	8391646	Formação Serra da Garapa/ Grupo Santo Onofre
TR	21	759840	8391486	Formação Serra da Garapa/ Grupo Santo Onofre
TR	22	760133	8391514	Formação Serra da Garapa/ Grupo Santo Onofre
TR	23	761012	8392200	Formação Serra da Garapa/ Grupo Santo Onofre
TR	24	761415	8392444	Formação Serra da Garapa/ Grupo Santo Onofre
TR	25	761714	8392346	Formação Serra da Garapa/ Grupo Santo Onofre
TR	49	758626	8378846	Formação Serra da Garapa/ Grupo Santo Onofre
TR	50	758955	8378986	Formação Serra da Garapa/ Grupo Santo Onofre
TR	51	759310	8379005	Formação Serra da Garapa/ Grupo Santo Onofre

TR	53	759371	8379451	Formação Serra da Garapa/ Grupo Santo Onofre
TR	54	759424	8379096	Formação Serra da Garapa/ Grupo Santo Onofre

ANEXO A – REGRAS DE FORMATAÇÃO DA REVISTA GONDWANA RESEARCH

GONDWANA RESEARCH
Official Journal of the International Association for Gondwana Research (IAGR)
ELSEVIER

AUTHOR INFORMATION PACK

TABLE OF CONTENTS

ISSN: 1342-937X

DESCRIPTION

Gondwana Research (GR) is an International Journal aimed to promote high quality research publications on all topics related to **solid Earth**, particularly with reference to the **origin** and **evolution** of **continents**, continental assemblies and their resources. *GR* is an "all earth science" journal with no restrictions on geological time, terrane or theme and covers a wide spectrum of topics in geosciences such as geology, geomorphology, palaeontology, structure, petrology, geochemistry, stable isotopes, geochronology, economic geology, exploration geology, engineering geology, geophysics, and environmental geology among other themes, and provides an appropriate forum to integrate studies from different disciplines and different terrains. In addition to regular articles and thematic issues, the journal invites high profile state-of-the-art reviews on thrust area topics for its column, 'GR FOCUS'. Focus articles include short biographies and photographs of the authors. Short articles (within ten printed pages) for rapid publication reporting important discoveries or innovative models of global interest will be considered under the category 'GR LETTERS'.

Benefits to authors
We also provide many author benefits, such as free PDFs, a liberal copyright policy, special discounts on Elsevier publications and much more. Please click here for more information on our author services.

Please see our Guide for Authors for information on article submission. If you require any further information or help, please visit our Support Center

IMPACT FACTOR

2015: 8.743 © Thomson Reuters Journal Citation Reports 2016

ABSTRACTING AND INDEXING

Chemical Abstracts
Current Contents
Mineralogical Abstracts
GeoRef
Science Citation Index
ScienceDirect
Scopus
Science Citation Index Expanded
Zoological Record
ISI Alerting Services
Journal Citation Reports - Science Edition
Current Abstracts (EBSCO)
TOC Premier

EDITORIAL BOARD

GUIDE FOR AUTHORS

Your Paper Your Way

We now differentiate between the requirements for new and revised submissions. You may choose to submit your manuscript as a single Word or PDF file to be used in the refereeing process. Only when your paper is at the revision stage, will you be requested to put your paper in to a 'correct format' for acceptance and provide the items required for the publication of your article.
To find out more, please visit the Preparation section below.

INTRODUCTION

Gondwana Research (GR) is an International Journal aimed to promote high quality research publications on all topics related to solid Earth, particularly with reference to the origin and evolution of continents, continental assemblies and their resources. GR is an "all earth science" journal with no restrictions on geological time, terrane or theme and covers a wide spectrum of topics in geosciences such as geology, geomorphology, palaeontology, structure, petrology, geochemistry, stable isotopes, geochronology, economic geology, exploration geology, engineering geology, geophysics, and environmental geology among other themes, and provides an appropriate forum to integrate studies from different disciplines and different terrains.

Types of papers

The types of contributions published in Gondwana Research are:
(1) Original research paper,
(2) high-profile state-of-the-art review on thrust area topics under the category 'GR FOCUS',
(3) short article (within ten printed pages) for rapid publication reporting important discoveries or innovative models of global interest under the category 'GR LETTERS'
(4) Comment and Reply.
(5) GR Focus papers that are primarily reviews (but that can also contain new data and discussion)

Letters to the Editors, carrying opinions, views, or other matter of general interest to the scientific community will be considered for occasional publication. Letters to the Editors should be addressed directly to the Editor-in-Chief, before submission through the EES.

For Book Reviews, the publisher/editor/author of the book should submit two copies of the publication to be reviewed to the Editor-in-Chief with a written request for publication of review, who shall then identify an appropriate reviewer. Unsolicited Book Reviews will not be published.

All contributions are subject to peer review except Comments and Replies (GR), Letters to the Editors, Conference reports, Announcements and Book Reviews . Comments on papers published in Gondwana Research must be submitted within six months of the publication of the printed version of the paper. The authors addressed by the Comment will be allowed one month time to submit a Reply. Both Comment and Reply will be limited to a maximum of three printed pages each, and will be accepted at the discretion of the handling Editor. Review papers under the 'GR FOCUS' category that give an overview of the current state of a subject in a certain field should not be directly submitted to the EES. Their submission should first be discussed with the Editor-in-Chief. Review papers are limited to 40 printed pages.

Contact details for submission

All manuscripts should be submitted electronically through Elsevier Editorial System (EES), which can be accessed at: http://ees.elsevier.com/gr

Submission checklist

You can use this list to carry out a final check of your submission before you send it to the journal for review. Please check the relevant section in this Guide for Authors for more details.

Ensure that the following items are present:

One author has been designated as the corresponding author with contact details:
- E-mail address
- Full postal address

All necessary files have been uploaded:

Manuscript:
- Include keywords
- All figures (include relevant captions)
- All tables (including titles, description, footnotes)
- Ensure all figure and table citations in the text match the files provided
- Indicate clearly if color should be used for any figures in print

Graphical Abstracts / Highlights files (where applicable)
Supplemental files (where applicable)

Further considerations
- Manuscript has been 'spell checked' and 'grammar checked'
- All references mentioned in the Reference List are cited in the text, and vice versa
- Permission has been obtained for use of copyrighted material from other sources (including the Internet)
- Relevant declarations of interest have been made
- Journal policies detailed in this guide have been reviewed
- Referee suggestions and contact details provided, based on journal requirements

For further information, visit our Support Center.

BEFORE YOU BEGIN

Ethics in publishing
Please see our information pages on Ethics in publishing and Ethical guidelines for journal publication.

Declaration of interest
All authors are requested to disclose any actual or potential conflict of interest including any financial, personal or other relationships with other people or organizations within three years of beginning the submitted work that could inappropriately influence, or be perceived to influence, their work. More information.

Submission declaration and verification
Submission of an article implies that the work described has not been published previously (except in the form of an abstract or as part of a published lecture or academic thesis or as an electronic preprint, see 'Multiple, redundant or concurrent publication' section of our ethics policy for more information), that it is not under consideration for publication elsewhere, that its publication is approved by all authors and tacitly or explicitly by the responsible authorities where the work was carried out, and that, if accepted, it will not be published elsewhere in the same form, in English or in any other language, including electronically without the written consent of the copyright-holder. To verify originality, your article may be checked by the originality detection service CrossCheck.

Changes to authorship
Authors are expected to consider carefully the list and order of authors **before** submitting their manuscript and provide the definitive list of authors at the time of the original submission. Any addition, deletion or rearrangement of author names in the authorship list should be made only **before** the manuscript has been accepted and only if approved by the journal Editor. To request such a change, the Editor must receive the following from the **corresponding author**: (a) the reason for the change in author list and (b) written confirmation (e-mail, letter) from all authors that they agree with the addition, removal or rearrangement. In the case of addition or removal of authors, this includes confirmation from the author being added or removed.
Only in exceptional circumstances will the Editor consider the addition, deletion or rearrangement of authors **after** the manuscript has been accepted. While the Editor considers the request, publication of the manuscript will be suspended. If the manuscript has already been published in an online issue, any requests approved by the Editor will result in a corrigendum.

Article transfer service
This journal is part of our Article Transfer Service. This means that if the Editor feels your article is more suitable in one of our other participating journals, then you may be asked to consider transferring the article to one of those. If you agree, your article will be transferred automatically on your behalf with no need to reformat. Please note that your article will be reviewed again by the new journal. More information.

Copyright

Upon acceptance of an article, authors will be asked to complete a 'Journal Publishing Agreement' (see more information on this). An e-mail will be sent to the corresponding author confirming receipt of the manuscript together with a 'Journal Publishing Agreement' form or a link to the online version of this agreement.

Subscribers may reproduce tables of contents or prepare lists of articles including abstracts for internal circulation within their institutions. Permission of the Publisher is required for resale or distribution outside the institution and for all other derivative works, including compilations and translations. If excerpts from other copyrighted works are included, the author(s) must obtain written permission from the copyright owners and credit the source(s) in the article. Elsevier has preprinted forms for use by authors in these cases.

For open access articles: Upon acceptance of an article, authors will be asked to complete an 'Exclusive License Agreement' (more information). Permitted third party reuse of open access articles is determined by the author's choice of user license.

Author rights

As an author you (or your employer or institution) have certain rights to reuse your work. More information.

Elsevier supports responsible sharing
Find out how you can share your research published in Elsevier journals.

Role of the funding source

You are requested to identify who provided financial support for the conduct of the research and/or preparation of the article and to briefly describe the role of the sponsor(s), if any, in study design; in the collection, analysis and interpretation of data; in the writing of the report; and in the decision to submit the article for publication. If the funding source(s) had no such involvement then this should be stated.

Funding body agreements and policies
Elsevier has established a number of agreements with funding bodies which allow authors to comply with their funder's open access policies. Some funding bodies will reimburse the author for the Open Access Publication Fee. Details of existing agreements are available online.

Open access

This journal offers authors a choice in publishing their research:

Open access
- Articles are freely available to both subscribers and the wider public with permitted reuse.
- An open access publication fee is payable by authors or on their behalf, e.g. by their research funder or institution.

Subscription
- Articles are made available to subscribers as well as developing countries and patient groups through our universal access programs.
- No open access publication fee payable by authors.

Regardless of how you choose to publish your article, the journal will apply the same peer review criteria and acceptance standards.

For open access articles, permitted third party (re)use is defined by the following Creative Commons user licenses:

Creative Commons Attribution (CC BY)
Lets others distribute and copy the article, create extracts, abstracts, and other revised versions, adaptations or derivative works of or from an article (such as a translation), include in a collective work (such as an anthology), text or data mine the article, even for commercial purposes, as long as they credit the author(s), do not represent the author as endorsing their adaptation of the article, and do not modify the article in such a way as to damage the author's honor or reputation.

Creative Commons Attribution-NonCommercial-NoDerivs (CC BY-NC-ND)
For non-commercial purposes, lets others distribute and copy the article, and to include in a collective work (such as an anthology), as long as they credit the author(s) and provided they do not alter or modify the article.

The open access publication fee for this journal is **USD 3300**, excluding taxes. There is a **20%** discount off the open access publication fee for members of the **International Association for Gondwana Research (IAGR)**. Learn more about Elsevier's pricing policy: http://www.elsevier.com/openaccesspricing.

Green open access
Authors can share their research in a variety of different ways and Elsevier has a number of green open access options available. We recommend authors see our green open access page for further information. Authors can also self-archive their manuscripts immediately and enable public access from their institution's repository after an embargo period. This is the version that has been accepted for publication and which typically includes author-incorporated changes suggested during submission, peer review and in editor-author communications. Embargo period: For subscription articles, an appropriate amount of time is needed for journals to deliver value to subscribing customers before an article becomes freely available to the public. This is the embargo period and it begins from the date the article is formally published online in its final and fully citable form. Find out more.

This journal has an embargo period of 24 months.

Language (usage and editing services)
Please write your text in good English (American or British usage is accepted, but not a mixture of these). Authors who feel their English language manuscript may require editing to eliminate possible grammatical or spelling errors and to conform to correct scientific English may wish to use the English Language Editing service available from Elsevier's WebShop.

Submission
Our online submission system guides you stepwise through the process of entering your article details and uploading your files. The system converts your article files to a single PDF file used in the peer-review process. Editable files (e.g., Word, LaTeX) are required to typeset your article for final publication. All correspondence, including notification of the Editor's decision and requests for revision, is sent by e-mail.

Submit your article
Please submit your article via http://ees.elsevier.com/gr

PREPARATION

NEW SUBMISSIONS
Submission to this journal proceeds totally online and you will be guided stepwise through the creation and uploading of your files. The system automatically converts your files to a single PDF file, which is used in the peer-review process.
As part of the Your Paper Your Way service, you may choose to submit your manuscript as a single file to be used in the refereeing process. This can be a PDF file or a Word document, in any format or lay-out that can be used by referees to evaluate your manuscript. It should contain high enough quality figures for refereeing. If you prefer to do so, you may still provide all or some of the source files at the initial submission. Please note that individual figure files larger than 10 MB must be uploaded separately.

References
There are no strict requirements on reference formatting at submission. References can be in any style or format as long as the style is consistent. Where applicable, author(s) name(s), journal title/book title, chapter title/article title, year of publication, volume number/book chapter and the pagination must be present. Use of DOI is highly encouraged. The reference style used by the journal will be applied to the accepted article by Elsevier at the proof stage. Note that missing data will be highlighted at proof stage for the author to correct.

Formatting requirements
There are no strict formatting requirements but all manuscripts must contain the essential elements needed to convey your manuscript, for example Abstract, Keywords, Introduction, Materials and Methods, Results, Conclusions, Artwork and Tables with Captions.

If your article includes any Videos and/or other Supplementary material, this should be included in your initial submission for peer review purposes.
Divide the article into clearly defined sections.

Figures and tables embedded in text
Please ensure the figures and the tables included in the single file are placed next to the relevant text in the manuscript, rather than at the bottom or the top of the file.

REVISED SUBMISSIONS

Use of word processing software
Regardless of the file format of the original submission, at revision you must provide us with an editable file of the entire article. Keep the layout of the text as simple as possible. Most formatting codes will be removed and replaced on processing the article. The electronic text should be prepared in a way very similar to that of conventional manuscripts (see also the Guide to Publishing with Elsevier). See also the section on Electronic artwork.
To avoid unnecessary errors you are strongly advised to use the 'spell-check' and 'grammar-check' functions of your word processor.

Article structure

Subdivision - numbered sections
Divide your article into clearly defined and numbered sections. Subsections should be numbered 1.1 (then 1.1.1, 1.1.2, ...), 1.2, etc. (the abstract is not included in section numbering). Use this numbering also for internal cross-referencing: do not just refer to 'the text'. Any subsection may be given a brief heading. Each heading should appear on its own separate line.

Material and methods
Provide sufficient detail to allow the work to be reproduced. Methods already published should be indicated by a reference: only relevant modifications should be described.

Results
Results should be clear and concise.

Discussion
This should explore the significance of the results of the work, not repeat them. A combined Results and Discussion section is often appropriate. Avoid extensive citations and discussion of published literature.

Conclusions
The main conclusions of the study may be presented in a short Conclusions section, which may stand alone or form a subsection of a Discussion or Results and Discussion section.

Essential title page information

• ***Title.*** Concise and informative. Titles are often used in information-retrieval systems. Avoid abbreviations and formulae where possible.
• ***Author names and affiliations.*** Please clearly indicate the given name(s) and family name(s) of each author and check that all names are accurately spelled. Present the authors' affiliation addresses (where the actual work was done) below the names. Indicate all affiliations with a lower-case superscript letter immediately after the author's name and in front of the appropriate address. Provide the full postal address of each affiliation, including the country name and, if available, the e-mail address of each author.
• ***Corresponding author.*** Clearly indicate who will handle correspondence at all stages of refereeing and publication, also post-publication. **Ensure that the e-mail address is given and that contact details are kept up to date by the corresponding author.**
• ***Present/permanent address.*** If an author has moved since the work described in the article was done, or was visiting at the time, a 'Present address' (or 'Permanent address') may be indicated as a footnote to that author's name. The address at which the author actually did the work must be retained as the main, affiliation address. Superscript Arabic numerals are used for such footnotes.

Abstract

A concise and factual abstract is required (up to 300 words within one paragraph). The abstract should state briefly the purpose of the research, the principal results and major conclusions. An abstract is often presented separately from the article, so it must be able to stand alone. For this reason, References should be avoided, but if essential, then cite the author(s) and year(s). Also, non-standard or uncommon abbreviations should be avoided, but if essential they must be defined at their first mention in the abstract itself.

Graphical abstract

A Graphical abstract is mandatory for this journal. Graphical Abstract should be a figure that captures, in as dramatic fashion as possible, the main points of your paper, i.e. the attention of a wide readership online. It must be in color, in landscape format (horizontal axis about 2.5 time that of the vertical) with no figure caption, and with minimal lettering in large font. Graphical abstracts should be submitted as a separate file in the online submission system. Image size: please provide an image with a minimum of 531 x 1328 pixels (h x w) or proportionally more. Preferred file types: TIFF, EPS, PDF or MS Office files. See http://www.elsevier.com/graphicalabstracts for examples.

Research highlights

Research highlights are mandatory for this journal. They must comprise three bulleted sentences that summarize the salient results reported in your paper. Research Highlights should be submitted as a separate Word file in the online submission system. Each sentence must contain no more than 85 characters (including spaces). See http://www.elsevier.com/researchhighlights for examples.

Keywords

Immediately after the abstract, provide a maximum of 6 keywords, using American spelling and avoiding general and plural terms and multiple concepts (avoid, for example, "and", "of"). Be sparing with abbreviations: only abbreviations firmly established in the field may be eligible. These keywords will be used for indexing purposes.

Text

The text should be typed in at least 12-point, double-spaced, with 1-inch margins. The lines must be numbered continuously. Headings of all subsections must be separated from the text by an empty line. The paragraphs must be zero spaced with 1 inch right indented first lines. Pdf files of the text are unacceptable.

Acknowledgements

Collate acknowledgements in a separate section at the end of the article before the references and do not, therefore, include them on the title page, as a footnote to the title or otherwise. List here those individuals who provided help during the research (e.g., providing language help, writing assistance or proof reading the article, assisting in analytical work, drawing pictures, etc.).

Formatting of funding sources

List funding sources in this standard way to facilitate compliance to funder's requirements:

Funding: This work was supported by the National Institutes of Health [grant numbers xxxx, yyyy]; the Bill & Melinda Gates Foundation, Seattle, WA [grant number zzzz]; and the United States Institutes of Peace [grant number aaaa].

It is not necessary to include detailed descriptions on the program or type of grants and awards. When funding is from a block grant or other resources available to a university, college, or other research institution, submit the name of the institute or organization that provided the funding.

If no funding has been provided for the research, please include the following sentence:

This research did not receive any specific grant from funding agencies in the public, commercial, or not-for-profit sectors.

Units

Follow internationally accepted rules and conventions: use the international system of units (SI). If other units are mentioned, please give their equivalent in SI.

Math formulae

Please submit math equations as editable text and not as images. Present simple formulae in line with normal text where possible and use the solidus (/) instead of a horizontal line for small fractional terms, e.g., X/Y. In principle, variables are to be presented in italics. Powers of e are often more conveniently denoted by exp. Number consecutively any equations that have to be displayed separately from the text (if referred to explicitly in the text).

Footnotes
Footnotes should be used sparingly. Number them consecutively throughout the article. Many word processors build footnotes into the text, and this feature may be used. Should this not be the case, indicate the position of footnotes in the text and present the footnotes themselves separately at the end of the article.

Artwork

Electronic artwork
General points
- Make sure you use uniform lettering and sizing of your original artwork.
- Preferred fonts: Arial (or Helvetica), Times New Roman (or Times), Symbol, Courier.
- Number the illustrations according to their sequence in the text.
- Use a logical naming convention for your artwork files.
- Indicate per figure if it is a single, 1.5 or 2-column fitting image.
- For Word submissions only, you may still provide figures and their captions, and tables within a single file at the revision stage.
- Please note that individual figure files larger than 10 MB must be provided in separate source files.

A detailed guide on electronic artwork is available.
You are urged to visit this site; some excerpts from the detailed information are given here.
Formats
Regardless of the application used, when your electronic artwork is finalized, please 'save as' or convert the images to one of the following formats (note the resolution requirements for line drawings, halftones, and line/halftone combinations given below):
EPS (or PDF): Vector drawings. Embed the font or save the text as 'graphics'.
TIFF (or JPG): Color or grayscale photographs (halftones): always use a minimum of 300 dpi.
TIFF (or JPG): Bitmapped line drawings: use a minimum of 1000 dpi.
TIFF (or JPG): Combinations bitmapped line/half-tone (color or grayscale): a minimum of 500 dpi is required.
Please do not:
- Supply files that are optimized for screen use (e.g., GIF, BMP, PICT, WPG); the resolution is too low.
- Supply files that are too low in resolution.
- Submit graphics that are disproportionately large for the content.

Color artwork
Please make sure that artwork files are in an acceptable format (TIFF (or JPEG), EPS (or PDF), or MS Office files) and with the correct resolution. If, together with your accepted article, you submit usable color figures then Elsevier will ensure, at no additional charge, that these figures will appear in color online (e.g., ScienceDirect and other sites) regardless of whether or not these illustrations are reproduced in color in the printed version. **For color reproduction in print, you will receive information regarding the costs from Elsevier after receipt of your accepted article.** Please indicate your preference for color: in print or online only. Further information on the preparation of electronic artwork.

Figure captions
Ensure that each illustration has a caption. A caption should comprise a brief title (**not** on the figure itself) and a description of the illustration. Keep text in the illustrations themselves to a minimum but explain all symbols and abbreviations used.

Tables

Please submit tables as editable text and not as images. Tables can be placed either next to the relevant text in the article, or on separate page(s) at the end. Number tables consecutively in accordance with their appearance in the text and place any table notes below the table body. Be sparing in the use of tables and ensure that the data presented in them do not duplicate results described elsewhere in the article. Please avoid using vertical rules.

References

Citation in text
Please ensure that every reference cited in the text is also present in the reference list (and vice versa). Any references cited in the abstract must be given in full. Unpublished results and personal communications are not recommended in the reference list, but may be mentioned in the text. If these references are included in the reference list they should follow the standard reference style of the

journal and should include a substitution of the publication date with either 'Unpublished results' or 'Personal communication'. Citation of a reference as 'in press' implies that the item has been accepted for publication.

Web references
As a minimum, the full URL should be given and the date when the reference was last accessed. Any further information, if known (DOI, author names, dates, reference to a source publication, etc.), should also be given. Web references can be listed separately (e.g., after the reference list) under a different heading if desired, or can be included in the reference list.

Data references
This journal encourages you to cite underlying or relevant datasets in your manuscript by citing them in your text and including a data reference in your Reference List. Data references should include the following elements: author name(s), dataset title, data repository, version (where available), year, and global persistent identifier. Add [dataset] immediately before the reference so we can properly identify it as a data reference. The [dataset] identifier will not appear in your published article.

[dataset] Oguro, M., Imahiro, S., Saito, S., Nakashizuka, T., 2015. Mortality data for Japanese oak wilt disease and surrounding forest compositions. Mendeley Data, v1. http://dx.doi.org/10.17632/xwj98nb39r.1.

References in a special issue
Please ensure that the words 'this issue' are added to any references in the list (and any citations in the text) to other articles in the same Special Issue.

Reference management software
Most Elsevier journals have their reference template available in many of the most popular reference management software products. These include all products that support Citation Style Language styles, such as Mendeley and Zotero, as well as EndNote. Using the word processor plug-ins from these products, authors only need to select the appropriate journal template when preparing their article, after which citations and bibliographies will be automatically formatted in the journal's style. If no template is yet available for this journal, please follow the format of the sample references and citations as shown in this Guide.

Users of Mendeley Desktop can easily install the reference style for this journal by clicking the following link:
http://open.mendeley.com/use-citation-style/gondwana-research
When preparing your manuscript, you will then be able to select this style using the Mendeley plug-ins for Microsoft Word or LibreOffice.

Reference formatting
There are no strict requirements on reference formatting at submission. References can be in any style or format as long as the style is consistent. Where applicable, author(s) name(s), journal title/book title, chapter title/article title, year of publication, volume number/book chapter and the pagination must be present. Use of DOI is highly encouraged. The reference style used by the journal will be applied to the accepted article by Elsevier at the proof stage. Note that missing data will be highlighted at proof stage for the author to correct. If you do wish to format the references yourself they should be arranged according to the following examples:

Reference style
References: All publications cited in the text should be presented in a list of references following the text of the manuscript. In the text refer to the author's name (without initials) and year of publication (e.g. "Since Condie (2001) has shown that..." or "This is in agreement with results obtained later (Meert, 2003; Burrett and Berry, 2000)."
For three or more authors use the first author followed by "et al.", in the text. The list of references should be arranged alphabetically by authors' names. The manuscript should be carefully checked to ensure that the spelling of authors' names and dates are exactly the same in the text as in the reference list. Full journal titles must be used.
References should be given in the following form:
Kusky, T.M., Stern, R.J., Tucker, R.D., 2003. Evolution of East African and related orogens, and the assembly of Gondwana. Precambrian Research 123, 81–85.
Pili, E., Sheppard, S.M.F., Lardeaux, J.M.,1999. Fluid–rock interaction in the granulites of Madagascar and lithospheric transfer of fluids. Gondwana Research 2, 341–350.

Suzuki, K., Adachi, M., 1992. Middle Precambrian detrital monazite and zircon from Hida gneiss in Oki-Dogo island, Japan: their origin and implications for the correlation of basement gneiss of Southwest Japan and Korea. Tectonophysics 235, 277–292.
Touret, J.L.R., 1985. Fluid regime in southern Norway, the record of fluid inclusions. In: Tobi, A.C., Touret, J.L.R. (Eds.), The Deep Proterozoic Crust in the North Atlantic Provinces. Reidel, Dordrecht, 517–549.
Kinny, P. D., Collins, A. S., Razakamanana, T., 2004. Provenance hints and age constraints of metasedimentary gneisses of Southern Madagascar from SHRIMP U–Pb zircon data. In: Chetty, T.R.K. and Bhaskar Rao, Y.J. (Eds.), International Field Workshop on the Southern Granulite Terrane. National Geophysical Research Institute, Hyderabad, India, 97–98.
Rogers, J.J.W. and Santosh, M., 2004. Continents and Supercontinents. Oxford University Press, New York. Li, Z.X., Metcalfe, I., Powell, C.M. (Eds.), 1996. Breakup of Rodinia and Gondwanaland and Assembly of Asia. Australian Journal of Earth Sciences 43.
Albee, H.F., Cullins, H.L., 1975. Geologic map of the Alpine Quadrangle, Bonneville County, Idaho, and Lincoln County Wyoming. United States Geological Survey Geologic Quadrangle Map GQ–1259, scale 1:24,000. Sajeev, K., 2003. Evolution and metamorphic zoning of Highland Complex, Sri Lanka: a comparison with Madurai Block, southern India. Ph.D. thesis, Okayama University.

Video

Elsevier accepts video material and animation sequences to support and enhance your scientific research. Authors who have video or animation files that they wish to submit with their article are strongly encouraged to include links to these within the body of the article. This can be done in the same way as a figure or table by referring to the video or animation content and noting in the body text where it should be placed. All submitted files should be properly labeled so that they directly relate to the video file's content. In order to ensure that your video or animation material is directly usable, please provide the files in one of our recommended file formats with a preferred maximum size of 150 MB. Video and animation files supplied will be published online in the electronic version of your article in Elsevier Web products, including ScienceDirect. Please supply 'stills' with your files: you can choose any frame from the video or animation or make a separate image. These will be used instead of standard icons and will personalize the link to your video data. For more detailed instructions please visit our video instruction pages. Note: since video and animation cannot be embedded in the print version of the journal, please provide text for both the electronic and the print version for the portions of the article that refer to this content.

Supplementary material

Supplementary material can support and enhance your scientific research. Supplementary files offer the author additional possibilities to publish supporting applications, high-resolution images, background datasets, sound clips and more. Please note that such items are published online exactly as they are submitted; there is no typesetting involved (supplementary data supplied as an Excel file or as a PowerPoint slide will appear as such online). Please submit the material together with the article and supply a concise and descriptive caption for each file. If you wish to make any changes to supplementary data during any stage of the process, then please make sure to provide an updated file, and do not annotate any corrections on a previous version. Please also make sure to switch off the 'Track Changes' option in any Microsoft Office files as these will appear in the published supplementary file(s). For more detailed instructions please visit our artwork instruction pages.

RESEARCH_DATA

This journal encourages and supports you to share data that underpins your research publication where appropriate, and enables you to interlink the data with your published articles. Research data refers to the results of observations or experimentation that are necessary to validate research findings. To facilitate reproducibility and data reuse, this journal also encourages you to share your software, code, models, algorithms, protocols, methods and other useful materials related to the project.

Below are a number of ways in which you can associate data with your article or make a statement about the availability of your data when submitting your manuscript.

For more information on depositing, sharing and using research data and other relevant research materials, visit the research data page.

Mendeley Data

This journal supports Mendeley Data, enabling you to deposit any research data and materials (including raw and processed data, video, code, software, algorithms, protocols, and methods) associated with your manuscript in a free-to-use, open access repository. During the submission process, after uploading your manuscript, you will have the opportunity to upload your relevant datasets directly to *Mendeley Data*. The datasets will be listed and directly accessible to readers next to your published article online.

For more information, visit the Mendeley Data for journals page.

Open data

This journal supports Open data, enabling authors to submit any raw (unprocessed) research data with their article for open access publication under the CC BY license. More information.

Database linking

Elsevier encourages authors to connect articles with external databases, giving readers access to relevant databases that help to build a better understanding of the described research. Please refer to relevant database identifiers using the following format in your article: Database: xxxx (e.g., TAIR: AT1G01020; CCDC: 734053; PDB: 1XFN). More information and a full list of supported databases.

Database linking

Once you have made your research data available in a data repository, you can link your article directly to the dataset. Elsevier collaborates with a number of repositories to link articles on ScienceDirect with relevant repositories, giving readers access to databases that give them a better understanding of the research described.

Transparency

To foster transparency, we encourage you to state the availability of your data in your submission. If your data is unavailable to access or unsuitable to post, this gives you the opportunity to indicate why. You can also include an email address so readers can request data that is unavailable for publication or under embargo. If you submit this form with your manuscript as a supplementary file, the statement will appear next to your published article on ScienceDirect.

ARTICLE ENRICHMENTS

AudioSlides

The journal encourages authors to create an AudioSlides presentation with their published article. AudioSlides are brief, webinar-style presentations that are shown next to the online article on ScienceDirect. This gives authors the opportunity to summarize their research in their own words and to help readers understand what the paper is about. More information and examples are available. Authors of this journal will automatically receive an invitation e-mail to create an AudioSlides presentation after acceptance of their paper.

Google Maps and KML files

KML (Keyhole Markup Language) files (optional): You can enrich your online articles by providing KML or KMZ files which will be visualized using Google maps. The KML or KMZ files can be uploaded in our online submission system. KML is an XML schema for expressing geographic annotation and visualization within Internet-based Earth browsers. Elsevier will generate Google Maps from the submitted KML files and include these in the article when published online. Submitted KML files will also be available for downloading from your online article on ScienceDirect. More information.

Interactive plots

This journal enables you to show an Interactive Plot with your article by simply submitting a data file. Full instructions.

AFTER ACCEPTANCE

Online proof correction

Corresponding authors will receive an e-mail with a link to our online proofing system, allowing annotation and correction of proofs online. The environment is similar to MS Word: in addition to editing text, you can also comment on figures/tables and answer questions from the Copy Editor. Web-based proofing provides a faster and less error-prone process by allowing you to directly type your corrections, eliminating the potential introduction of errors.

If preferred, you can still choose to annotate and upload your edits on the PDF version. All instructions for proofing will be given in the e-mail we send to authors, including alternative methods to the online version and PDF.
We will do everything possible to get your article published quickly and accurately. Please use this proof only for checking the typesetting, editing, completeness and correctness of the text, tables and figures. Significant changes to the article as accepted for publication will only be considered at this stage with permission from the Editor. It is important to ensure that all corrections are sent back to us in one communication. Please check carefully before replying, as inclusion of any subsequent corrections cannot be guaranteed. Proofreading is solely your responsibility.

Offprints

The corresponding author will, at no cost, receive a customized Share Link providing 50 days free access to the final published version of the article on ScienceDirect. The Share Link can be used for sharing the article via any communication channel, including email and social media. For an extra charge, paper offprints can be ordered via the offprint order form which is sent once the article is accepted for publication. Both corresponding and co-authors may order offprints at any time via Elsevier's Webshop. Corresponding authors who have published their article open access do not receive a Share Link as their final published version of the article is available open access on ScienceDirect and can be shared through the article DOI link.

AUTHOR INQUIRIES

Visit the Elsevier Support Center to find the answers you need. Here you will find everything from Frequently Asked Questions to ways to get in touch.
You can also check the status of your submitted article or find out when your accepted article will be published.

ANEXO B – COMPROVANTE DE SUMISSÃO DO ARTIGO

Gmail

Caroline Novais <carolcnb@gmail.com>

Submission Confirmation
2 mensagens

Gondwana Research <eesserver@eesmail.elsevier.com> 14 de setembro de 2017 13:40
Responder a: Gondwana Research <santosh@cugb.edu.cn>
Para: carolcnb@gmail.com, carolbit@hotmail.com

Article Type: Research Paper

Dear Caroline,

Your submission entitled "Statherian and Tonian rifts from the southern sector of the Paramirim Aulacogen, São Francisco-Congo paleo-plate: new data, regional correlations" has been received by Gondwana Research

You may check on the progress of your paper by logging on to the Elsevier Editorial System as an author. The URL is https://eeslive.elsevier.com/gr/.

Your username is: carolcnb@gmail.com
Your password is: *******

Your manuscript will be given a reference number once an Editor has been assigned.

Thank you for submitting your work to this journal.

Kind regards,

Elsevier Editorial System
Gondwana Research